AN INVESTIGATION OF UBC SERVICEABILITY REQUIREMENTS FROM BUILDING RESPONSES RECORDED DURING THE 1989 LOMA PRIETA EARTHQUAKE

by

Chia-Ming Uang and Ahmed Maarouf

Department of Civil Engineering
Northeastern University, Boston

Data Utilization Report CSMIP/96-01

California Strong Motion Instrumentation Program

September 1996

CALIFORNIA DEPARTMENT OF CONSERVATION
DIVISION OF MINES AND GEOLOGY
OFFICE OF STRONG MOTION STUDIES

OSMS 96-09

DIVISION OF MINES AND GEOLOGY
JAMES F. DAVIS
STATE GEOLOGIST

DISCLAIMER

The content of this report was developed under Contract No. 1090-515 from the Strong Motion Instrumentation Program in the Division of Mines and Geology of the California Department of Conservation. This report has not been edited to the standards of a formal publication. Any opinions, findings, conclusions or recommendations contained in this report are those of the authors, and should not be interpreted as representing the official policies, either expressed or implied, of the State of California.

AN INVESTIGATION OF UBC SERVICEABILITY REQUIREMENTS FROM BUILDING RESPONSES RECORDED DURING THE 1989 LOMA PRIETA EARTHQUAKE

by

Chia-Ming Uang* and Ahmed Maarouf

Department of Civil Engineering
Northeastern University, Boston

Data Utilization Report CSMIP/96-01

California Strong Motion Instrumentation Program

September 1996

* Now at Department of Applied Mechanics and Engineering Sceiences, University of California, San Diego.

This study was conducted at the Northeastern University in Boston, Massachusetts and was supported by the Department of Conservation under Contract No. 1090-515.

California Department of Conservation
Division of Mines and Geology
Office of Strong Motion Studies
801 K Street, MS 13-35
Sacramento, California 95814-3531

PREFACE

The California Strong Motion Instrumentation Program (CSMIP) in the Division of Mines and Geology of the California Department of Conservation promotes and facilitates the improvement of seismic codes through the Data Interpretation Project. The objective of the this project is to increase the understanding of earthquake strong ground shaking and its effects on structures through interpretation and analysis studies of CSMIP and other applicable strong motion data. The ultimate goal is to accelerate the process by which lessons learned from earthquake data are incorporated into seismic code provisions and seismic design practices.

The specific objectives of the CSMIP Data Interpretation Project are to:

1. Understand the spatial variation and magnitude dependence of earthquake strong ground motion.

2. Understand the effects of earthquake motions on the response of geologic formations, buildings and lifeline structures.

3. Expedite the incorporation of knowledge of earthquake shaking into revision of seismic codes and practices.

4. Increase awareness within the seismological and earthquake engineering community about the effective usage of strong motion data.

5. Improve instrumentation methods and data processing techniques to maximize the usefulness of SMIP data. Develop data representations to increase the usefulness and the applicability to design engineers.

This report is the fourteenth in a series of CSMIP data utilization reports designed to transfer recent research findings on strong-motion data to practicing seismic design professionals and earth scientists. CSMIP extends its appreciation to the members of the Strong Motion Instrumentation Advisory Committee and its subcommittees for their recommendations regarding the Data Interpretation Research Project.

Anthony F. Shakal
CSMIP Program Manager

Moh J. Huang
CSMIP Data Interpretation
Project Manager

ABSTRACT

The Uniform Building Code (UBC) seismic design procedure does not address the serviceability limit state explicitly. In the light of significant economic losses of building damage in the 1989 Loma Prieta earthquake, the UBC seismic serviceability requirements are examined from the recorded responses of four multistory buildings. An analytical study showed that the intensity of the UBC-implied "moderate" design earthquake for buildings with a fundamental period greater than 0.7 seconds is only one-sixth that of the "severe" design earthquake. The four buildings (one steel building and three reinforced concrete buildings) selected in this study have effective peak ground accelerations similar that of the UBC-implied moderate design earthquake.

Detailed structural responses of each building at peak responses are computed by imposing lateral displacements to a three-dimensional finite element model; a modal superposition technique is used to "recover" lateral displacements at floors that are not instrumented. An analytical study shows that member forces in ductile building systems may exceed member capacities if the structure were to respond elastically during moderate earthquakes. This is confirmed by the structural analyses of a 13-story steel frame; the actual stress ratio may exceed 1.4, and the maximum story drift ratio is about one percent. Because of the large lateral stiffness, not the UBC drift limits, the serviceability performance tends to be satisfactory for the types of reinforced concrete buildings studied.

It is recommended that, in addition to considering the ultimate limit state for sever design earthquakes, the serviceability limit state for moderate design earthquakes be considered explicitly to limit story drifts and member forces in UBC.

ACKNOWLEDGMENTS

The contents of this report were developed under Contract No. 1090-515 from the California Department of Conservation, Division of Mines and Geology, Strong Motion Instrumentation Program. However, these contents do not necessarily represent the policy of that agency nor do endorsement by the State Government. Much appreciation is given to the staff of the SMIP, especially Drs. M. J. Huang and A. F. Shakal, for providing processed data and design drawings.

Table of Contents

Chapter 1
Introduction

1.1. Problem Statement

Modern building seismic design provisions generally require that a well designed building structure satisfy the following performance criteria (25):

Serviceability Limit State — During minor or moderate earthquakes a building should have sufficient stiffness and strength to avoid nonstructural and structural damage.

Ultimate Limit State — During severe earthquakes a building should have sufficient strength and energy dissipation capacity to avoid structural collapse.

While the ultimate limit state deals with the life-safety considerations for severe earthquakes, the serviceability limit state attempts to reduce economic losses by minimizing nonstructural damage and by avoiding structural yielding in moderate earthquakes. Therefore an ideal seismic code should include a two-phase design procedure.

The idea of using two levels of design earthquakes is not new in the United States (5, 7, 28). In 1974 a two-phase design procedure was proposed in the ATC-2 project (7), although this procedure was not adopted in the ATC 3-06 document (30). The ATC 3-06 design procedure [or the NEHRP Recommended Provisions (19), which is a revised version of the ATC 3-06 document] considers the ultimate limit state only. That is, the ATC 3-06 design procedure only intends to safeguard against major failure and loss of life in severe earthquakes; no attempt is made to limit damage, maintain functions, or provide for easy repair. This document does not consider the serviceability limit state, nor does it attempt to minimize economic losses produced by minor or moderate earthquake excitations. Similar attitude towards designing buildings to meet mainly the life-safety criterion in severe earthquakes has also been adopted by the SEAOC Recommended Lateral Force Requirements (25) and the Uniform Building Code (36).

In order to consider the serviceability limit state in seismic provisions, it is necessary to

(i) define "moderate" design earthquakes in the form of, say, elastic design spectra;

(ii) limit story drifts to, say, 0.5% of the story height to avoid nonstructural damage; and

(iii) limit member forces and stresses to avoid structural damage or yielding.

A review of the seismic codes in other countries indicates that the 1981 Building Standard Law of Japan (6) follows a two-phase design procedure. In design phase-one for the serviceability limit state, a moderate design earthquake is specified in the form of an elastic design spectrum; the intensity of the moderate design earthquake is one-fifth that of the severe design earthquake. The story drift limit is set to 0.5% of the story height to minimize nonstructural damage. To control structural damage, the allowable stress for steel design is set to approximately 90% of the yield stress. In design phase-two for the ultimate limit state, designers are required to check the ultimate strength of the structure (13, 32).

1.2. Loma Prieta Earthquake

The Loma Prieta earthquake of October 17,1989, a Magnitude 7.1 earthquake that occurred in a sparsely settled portion of the Santa Cruse mountains, caused 6 billion dollars damage and the collapse of buildings as far as 60 miles in San Francisco and Oakland (10). It is generally recognized that multistory buildings in the San Francisco Bay Area performed well during the Loma Prieta Earthquake (16, 20, 23, 24). It is also widely accepted that these buildings (or the seismic design provisions in the United States) were not attested for their ultimate limit state against severe structural damage or collapse because the epicenter of this earthquake was not located in the Bay Area, and the strong motion duration lasted for only 10 seconds. Nevertheless, in the light of the significant economic losses and building damage at this level of ground excitations, this earthquake provides an excellent opportunity to evaluate the serviceability limit state philosophy of the Uniform Building Code (UBC). This study is feasible because significant number of seismic records in extensively instrumented buildings have been collected by CDMG (29), and the recorded peak ground motions at the base of many buildings fall in the range 0.06-0.15 g, which is representative of "moderate" design earthquakes implicitly assumed by the UBC (to be discussed in Chapter 2).

1.3. Objectives

The objectives of this research are:

(1) Evaluate building responses including story drifts and member forces from recorded data of a limited number of floors in four multistory buildings excited during the Loma Prieta Earthquake. The computed story drifts and member forces are related to nonstructural and structural component damage, respectively.

(2) Examine the adequacy of the serviceability requirements of the UBC seismic provisions from the calculated building response and the observed damage.

(3) Recommend guidelines to improve the UBC serviceability requirements.

1.4. Scope

Four medium-rise buildings (6- to 13-story high) that were extensively instrumented by CDMG (29) have been selected for this study. See Table 1.1 for a list of these buildings. The selected database covers buildings constructed with different materials and different lateral-force-resisting framing systems (i.e., different K or R_w factors). Recorded peak ground accelerations fall in the range 0.11-0.13 g.

Chapter 2
Problems of UBC Seismic Serviceability Requirements

2.1. UBC Seismic Design Philosophy

2.1.1. Ultimate Limit State for Severe Earthquakes

To satisfy the ultimate limit state, UBC specifies elastic design spectra corresponding to "severe" design earthquakes. For design purposes, the elastic design spectra are reduced to the inelastic design spectra by a force reduction factor R_w; that is, the design base shear ratio C_w is:

$$C_w = \frac{C_{eu}}{R_w} \tag{2.1}$$

where C_{eu} is the minimum design base shear ratio if the structure were to remain in the elastic range (see Fig. 2.1). The force reduction facto R_w mainly accounts for structural energy dissipation (or ductility) capacity and structural overstrength. (3, 27, 33).

2.1.2. Serviceability Limit State for Moderate Earthquakes

UBC Drift Control — To satisfy the serviceability requirements, UBC combines its definition of "moderate" design earthquakes and its drift control in the follow requirement (36):

> "Calculated story drift [which corresponds to a design base shear ratio C_w] shall not exceed $0.04/R_w$ or 0.005 times the story height for structures having a fundamental period of less than 0.7 seconds. For structures having a fundamental period of 0.7 seconds or greater, the calculated story drift shall not exceed $0.03/R_w$ or 0.004 times the story height."

First, consider structures with fundamental periods of 0.7 seconds or greater. For buildings designed with $R_w \geq 7.5$, the story drift ratio is controlled by the $0.03/R_w$ limit*. Figure 2.2 shows the expected building response, where point A represents the UBC design. Define the elastic design base shear ratio for the moderate design earthquake as C_{es} (= C_{eu}/R_{ser}), and accept a story drift ratio of 0.5% as the limiting value to control nonstructural damage at this design earthquake level. Although in UBC the C_w level for the ultimate limit state and the C_{es} level for the serviceability limit state are not related at all from the viewpoint of the limit state concept, they do relate to each other by a simple relationship because both assume that the structural responses are in the elastic range. Using a linear relationship between points A and B in Fig. 2.2, the elastic design base shear ratio (C_{es}) implicitly assumed by UBC for the moderate design earthquake can be computed by the following relationship:

$$\frac{C_{es}}{C_w} = \frac{0.005}{\left(\frac{0.03}{R_w}\right)} \tag{2.2}$$

Solving the above equation for C_{es} gives the following:

$$C_{es} = \left(\frac{R_w}{6}\right) C_w = \left(\frac{R_w}{6}\right) \frac{C_{eu}}{R_w} = \frac{C_{eu}}{6} \tag{2.3}$$

That is, the intensity of the moderate design earthquake for the serviceability limit state is one-sixth that of the severe design earthquake for the ultimate limit state. Since the effective peak ground acceleration adopted in UBC in high seismic risk areas is 0.4 g, UBC assumes an effective peak acceleration of 0.07 g (= 0.4/6) for moderate design earthquakes.

For buildings with fundamental periods shorter than 0.7 seconds (or a height less than 65 ft. in the 1988 UBC), the drift limit specified by UBC is $0.04/R_w$. It can be shown by a similar derivation that the effective peak acceleration for such buildings is one-eighth that of 0.4 g, i.e., 0.05 g. In other words, in a particular seismic zone the moderate design earthquake adopted by UBC is not the same for all buildings; the intensity of the moderate design earthquake is lower for

* Because UBC does not use a two-phase design procedure by specifying a separate elastic design spectrum for the moderate design earthquake, it has been shown by Uang and Bertero (35) that the UBC story drift limit of 0.004 for buildings with a fundamental period greater than 0.7 seconds should not apply.

stiffer structures with fundamental periods less than 0.7 seconds. Note that in the 1981 Building Standard Law of Japan the intensity of the moderate design earthquake is always equal to one-fifth that of the severe design earthquake. It is difficult to justify why the intensity of the UBC moderate design earthquake should be dependent on the fundamental period (or height) of the structure†.

UBC Stress (or Member Force) Control — The effectiveness with which UBC controls member's maximum stresses (or yielding) can be evaluated by examining the allowable stresses at the force level of moderate design earthquakes. At the UBC prescribed seismic force level, the allowable stress for steel design (1) can be taken as (see point B in Fig. 2.2)

$$F_a^{(w)} = \left(\frac{4}{3}\right) \times 0.66\, F_y = 0.88\, F_y \tag{2.4}$$

that is, the allowable stress ($0.66 F_y$) for gravity load design can be increased by one-third under seismic loading, F_y being the nominal yield stress. Again using the linear relationship between points A and B in Fig. 2.2, the allowable stress implicitly assumed by UBC at the moderate design earthquake force level (i.e., C_{es} level in Fig. 2.2) is

$$\frac{C_{es}}{C_w} = \frac{F_a^{(es)}}{F_a^{(w)}} \tag{2.5}$$

that is, for buildings with a fundamental period greater than 0.7 seconds (or taller than 65 ft. in the 1988 UBC),

$$F_a^{(es)} = \left(\frac{C_{es}}{C_w}\right) F_a^{(w)} = \frac{\left(\dfrac{C_{eu}}{6}\right)}{\left(\dfrac{C_{eu}}{R_w}\right)} F_a^{(w)} = \left(\frac{R_w}{6}\right) F_a^{(w)} = \left(\frac{R_w}{6}\right) 0.88\, F_y \tag{2.6}$$

For ductile moment frames ($R_w = 12$), the UBC-implied allowable stress for the moderate design earthquake may be as high as $1.76 F_y$.

† It should be noted that the conservatism for long period structures has already been included in the UBC elastic design spectra for severe design earthquakes. Since the moderate design earthquake implied by UBC can be scaled directly from its severe design earthquake by a constant factor (= 6 for buildings with a fundamental period greater than 0.7 seconds), this conservatism has also been carried over to the UBC "moderate" design earthquake.

Equation 2.6 is based on the assumption that the stress produced by gravity loads can be ignored. In a more general case, the gravity load effect can be measured by a parameter G:

$$G = \frac{f^{(g)}}{F_a^{(g)}} \tag{2.7}$$

where $f^{(g)}$ is the stress produced by gravity loads, and $F_a^{(g)}$ ($= 0.66F_y$) is the allowable stress for gravity load design. Then the UBC-implied allowable stress at the force level of moderate design earthquakes is (35):

$$F_a^{(es)} = \left[\frac{2R_w}{9} + G\left(1 - \frac{R_w}{6}\right)\right]0.66F_y \tag{2.8}$$

Figure 2.3 shows the variations of the allowable stress. It is shown that the gravity load effect will help reducing the stress level of $F_a^{(es)}$; nevertheless this UBC-implied allowable stress will still exceed F_y, especially for ductile building systems. For reinforced concrete structures, similar derivations for the design strength which is implicitly assumed by UBC for the moderate design earthquake can be found in Ref. 34.

To summarize the results presented above, the intensity level of moderate design earthquakes implied by the UBC drift requirements is only one-sixth to one-eighth that of severe design earthquakes. It is also shown that the UBC design procedure cannot prevent structures from yielding during moderate earthquakes.

2.2. Case Studies

2.2.1. Building Descriptions

Motivated by the results of the simple analytical study presented in the previous section, four buildings located in the Bay Area have been selected for this study (see Table 1.1). The first three buildings, which are located in San Jose, are about 20 miles away from the epicenter of the Loma Prieta Earthquake (see Fig. 2.4). The fourth building is located in Hayward, about 45 miles away from the epicenter.

2.2.2. Method of Analysis

For each selected building, design drawings and recorded data were obtained from California Division of Mines and Geology (CDMG); recorded data include absolute accelerations, velocities, and displacements. The building design was then reviewed in accordance with UBC; both the latest edition and the edition used in the original design were considered. Dead loads were estimated from the design drawings and live loads as specified by UBC were used.

One important task of this study was to evaluate maximum story drifts and member forces that developed during the Loma Prieta Earthquake. Since CDMG usually instruments only a few floors in each building, the story drift, which is the difference of lateral displacements in two adjacent floors, cannot be computed directly. (It will be shown in Chapter 3 that assuming a constant story drift ratio between two instrumented floors, which are not adjacent to each other, may significantly underestimate the maximum story drift ratio.) Furthermore, no member force measurement was made by CDMG. To overcome the limitations of the recorded data, structural analyses had to be performed in order to obtain detailed structural responses. Since this study is only interested in peak responses, and considering the relatively low level of ground excitations experienced by these buildings, time-history dynamic correlation was not considered. Instead, the following "static" approach was used:

(1) Estimate dead loads from design drawings and estimate realistic live loads at the time the earthquake struck.

(2) Establish a three-dimensional finite element model for each building. Compute natural periods and mode shapes by using the computer program ETABS (18).

(3) Perform system identification to obtain natural periods from recorded response. The identified natural periods are then correlated with those predicted by ETABS.

(4) Compute lateral displacements at floors that were not instrumented by a modal superposition technique. To demonstrate this technique, consider a 2-dimensional frame which is instrumented at the roof and the fifth floor only (see Fig. 2.5). To "recover" the lateral displacements of all other floors at any instant of time, say at a selected peak response, the following relationship is used:

$$\sum_{i=1}^{2} C_i \{\phi_i\} = \{d\} \tag{2.9}$$

where $\{\phi_i\}$ = i-th mode shape;

$\{d\}$ = relative displacement vector;

C_i = i-th modal amplitude.

That is,

$$C_1 \begin{Bmatrix} \phi_{10,1} \\ \phi_{9,1} \\ \phi_{8,1} \\ \phi_{7,1} \\ \phi_{6,1} \\ \phi_{5,1} \\ \phi_{4,1} \\ \phi_{3,1} \\ \phi_{2,1} \\ \phi_{1,1} \end{Bmatrix} + C_2 \begin{Bmatrix} \phi_{10,2} \\ \phi_{9,2} \\ \phi_{8,2} \\ \phi_{7,2} \\ \phi_{6,2} \\ \phi_{5,2} \\ \phi_{4,2} \\ \phi_{3,2} \\ \phi_{2,2} \\ \phi_{1,2} \end{Bmatrix} = \begin{Bmatrix} d_{10} \\ d_9 \\ d_8 \\ d_7 \\ d_6 \\ d_5 \\ d_4 \\ d_3 \\ d_2 \\ d_1 \end{Bmatrix} \tag{2.10}$$

Extracting the equations that correspond to the two instrumented floors gives the following:

$$\begin{bmatrix} \phi_{10,1} & \phi_{10,2} \\ \phi_{5,1} & \phi_{5,2} \end{bmatrix} \begin{Bmatrix} C_1 \\ C_2 \end{Bmatrix} = \begin{Bmatrix} d_{10} \\ d_5 \end{Bmatrix} \tag{2.11}$$

from which the modal amplitudes C_1 and C_2 can be solved. The complete lateral displacement profile then can be established by substituting C_1 and C_2 into Eq. 2.10. When the structural response involves significant torsional response, a similar procedure which considers 3-dimensional mode shapes is adopted.

(5) Perform static structural analyses at some selected response peaks using the computer program ETABS. The structural analysis is performed by first loading the structure with dead and live loads, and then *imposing* the lateral displacements computed from the previous step at every floor level. Assuming that the floors are rigid in their own plane, two translational and one torsional displacements are imposed to each floor of the structure. Note that ETABS can only perform elastic structural analysis. In case where nonlinear characteristics of the response cannot be ignored, this is especially true for reinforced concrete shear wall

structures, an iterative procedure is used to adjust the element stiffness in the ETABS analyses.

(6) From the static analyses in the previous step, detailed structural responses which include story drifts and member forces are obtained.

Chapter 3
San Jose 13-story Government Office Building

3.1. Building Description

The 13-story Government Office Building (see Fig. 3.1) is located in the City of San Jose, California, at a distance of 21 miles from the epicenter of the Loma Prieta earthquake. The building, which is designated as CSMIP357, was designed in 1972 and constructed in 1975-76. This steel office building consists of 13 stories and a penthouse, all above grade. The building is generally regular in plan, except that two extra bays along the south and west sides of the building were provided to accommodate the elevators and stairs (see Fig. 3.2). Typical floor system of the building consists of 3.5-in. light-weight concrete slab on metal deck supported by a complete steel space frame. The lateral-force-resisting system of the structure consists of moment-resisting steel space frame. With a few exceptions, Grade 50 steel was used for the frame members. The building foundation is a 173 by 167 square ft., 4-ft. thick reinforced concrete mat founded on alluvial soil.

3.2. UBC Seismic Lateral Forces

3.2.1. Building Reactive Weight

It is assumed that the reactive weight of the building includes all the dead load of the bare structure, as well as an additional 15 pounds per square foot for partitions, ceiling, or anything else that might be tied down to the floors. The reactive weights for a typical floor and the roof are estimated to be 1,900 and 1,800 kips, respectively. The reactive weights of the mechanical floor (12th floor) and the penthouse are estimated to be 2,100 and 400 kips, respectively. The reactive weight of the building, W, was estimated to be 25,200 kips.

3.2.2. 1970 UBC Design Base Shear

According to the 1970 UBC, the minimum design base shear V was calculated by the following formula:

$$V = ZKCW \tag{3.1}$$

where Z (= 1.0) is the zone factor and K (= 1.0) is the building system coefficient. It is worth noting that the 1970 UBC did not include a soil factor. The factor C was calculated by the following formula:

$$C = \frac{0.05}{T^{1/3}} \tag{3.2}$$

The fundamental period, T, of the building in the above equation was calculated as

$$T = \frac{0.05h_n}{D^{1/2}} \quad \text{or} \quad 0.1N \tag{3.3}$$

where h_n is the building height in feet, D is the dimension of the building in feet in a direction parallel to the applied lateral seismic forces, and N is the number of stories. The period computed from Eq. (3.3) is equal to 0.77 or 1.30 seconds. Using a more realistic value of 1.30 seconds (to be shown later), the design base shear V is equal to 1,154 kips (the design base shear ratio is 4.6%). If the original design had chosen a ductile frame design ($K = 0.67$) and used a period equal to 0.77 seconds, the design base shear ratio would be 3.7%.

3.2.3. 1991 UBC Design Base Shear

According to the 1991 UBC, the minimum design base shear V is calculated by the following formula:

$$V = \frac{ZIC}{R_w}W \tag{3.4}$$

where Z (= 0.4) is the seismic zone factor. Because the building height exceeds the 160 ft. height limitation for ordinary moment-resisting space frames, this building has to be designed as a special moment-resisting space frame, i.e., R_w = 12. The factor C is calculated by the following formula:

$$C = \frac{1.25S}{T^{2/3}} \tag{3.5}$$

where the period T of the building in both directions is calculated as

$$T = 0.035(h_n)^{3/4} = 1.77 \text{ seconds} \tag{3.6}$$

The soil factor S is taken as 1.5, which corresponds to soil type S_3 (alluvial soil). Therefore the minimum design base shear V is equal 1,075 kips (the base shear ratio is equal to 4.3%).

One can notice that the 1991 and 1970 UBC design base shears for this building are nearly identical. This could lead to the expectation that the original member design will also satisfy the 1991 UBC.

3.3. Review of the 1991 UBC Seismic Design

3.3.1. Mathematical Model of the Building

Based on the design drawings of the building a three-dimensional elastic model was established. It was assumed that the floors are rigid in their own plane. Since no shear connectors between the girders and slabs were used in the original building design, composite action was not considered. The column bases were assumed to be fixed to the foundation. The columns and girders were framed together through welded connections. A 50% rigid end zones were used to model the panel zone flexibility of the rigid connections (31).

3.3.2. Story Drifts and Member Forces

An elastic structural analysis was carried out by using the ETABS computer program. The UBC lateral seismic forces together with the gravity loads were applied to the mathematical model of the structure. A 50 pounds per square foot live load and 5% accidental torsion were considered in the analysis. The live load reduction, as permitted by the UBC, was also considered.

Figure 3.3 shows the calculated story drift ratios. The results indicate that the maximum story drift ratio is 0.23%, which is very close to the 1991 UBC drift limit of 0.25% (= $0.03/R_w$).

Using the AISC allowable stress design procedure for steel structures (1), the member stress ratios were calculated. The stress ratio is defined as the ratio between the actual stress and the seismic allowable stress, which includes a one-third increase as is permitted by the code; the AISC interaction formulas were used for column design. Figure 3.4 shows the stress ratio of some critical members. These ratios, which should be less than one for the design to be acceptable, are much smaller than one (less than 0.5).

It is therefore concluded that this structure conforms with the 1991 UBC seismic design requirements for member strengths and story drifts. The design of this structure was governed by the story drift limitation.

3.4. Analysis of Recorded Response

3.4.1. Effective Peak Acceleration

Under the California Strong Motion Instrumentation Program (CSMIP) the building has been instrumented with 22 sensors at 5 different floors (see Fig. 3.5). Figure 3.6 shows the acceleration time history of each sensor. The peak ground acceleration at the base of the building was 0.09 g in the E-W direction and 0.10 g in the N-S direction. The recorded peak acceleration at the roof level was 0.34 g.

Using the ATC procedure (30), the effective peak accelerations (EPA) in the E-W and N-S directions were calculated from the elastic response spectra (see Fig. 3.7) of the base acceleration records. The EPA was found to be about 0.08 g, i.e., about one-fifth that of the 1991 UBC severe design earthquake (0.4 g). Note that the 1991 UBC response amplification for soil type S_3 and a period of 2.2 seconds (the measured fundamental period of the building, to be shown in the next section) is 1.1 (= 0.44/0.4). The elastic response spectra of the recorded base accelerations show that the response amplification in the vicinity of 2.2 seconds is very significant (0.22/0.08 = 2.8). This remarkable difference might suggest that the response of the structure itself is reflected in the recorded base motions, which are not free-field measurements.

3.4.2. Measured Natural Periods

In order to identify natural periods from the records, transfer functions between the base and roof accelerations were computed (see Fig. 3. 8). The acceleration at sensor i is denoted as A_i in the following discussion.

N-S direction — The transfer function was computed from the average horizontal acceleration of A_6 and A_7 at the roof and the base horizontal acceleration, which was computed from three available horizontal records at the base. The identified fundamental period was 2.23 seconds (or 0.45 Hz). A similar computation was conducted for the building records obtained from the 1984 Morgan Hill earthquake (11). The identified fundamental period was 2.06 seconds (or 0.48 Hz); a similar value was also reported by other researchers (17,21). Therefore the period in this direction has lengthened by 8%.

E-W direction — The transfer function was computed from the average horizontal acceleration of A_4 and A_5 at the roof and the average horizontal acceleration of A_{20} and A_{21} at the base. The identified fundamental period was 2.18 seconds (or 0.46 Hz). This value is almost the same as that (2.19 seconds) identified from the Morgan Hill earthquake (see Table 3.1).

Torsional direction — The transfer function was computed from (A_5 - A_4) at the roof and (A_{21} - A_{20}) at the base. The identified fundamental period was 1.69 seconds (or 0.59 Hz). This value is slightly larger than that (1.63 seconds) identified from the Morgan Hill earthquake.

3.4.3. Relative Displacement Response

The relative displacements at the center of mass of each instrumented floor (see Fig. 3.9) were calculated by subtracting the base displacement from the corresponding absolute displacement record. Figure 3.10 shows that the peak roof response (= 14.01 in.) in the E-W direction occurred at the 12.24 second mark from the beginning of the record, while the peak roof response (=13.49 in.) in the N-S direction occurred later at 18.42 seconds. The relative displacement records show the beating phenomenon. Similar behavior was observed previously by other researchers (15,17,21) during the 1984 Morgan Hill earthquake.

3.4.4. Rocking and Torsion Responses

The rocking motion of this building was examined from three vertical acceleration records at the base. The ratio between the rigid-body relative displacements due to rocking and the total relative displacements was less than 3%. Therefore no rocking will be considered later on in the structural analysis of the building.

The torsional vibration was examined to quantify the torsional component in the relative displacement records. The lateral displacement due to torsion in any instrumented floor was calculated by multiplying the torsional angle of the floor times the perpendicular distance from the center of the mass to the sensor. These "torsional" displacements were compared with the net relative displacements, i.e., the relative displacements without the torsional component, at two different sensor locations (see Fig. 3.11). The ratio between the torsional and the net relative displacements could be as high as 30%. Because of the significant torsional response, a three-dimensional mathematical model will be used later on to better represent the actual building response.

3.5. Building Response during the 1989 Loma Prieta Earthquake

3.5.1. Method of Analysis

A linear structural analysis using the ETABS computer program was carried out to calculate the member forces and story drifts at the peak response in the E-W direction. Gravity loads (dead loads and 50% of the live load) were first applied to the model, and then the three (two translational and one torsional) components of the relative displacements were imposed at the center of mass of each floor. The relative displacements of the floors that were not instrumented were estimated by the technique described below.

First, the dynamic characteristics (mode shapes and natural periods) of the model were calculated from ETABS. Table 3.2 shows the sequence of the mode shapes and the corresponding periods. The first two modes are mainly translational while the third mode is mainly torsional. This pattern repeats itself for the higher modes. The fundamental periods of the translational modes in the E-W and N-S directions are very close. The torsional period is about 80% of the corresponding translational periods.

The natural periods of the model were compared with those identified from the records (see Table 3.1). The periods of the model show a good agreement with those calculated from the records.

The relative displacements at the center of mass of the four instrumented floors were then calculated from the available records and the floor geometry. These displacements together with twelve mode shapes were used to calculate the lateral displacements at the center of mass of the floors that were not instrumented. The modal amplitudes C_i for the first twelve modes were solved from the lateral displacements of the four instrumented floors by the following equation:

$$\sum_{i=1}^{12} C_i \{\phi_i\} = \{d\} \tag{3.7}$$

where $\{\phi_i\}$ is the i-th mode shape and $\{d\}$ is the relative displacement vector in the direction under consideration. Figure 3.12 shows the relative displacement profile at the 12.24 second mark in the E-W direction; the contribution of each mode is also shown. The figure shows that the contribution of higher modes cannot be neglected in estimating lateral displacements of the floors that were not instrumented. These displacements were then used to calculate the story drift ratios.

3.5.2. Story Drift Ratios

Figure 3.13 shows that, at the 19.6 second mark of the Loma Prieta earthquake, the maximum story drift ratio at the center of mass in the N-S direction was 0.93%. This drift ratio is about 4.0 times that produced by the 1991 UBC seismic lateral loads and 1.9 times the serviceability level drift ratio (= 0.5%). Figure 3.13 also shows the "average" story drift ratios which were computed by assuming a straight lateral displacement profile between instrumented floors. A comparison of the average story drift ratios and the ratios obtained from the modal combination method shows that the average drift ratio may significantly underestimate the maximum story drift ratios. The recorded response at eight selected time marks was used to calculate the envelope of the story drift ratios. Figure 3.14 shows the envelope of the maximum story drift ratios at the center of mass in both the N-S and E-W directions. The figure also shows the envelope of the story drift ratios at the corner column locations. The maximum story drift ratio calculated at these locations occurred in the eleventh story and was as high as 0.97%.

3.5.3. Correlation between Story Drift Ratios and Observed Nonstructural Damage

Damage to nonstructural elements is usually related to both high (absolute) accelerations and large story drift ratios (9). Exterior facades and partitions are affected primarily by large drift ratios, while the high accelerations contribute mostly to equipment and content damage.

The calculated story drift ratios in Fig. 3.14 suggest that the most severe damage to nonstructural elements in the upper half of the building has occurred in the eleventh and twelfth stories. The high story drifts combined with the high floor accelerations (0.29 g and 0.26 g on the twelfth and eleventh floors, respectively) in these two floors indicate severe nonstructural damage. This conclusion is consistent with the observed damage to nonstructural elements after the earthquake (26).

The calculated story drift ratios also suggest that severe nonstructural damage should have occurred in the lower stories, especially in the second and third stories. Field observation show that, relative to upper stories, the damage is not that severe in these lower stories. One possible reason is that the maximum accelerations (0.13 g on the second floor) in the lower stories were relatively small.

3.5.4. Member Forces and Stress Ratios

The resulting member forces from structural analyses were used to calculate member stress ratios. The stress ratios indicate that the perimeter frame of this structure is more critical than the interior members. Figure 3.15 shows the stress ratios in some selected members of the structure. The results indicate that, if the structure were to remain elastic, stress ratios as high as 1.41 and 1.21 would have developed in the beams and columns, respectively. As the UBC allowable bending stress for earthquake loading is equal to $0.88F_y$, a beam stress ratio of 1.14 (= 1.0/0.88) means that a cross section has reached the first yielding. For a typical steel W-shape section, the plastic shape factor is about 1.14; this means that a beam stress ratio of 1.3 (= 1.14/0.88) indicates that the full plastic moment capacity has been reached. Therefore a number of beams, especially in the tenth and eleventh stories of the N-S frames, must have yielded during the earthquake. The results also show that the stresses produced by the 1989 Loma Prieta earthquake are more than three times the stresses produced by the 1991 UBC lateral loads.

3.6. Design Implications of the UBC Serviceability Requirements

UBC anchors the level of elastic design spectrum to an EPA, which is expressed as a Z factor. It has been shown in Chapter 2 that the UBC-implied EPA for the moderate design earthquake is about 0.07 g. By examining only the EPA, the level of the base motions of this building recorded during the Loma Prieta earthquake is comparable to the UBC "moderate" design earthquake. Nevertheless, examining the spectral shapes of the recorded motions and the UBC design spectrum in Fig. 3.7 indicates a significant difference in spectral ordinates in the period range of interest. Although it is well recognized that large variations in spectral shapes always exist from one earthquake record to the other (or to the design spectrum), for the purpose of correlating a particular building's response to code requirements, it may be worthwhile to scale the observed responses to account for the difference in spectral ordinates or shapes.

As demonstrated earlier, the EPA of the 1991 UBC "moderate" design earthquake is about 0.07 g. At this level of earthquake excitation, the elastic spectral acceleration for a structure with a period of 1.77 seconds — the period of this building according to the 1991 UBC formula (see Eq. 3.6) — and soil type S_3 is 0.085 (see Fig. 3.7). By examining the elastic response spectra of the base accelerations, it was found that the spectral acceleration corresponding to the fundamental period of the building (which was about 2.2 seconds during the Loma Prieta earthquake) was 0.22 g, i.e., 2.59 times the UBC value. Scaling the maximum story drift ratio (= 0.97%) developed during the earthquake by a factor of 2.59 and taking into account the fact that the design drift ratio was 92% of the UBC drift limit, then the maximum story drift ratio corresponding to an EPA of 0.07 g is equal to 0.41% (= 0.0097/2.59/0.92). This value is smaller than the widely accepted 0.5% drift limit for controlling nonstructural damage during moderate earthquakes.

If the maximum stress ratio (= 1.41) in the eleventh story beam was scaled by the same manner and considering that the original design stress ratio of the beam was as low as 0.40, the stress ratio would be equal to 1.36 (= 1.41/2.59/0.40). Should the UBC design stress ratios be close to 1.0, many more members would have yielded during the Loma Prieta earthquake.

3.7. Conclusions

Based on a review of the UBC design, a detailed study of the response of building CSMIP355 during the Loma Prieta earthquake, and a correlation of the calculated response with the observed damage, the following conclusions can be made.

(1) The EPA of the base accelerations recorded during the 1989 Loma Prieta earthquake is about the same as that of the UBC-implied moderate design earthquake.

(2) The CSMIP357 building satisfies the 1991 UBC. The design stress ratios are generally low and the design is governed by the story drift requirement.

(3) A comparison of natural periods computed from the records of the 1984 Morgan Hill earthquake and the 1989 Loma Prieta earthquake indicates that the natural periods have lengthened. The identified natural periods also correlate well with those predicted from a 3-D mathematical model.

(4) Higher modes cannot be ignored in computing lateral displacements of the floors that were not instrumented. Furthermore, assuming a constant story drift ratio between two instrumented floors that are not adjacent to each other may significantly underestimate actual story drift ratios.

(5) During the Loma Prieta earthquake the story drift ratio is as high as 0.97%, which is about twice the 0.5% drift limit commonly used to control nonstructural damage for moderate earthquakes. Based on the elastic structural analyses, stress ratios as high as 1.4 may have been developed if the structure were to respond elastically during the earthquake.

(6) The damage to nonstructural elements predicted by story drift ratios and floor accelerations correlates well with the observed damage in the eleventh and twelfth stories. Although the computed maximum story drift ratio occurs in the second story, low accelerations at the bottom floors help to reduce nonstructural damage.

(7) Although the EPA of the base accelerations recorded during the 1989 Loma Prieta earthquake is about the same as that of the UBC-implied moderate earthquake, unusual high

response amplification exists in the elastic response spectra of the base acceleration records. If the response of the structure is scaled so that the spectral ordinates match the UBC elastic design base shear ratio for the moderate design earthquake and the original design stress ratios of the beams were close to one, stress ratios as high as 1.36 could have been developed.

(8) The CSMIP357 building demonstrates that the 1991 UBC seismic design requirements cannot insure desired serviceability performance during moderate earthquakes.

Chapter 4
Hayward 6-story Office Building

4.1. Building Description

The Hayward six-story office building (see Fig. 4.1) is located in the City of Hayward, California, at a distance of about 45 miles from the epicenter of the Loma Prieta earthquake. The building, which is designated as CSMIP462, was designed in 1966 and constructed in 1967. This reinforced concrete office building consists of 6 stories above grade and a basement. The gravity-load-carrying system consists of concrete waffle floors with 4-in. light-weight concrete slabs and 10-in. deep two-way joists. The gravity load is transferred to the foundation by reinforced concrete columns. The lateral-force-resisting system of the structure consists of normal-weight concrete shear walls. The structure is not symmetric in plan (see Fig. 4.2), as the concrete shear walls are shifted toward south end of the building. The column foundations consists of spread footings, and shear walls are founded on combined footings. The building materials are 3,750 and 5,000 psi normal-weight concrete for the walls and columns, respectively, and Grade 40 reinforcements are used. The soil at the building site is alluvium.

4.2. UBC Seismic Lateral Loads

4.2.1. Building Reactive Weight

It is assumed that the reactive weight of the building includes all the dead load of the bare structure, as well as an additional 15 pounds per square foot for partitions, ceiling, or anything else that might be tied down to the floors. The reactive weights for a typical floor and the roof are estimated to be 2,550 and 2,000 kips, respectively. The reactive weight of the building, W, was estimated to be 14,750 kips.

4.2.2. 1964 UBC Design Base Shear

According to the 1964 UBC, the minimum design base shear V was calculated by the following formula:

$$V = ZKCW \tag{4.1}$$

where Z (= 1.0) is the zone factor and K (= 1.0) is the building system coefficient. The factor C was calculated by the following formula:

$$C = \frac{0.05}{T^{1/3}} \tag{4.2}$$

The fundamental period T of the building was calculated as

$$T = \frac{0.05 h_n}{D^{1/2}} \tag{4.3}$$

The periods computed from Eq. (4.3) are equal to 0.38 and 0.24 seconds in the E-W and N-S directions, respectively. The design base shears are equal to 870 and 1,010 kips in the E-W and N-S directions, respectively. The design base shear ratios in the E-W and N-S directions are 6.9% and 8.0%, respectively.

4.2.3. 1991 UBC Design Base Shear

According to the 1991 UBC, the minimum design base shear V is calculated by the following formula:

$$V = \frac{ZIC}{R_w} W \tag{4.4}$$

where Z (= 0.4) is the zone factor. The building could be classified as a building frame system (R_w = 8). The factor C was calculated by the following formula:

$$C = \frac{1.25S}{T^{2/3}} \quad \leq 2.75 \tag{4.5}$$

where S (= 1.5 for alluvial soil) is the soil factor and the period T of the building was calculated as

$$T = 0.02(h_n)^{3/4} \tag{4.6}$$

The period computed from Eq. (4.6) is equal to 0.50 seconds in both directions. The design base shear V in both directions is equal to 2,028 kips in both directions. The corresponding design base shear ratio is 13.8%.

The ratios between the prescribed design base shears of the 1991 and 1964 UBC are 200% and 173% in the E-W and N-S directions, respectively. This remarkable difference, which is attributed mainly to the absence of the soil factor S in the 1964 UBC, leads to the expectation that the design strengths of the building shear walls might not satisfy the 1991 UBC, unless the building was conservatively designed.

4.3. Review of the 1991 UBC Seismic Design

4.3.1. Mathematical Model of the Building

Based on the design drawings of the building a three-dimensional elastic model was established. It was assumed that the floors are rigid in their own plane. The shear walls were assumed to be fixed at the base. The mathematical model included walls extending along the whole height of the building (see Fig. 4.3).

4.3.2. Story Drifts and Member Forces

A static structural analysis was carried out by using the ETABS computer program. The factored 1991 UBC lateral seismic forces together with the gravity loads were applied to the mathematical model of the structure. Because of the torsional irregularity of the building, the UBC accidental torsion amplification factor, A_x, was calculated as follows:

$$A_x = \left[\frac{\delta_{\max}}{1.2\delta_{avg}} \right]^2 \tag{4.7}$$

where $\delta_{\max}$ is the maximum displacement at level x, and δ_{avg} is the average of the displacements at the extreme points of the structure at level x. The torsional amplification factor was found to be equal to 2. Therefore, a 10% (= $2 \times 5\%$) accidental torsion was considered in the structural analysis.

Figure 4.4 shows the calculated story drift ratios at the center of mass and one end of the building; the effect of mass eccentricity is very significant. The results indicate that the maximum story drift ratio is 0.45% in the E-W direction. According to the 1991 UBC, the allowable story drift ratio for this frame is equal to 0.5% for T less than 0.7 seconds. Thus, the maximum drift ratio obtained from the analysis was 90% of the UBC drift limit.

Using the ACI design procedure (4), the wall capacity ratios were calculated; the wall capacity ratio is defined as the ratio $\frac{OA}{OB}$ as shown in a typical interaction diagram of a reinforced concrete shear wall (see Fig. 4.5). The wall capacity ratio, which gives an indication of the force demand of the wall with respect to its capacity, should not be greater than one for the design to be adequate. Figure 4.6 shows the wall capacity ratios of selected walls. Notice that the maximum ratio is 3.0. Therefore it is concluded that this structure does not conform with the 1991 UBC seismic design requirement for member strengths.

4.4. Analysis of Recorded Response

4.4.1. Effective Peak Acceleration

Under the California Strong Motion Instrumentation Program (CSMIP) the building has been instrumented with 13 sensors at 4 different floors (see Fig. 4.2). Figure 4.7 shows the acceleration time history of each sensor. The peak ground acceleration (PGA) recorded at the base of the building was 0.12 g in the E-W direction and 0.09 g in the N-S direction. The recorded peak acceleration at the roof level was 0.45 g (in the E-W direction).

The effective peak accelerations (EPA) in the E-W and N-S directions were calculated from the elastic response spectra of the base acceleration records (see Fig. 4.8). The EPAs were found to be about 0.09 g and 0.08 g in the E-W and N-S directions, respectively. That is, the intensity of the base motion is about one-fifth that of the 1991 UBC severe design earthquake (0.4 g).

4.4.2. Measured Natural Periods

In order to identify natural periods from the records, transfer functions between the base and roof accelerations were computed (see Fig. 4.9).

E-W direction — The transfer function was computed from the average horizontal acceleration (A_2 + A_3) at the roof and the average horizontal acceleration (A_7 + A_9) at the base. The identified fundamental period is 0.95 seconds (or 1.05 Hz). The identified mode shape at the roof level in Fig. 4.10 shows that this is a translational-torsional coupling mode.

N-S direction — The transfer function was computed from the horizontal acceleration (A_{10}) at the roof and the base horizontal acceleration (A_{13}). The identified natural period, which is the second mode of the structure, is 0.85 seconds (or 1.18 Hz). Figure 4.10 shows the identified mode shape at the roof level. The motion in the N-S direction is primarily translational.

Torsional direction — The transfer function was computed from the torsional acceleration (A_2 - A_3) and the average horizontal acceleration (A_7 + A_9) at the base. The identified natural period, which is the third mode of the structure, is 0.68 seconds (or 1.47 Hz). The identified mode shape at the roof level in Fig. 4.10 also indicates that this is a translational-torsional coupling mode.

Strictly speaking, both the first and third modes are strongly coupled in the E-W and torsional directions; none of them can be classified as a predominant E-W mode.

4.4.3. Relative Displacement Response

Relative displacements were calculated by subtracting base displacements from the corresponding absolute displacement record (see Fig. 4.11). Two peak responses can be identified from the relative displacement time histories. These peak displacement responses occurred at the 12.08 and 15.04 second time marks. Figure 4.12 shows the roof relative displacement response at these time marks (cases 1 and 3). Another peak response, which occurred at 13.96 seconds, corresponds to the peak torsional response.

4.4.4. Torsion

The plan of this building shows a significant mass eccentricity which should result in torsional vibration. The torsional vibration was examined to quantify the torsional component in the relative displacement records. The displacements due to torsion were calculated by multiplying the torsional angle of the floor where a particular set of sensors is located times the perpendicular distance from the center of the mass to the sensor. These "torsional" displacements were compared with the net relative displacements, i.e., the relative displacements without the torsional component, at two different sensor locations (see Fig. 4.13). The ratio between the torsional and the net relative displacements was as high as 1.1. The peak torsional angle occurred at the 13.96 second mark of the earthquake (see case 2 in Fig. 4.12). In fact, the relative displacement at the south end of the building at this time mark was 1.34 inches, which is larger than the relative displacements at the center of mass at the E-W peak response. Because of the significant torsional response, a three-dimensional mathematical model is necessary to study the actual building response.

4.5. Building Response during the 1989 Loma Prieta Earthquake

4.5.1. Method of Analysis

A linear structural analysis by the ETABS computer program was carried out to calculate the member forces at three selected peak responses by imposing three components (two translational and one torsional) of the relative displacements at the center of mass of each floor.

The building was instrumented at the roof, fourth, and first floors. Since a perimeter wall exists at the basement level, the measured relative displacement at the first floor is small. In order to maintain numerical accuracy and to limit the number of modes to six in the mode superposition procedure, six measured displacements at the roof and fourth floor were used to estimate the relative displacements of the floors that were not instrumented. Table 4.1 shows that the natural periods computed from the 3-dimensional model are consistent with the measured ones. Figure 4.10 shows the first three mode shapes at the roof level.

Figure 4.14 shows the relative displacement profile at the 12.08 second mark in the N-S direction; the contribution of each mode is also shown. The figure shows that the response of the structure in the N-S direction is dominated by the second mode. The measured relative displacements at the first floor level were larger than the calculated ones. The difference between the measured and calculated displacements at the first floor level is an indication of the stiffness loss that might have occurred in the first two story walls of the building. However, the measured rather than calculated relative displacement in the first floor were used in the structural analysis.

4.5.2. Story Drift Ratios

Considering all three cases of peak responses, Fig. 4.15 shows that the maximum story drift ratio in the E-W direction was 0.41%, which corresponds to the case of maximum torsional angle. The maximum story drift ratio in the N-S direction was 0.18%. Since both story drift ratios are less than 0.5%, it is expected that little damage in nonstructural components would have occurred during the Loma Prieta earthquake.

4.5.3. Member Forces and Wall Capacity Ratios

The resulting member forces obtained from static analyses were used to calculate the wall capacity ratios. Figure 4.16 shows the wall capacity ratios in some selected walls. The results indicate that if the structure were to remain elastic, a wall capacity ratio as high as 3.4 would have occurred. Therefore a number walls, especially in the lower two stories, must have yielded during the earthquake. This conclusion is consistent with the observations of period elongation after the earthquake ground shaking (see Fig. 4.11). Furthermore, the observation that the measured relative displacements at the first floor level are larger than those computed from the modal superposition method also supports the conclusion that the walls in the first two stories must have suffered some yielding. The results also show that the internal forces produced by the 1989 Loma Prieta earthquake are 1.1 times (= 3.4/3.0) those produced by the 1991 UBC design seismic forces.

4.6. Conclusions

Based on a review of the UBC design and a detailed study of the response of building CSMIP462, the following conclusions can be made.

(1) The EPA of the base accelerations recorded during the 1989 Loma Prieta earthquake is about the same as that of the moderate design earthquake.

(2) As a result of the large eccentricity between centers of mass and rigidity, the response of this building is primarily torsional.

(3) The design base shear of the 1991 UBC is twice that of the 1964 UBC. As a result of mass eccentricity, the 5% accidental eccentricity has to be doubled. Although the story drift ratios satisfy the UBC drift limit, the wall capacity ratios are as high as 3.0.

(4) The identified natural periods in the first three modes are consistent with those predicted analytically. The measured periods are longer than those predicted analytically; this observation is consistent with the conclusion that some walls must have yielded during the Loma Prieta earthquake.

(5) While no severe nonstructural damage due to excessive drift ratios is observed from the analysis, wall yielding must have occurred during the Loma Prieta earthquake. The wall capacity ratio is as high as 3.4.

Chapter 5
San Jose 10-story Residential Building

5.1. Building Description

The 10-story Residential Building (see Fig. 5.1) is located in the City of San Jose, California, at a distance of 20 miles from the epicenter of the Loma Prieta earthquake. The building was designed in 1971 and constructed in 1971-72. This building, which is designated as CSMIP356, is a 10-story residential building with a rectangular plan (see Fig. 5.2). A typical floor system of the building consists of one-way post-tensioned concrete slabs spanning load-bearing concrete shear walls. The lateral-force-resisting system of the structure consists of reinforced concrete shear walls at regular intervals in the transverse (E-W) direction and reinforced concrete shear walls along the interior corridors in the longitudinal (N-S) direction. The longitudinal corridor walls are stepped at the sixth floor. The foundations of the structure consists of precast-prestressed concrete piles located under all bearing walls. The building is founded on alluvial soil with a base dimensions of 210 by 64 square ft. The materials used for the construction of the building are: 3,000 psi normal-weight concrete for the walls, 4,000 psi light-weight concrete for the slabs, Grade 60 steel reinforcement for bars larger than No. 5, and Grade 40 steel otherwise.

5.2. UBC Seismic Lateral Forces

5.2.1. Building Reactive Weight

The reactive weight of the building includes all the dead load of the slabs, walls, as well as additional 10 pounds per square foot for partitions, ceiling, or anything else that might be tied down to the floors. The reactive weights for typical floors and the roof are 2,183 and 1,720 kips, respectively. The total reactive weight, W, was estimated to be 21,370 kips.

5.2.2. 1967 UBC Design Base Shear

According to the 1967 UBC, the minimum design base shear V was calculated by the following formula:

$$V = ZKCW \tag{5.1}$$

where Z (= 1.0) is the zone factor and K (= 1.0) is the building system coefficient. The factor C was calculated by the following formula:

$$C = \frac{0.05}{T^{1/3}} \tag{5.2}$$

The period T of the building was calculated as

$$T = \frac{0.05h_n}{D^{1/2}} \tag{5.3}$$

The periods computed from Eq. (5.3) are equal to 0.60 and 0.33 seconds in the E-W and N-S directions, respectively. The design base shears are equal to 1,270 and 1,540 kips in the E-W and N-S directions, respectively. The design base shear ratios in the E-W and N-S directions are 5.9% and 7.2%, respectively.

5.2.3. 1991 UBC Design Base Shear

According to the 1991 UBC, the minimum design base shear V is calculated by the following formula:

$$V = \frac{ZIC}{R_w} W \tag{5.4}$$

where Z (= 0.4) is the zone factor. The building could be classified as a building frame system in the N-S direction (R_w = 8) and a bearing wall system in the E-W direction (R_w = 6). According to the 1991 UBC, in seismic zones 3 and 4 where a structure has a bearing wall system in only one direction the value of R_w used for design in the orthogonal direction shall not be greater than that used for the bearing wall system. Therefore the value of R_w in the N-S direction should be taken as 6. The factor C was calculated by the following formula:

$$C = \frac{1.25S}{T^{2/3}} \leq 2.75 \tag{5.5}$$

where S (= 1.5 for alluvial soil) is the soil factor, and the period T of the building was calculated as

$$T = 0.02(h_n)^{3/4} = 0.61 \text{ seconds} \tag{5.6}$$

If the 1991 UBC formula (34-4) was used, the period in the E-W and N-S directions would be 0.33 and 0.52 seconds, respectively.

Using a value of T equal to 0.61 seconds gives a design base shear equal to 3,710 kips in both directions. The corresponding design base shear ratio is 17.3%. If the period in the N-S direction was taken as 0.67 seconds (the fundamental period from the mathematical model of the building, as will be shown later), the base shear ratio would be 16.3%.

The ratios between the design base shears of the 1991 and 1967 UBC are 290% and 230% in the E-W and N-S directions, respectively. This remarkable difference, which in large part is attributed to the absence of the soil factor S in the 1967 UBC, leads to the expectation that the design strengths of the building walls will not satisfy the 1991 UBC, unless the building was conservatively designed.

5.3. Review of the 1991 UBC Seismic Design

5.3.1. Mathematical Model of the Building

Based on the design drawings of the building, a three-dimensional elastic model was established. The model included sixteen walls in the E-W direction and four walls in the N-S direction (see Fig. 5.3). It was assumed that the walls are fixed at the base and that the floor slabs are rigid in their own plane. The openings in the walls (not shown in figure) were considered in the calculation of the stiffness and strength of the walls.

5.3.2. Materials Characteristics and Wall Strengths

Concrete — The walls of the building were constructed using 3,000 psi normal-weight concrete. Figure 5.4a shows the model used to represent the concrete stress-strain relationship.

The concrete compressive strength, f'_c, at the time the earthquake struck may exceed the specified value of 3,000 psi for a number of reasons. The high strain rate of the earthquake loading can increase f'_c by 17% (22). The margin of safety assumed in the concrete mix design and the aging of the concrete will also increase the compressive strength. In this study an upper bound f'_c is assumed to be 4,000 psi.

The modulus of elasticity, E_c, obtained from the ACI 318-89 (4) formula (8.5.1) was found to be 3,300 ksi. To establish an upper bound estimate of the modulus of elasticity, the high strain rate of the earthquake loading should also be taken into account. This high strain rate alone can increase E_c by more than 17%. In this study, an upper bound value of E_c will be taken as 3,800 ksi.

The modulus of rupture, f_r, calculated from the ACI 318-89 formula (9-9) was found to be 411 psi. Based on $f'_c = 3,000$ psi and using Kent's formula (14), an upper bound estimate is

$$f_r = \frac{1400 f'_c}{4000 + f'_c} = 600 \text{ psi} \tag{5.7}$$

Reinforcing steel — The steel model used (see Fig. 5.4b) has a specified yield stress of 40 ksi. Considering the margin of safety in the specified value and the high strain rate of the earthquake loading, an upper bound estimate of 50 ksi was assumed. A bilinear steel model with no strain hardening was used; strain hardening was judged to be insignificant at the level of this moderate earthquake excitation.

Flexural strength of walls

Based on the concrete and steel models just presented, the flexural strength of the walls was calculated assuming that a plane section remains plane after bending. Both the nominal and upper bound values of the models were considered. Strengths based on nominal values were used for the UBC design review, and realistic strengths based on upper bound values were used to evaluate the structure's performance during the Loma Prieta earthquake. The axial gravity loads on the walls were calculated from the tributary areas. The moment-curvature relationships, cracking moments, and nominal moments were obtained by using the computer program UNCOLA (12). Figure 5.5 shows typical moment-curvature relationships of two wall sections.

Since all the wall cross sections are lightly reinforced, the moment-curvature diagrams in Fig. 5.5 indicated that the walls are relatively ductile.

Shear strength of walls

The nominal shear strength V_n of the wall sections was estimated using the ACI 318-89 formula (21-6):

$$V_n = A_{cv}(2\sqrt{f_c'} + \rho f_y) \tag{5.8}$$

where A_{cv} is the area of the wall cross section in the direction of the shearing force, and ρ is the ratio of the shear reinforcement.

5.3.3. Story Drifts and Member Forces

The factored 1991 UBC lateral seismic forces together with the factored gravity loads were applied to the mathematical model of the structure. A live load of 40 pounds per square foot, as recommended by UBC for the design of residential buildings, was applied to floors in the analysis. An elastic structural analysis was carried out by the ETABS computer program.

In the N-S direction, the calculated lateral displacements and story drift ratios produced by the UBC design forces are shown in Fig. 5.6. The limit of the story drift ratio specified by UBC is 0.5%. The maximum drift ratio obtained from the analysis was 42% of the UBC drift limit.

Figure 5.7a compares the shear capacity of the walls as computed from Eq. 5.8 and the design story shears of the 1991 and 1967 UBC in the N-S direction. The figure shows that the shear strength of the walls is smaller than the UBC design forces in a number of stories. The base shear corresponding to shear failure of the building (in the seventh story) was estimated to be $0.14W$. Figure 5.7b compares the UBC overturning moments and the flexural capacity of the walls. The base shear corresponding to the flexural failure at the second story (the critical story) was estimated to be $0.12W$. By comparing the base shears corresponding to the shear and flexural modes of failure, it is evident that the building will yield in flexure, which is desirable for earthquake resistant design. Figure 5.7 also shows that the flexural capacities of four of the ten stories were less than the 1991 UBC factored moments. The overturning moments produced by the 1991 UBC seismic forces exceeded the wall flexural capacity by about 40% in the second story. It was concluded that this structure does not conform with the strength requirements of the 1991 UBC.

5.4. Analysis of Recorded Response

5.4.1. Effective Peak Acceleration

CSMIP has instrumented this building at three level with 13 sensors (see Fig. 5.2). Figure 5.8 shows the acceleration time history of each sensor. The peak ground accelerations recorded at the base of the structure were 0.12 g and 0.09 g in the E-W and N-S directions, respectively. The recorded peak accelerations at the roof level was 0.23 g and 0.36 g in the E-W and N-S directions, respectively.

The effective peak accelerations (EPA) were calculated from the elastic response spectra of the base acceleration records (see Fig. 5.9). The EPA was found to be about 0.08 g in both directions, i.e., one-fifth that of the 1991 UBC severe design earthquake (0.4 g).

5.4.2. Measured Natural Periods

In order to identify natural periods from the records, transfer functions between the base and roof accelerations were computed (see Fig. 5.10).

N-S direction — The transfer function was computed from the horizontal acceleration (A_7) at the roof and the base horizontal acceleration (A_{13}). The identified fundamental period varied from 0.68 seconds (1.47 Hz) to 0.78 seconds (1.28 Hz). The measured period identified from the records of the 1984 Morgan Hill earthquake varied from 0.58 to 0.64 seconds (21).

E-W direction — The transfer function was computed from the average horizontal acceleration (A_4 + A_6) at the roof and the average horizontal acceleration (A_{11} + A_{12}) at the base. The identified fundamental period was about 0.42 seconds (or 2.38 Hz). This value is almost the same as that identified from the Morgan Hill earthquake (see Table 5.1).

Torsional direction — The transfer function was computed from (A_6 - A_4) and (A_{11} + A_{12}). The identified fundamental period was 0.36-0.38 seconds (or about 2.7 Hz). This value is also very close to that identified from the Morgan Hill earthquake.

5.4.3. Relative Displacement Response

E-W direction

Relative displacement was computed by subtracting base displacement record from absolute displacement record. For example, the roof relative displacement at sensor 6, d_6, was computed as follows:

$$d_6 = D_6 - D_{12} \tag{5.9}$$

where D_6 and D_{12} are the absolute displacement records of sensors 6 and 12, respectively. Examining the relative displacement time history d_6 in Fig. 5.11a shows a low frequency noise component. After comparing the short period of the structure (= 0.44 seconds) with the long period noise observed in the relative displacement records, it was found reasonable to truncate numerically this noise up to 0.6 Hz (see Fig. 5.11b). One can notice the significant effect of this filtering by comparing the peak values in these two figures.

Rocking motion

The arrangement of the sensor locations in the E-W direction was adequate to evaluate the rocking motion of the building. Assuming that the foundation under the south end walls in the E-W direction is rigid, then the rocking acceleration $\ddot{\alpha}$ of the south end walls can be calculated from the following equation:

$$\ddot{\alpha} = \frac{A_3 - A_1}{L_{1-3}} \tag{5.10}$$

where L_{1-3} is the distance between sensors 1 and 3. Rocking motion introduces a rigid-body displacement component that should be subtracted from the relative displacements on the sixth floor and the roof to obtain the "net" relative displacements. The horizontal acceleration due to rocking, $\ddot{r}$, at the sixth floor is calculated as

$$\ddot{r} = \ddot{\alpha}\, h_6 \tag{5.11}$$

where h_6 is the elevation of the sixth floor above the base.

A very high degree of correlation was observed between the relative acceleration (including the effect of rocking) and the rocking component, as shown in Fig. 5.12. The correlation coefficient was found to be 97% (see Fig. 5.13).

The net relative displacements at the sensor locations were then calculated by subtracting the horizontal displacement due to rocking from the relative displacement records. The resulting displacements (see Fig. 5.14) represent the deformations due to the flexibility of the walls. These displacements will be imposed on the mathematical model of the building to obtain wall internal forces and story drifts.

In fact, the rigid-body component of the displacements due to rocking accounted for about 49% to 57% of the (total) relative displacements. It is interesting to note that this value is similar to that reported by Bard (2) from a study of the response recorded during the Morgan Hill earthquake.

N-S direction

The building was equipped with three sensors to measure the response in this direction. The base motion was recorded by sensor 13 which is located at the south end of the building. Following the technique which was used in the E-W direction, the records of the other two sensors were used to compute the relative response at the sixth floor and the roof. Since the arrangement of the sensor locations in the N-S direction was not adequate to evaluate the rocking motion of the building, no rigid-body rocking component was removed from the relative displacement records. Because of the large dimension in the N-S direction, it is believed that the rocking component in this direction is less significant than that in the E-W direction.

Torsional direction

The contribution of torsion to the translational displacement at any sensor location was computed by multiplying the torsional angle of the instrumented floor times the perpendicular distance between the center of mass and the sensor location. It was found that the torsional vibration of this building is not that significant, as one can expect from the regular plan of the structure. It should be noted that by imposing the translational components in two perpendicular directions on the structural model, the torsional effect will be included automatically in the resulting response.

5.5. Building Response during the 1989 Loma Prieta Earthquake

Three types of structural analyses (linear elastic analysis, response spectrum analysis, and nonlinear static analysis) were performed to calculate member forces and story drifts produced by the Loma Prieta earthquake. A three-dimensional model of the building was used in these analyses.

5.5.1. Elastic Analysis

Because of the low level of excitation during the Loma Prieta earthquake, it was decided to start with an elastic analysis. The building was instrumented at the roof and sixth floor. Using the modal combination technique described in Chapter 2, two mode shapes were used in each direction to estimate the relative displacements of the floors that were not instrumented. For example, Fig. 5.15 shows the relative displacement profile at peak response, which occurred at the 15.08 second time mark, to be imposed on the mathematical model in the N-S direction; the contribution of each mode is also shown.

In the E-W direction, the fundamental period calculated from the mathematical model was 0.44 seconds, which is practically the same as that obtained from the record. In the N-S direction, the fundamental period computed from the mathematical model was 0.67 seconds, which is about 14% less than that identified from the record. In fact, the larger measured period in the N-S direction indicates that some cracking must have occurred.

Member forces were computed by first applying the gravity loads and then imposing the relative displacements at every floor of the 3-D mathematical model. The response in the E-W direction was found to be elastic, as the resulting member forces were significantly smaller than the member strength (see Fig. 5.16a). In the N-S direction, the moments obtained from the structural analysis exceeded the cracking moments and even the overturning moment capacity (see Fig. 5.16b). In the second story, the ratio between the elastic overturning moment and the summation of the nominal moments was 1.3. Therefore it was concluded that the walls in the bottom stories must have cracked or yielded.

5.5.2. Response Spectrum Analysis

To confirm the previous results, a dynamic response spectrum analysis was performed. The computer program ETABS was used for this purpose. In this analysis a 5% damping ratio, which was identified by Papageorgiou and Lin (21), was used. Elastic response spectra (5% damping ratio) of the recorded base accelerations were used as the input motion. Three modes of vibration in each direction were considered in the analysis and the results were combined by the CQC technique (37).

The results obtained from the response spectrum analysis are also shown in Fig. 5.16b. It is observed that the overturning moment predicted by the response spectrum method is less than that predicted by the static analysis in the bottom five stories and vise versa for the upper stories. It is believed that the discrepancy is due to the following reasons. First of all, the input response spectrum was not based on free field motions. Second, the structure's rocking motion was not modeled in the response spectrum analysis. Third, the relative displacement profile used in the static analysis was constructed on the basis of elastic theory, although in reality nonlinear behavior must have developed.

5.5.3. Nonlinear Analysis

Since the results of linear analyses indicated that the moments produced by the earthquake excitation in the N-S direction were much larger than the cracking moments in the lower stories, the cracked stiffness of the walls rather than the elastic stiffness should be used to calculate the actual member forces. Because the stiffness of a reinforced concrete member depends on the level of member forces, an iterative technique was used to estimate the cracked stiffness, and hence the realistic member forces, of the walls in the N-S direction.

As the ratio between the elastic moment and the cracking moment was the greatest at the second story walls, it was concluded that this story should have cracked first. To estimate the cracked stiffness of this story, different values were used in the mathematical model. Similar to the procedure used in the elastic analysis, for each trial value of the cracked stiffness the mode shapes were first computed and then a modal combination procedure was used to establish the lateral displacement profile. Together with gravity loads, the lateral displacements were then imposed on the model. The resulting moments of the cracked sections were then used to calculate the corresponding curvatures of the walls. For each trial cracked stiffness, a point which corresponded to the moment and curvature from the structural analysis were plotted on the actual moment-curvature diagram of the walls (see Fig. 5.17). The intersection of the two curves represents the cracked stiffness which satisfies the characteristics of the cross section and the behavior of the whole structure.

Results determined from an iterative procedure by changing the stiffness of the walls in the lower stories have shown that the second, third, and fourth story walls were cracked. The calculated fundamental period of this cracked model, which represent the maximum "instantaneous" period during the earthquake, was about 0.85 seconds.

Story drift ratios

Figure 5.18 shows the calculated story drift ratios in the E-W and N-S directions. The figure shows that the maximum story drift ratios were only 0.03% and 0.19% in the E-W and N-S directions, respectively. These ratios are significantly smaller than the ratio of 0.5%, commonly used to limit nonstructural damage during moderate earthquakes.

Member forces

Figure 5.19 shows that the bending moment along Axis 1*A* (see Fig. 5.3a) exceeded the wall cracking moment in the second, third, and fourth stories, while the remaining parts of the structure remained uncracked. Figure 5.20a shows that the story shears are smaller than the shear capacity of the walls.

To confirm this solution, a response spectrum analysis was also carried out. The ratio between the resulting base shear from the response spectrum analysis and that obtained from the nonlinear static analysis is 0.92 (= 3,481/3,770).

Stresses in the critical cross section

The interaction diagram of wall section 19 (see Fig. 5.3a), which is a critical section, is shown in Fig. 5.21. The moment-axial force combination at the peak response indicated that the capacity was not exceeded.

5.6. Conclusions

Based on a review of the UBC design and a detailed study of the response of building CSMIP356 during the Loma Prieta earthquake, the following conclusions can be made.

(1) The EPA of the base acceleration recorded during the 1989 Loma Prieta earthquake is about the same as that of the UBC-implied moderate design earthquake.

(2) The CSMIP356 building satisfies the 1991 UBC strength requirements in the E-W direction, while the wall flexural capacities in the N-S direction are significantly less than the UBC required flexural capacities.

(3) A comparison of natural periods obtained from the records in the 1984 Morgan Hill and 1989 Loma Prieta earthquakes indicates that the fundamental period in the N-S direction has elongated by 16%. The fundamental period in the E-W direction remains the same. It implies that structural damage must have occurred in the N-S direction, but not in the E-W direction.

(4) Because of the large lateral stiffness of this shear wall building, the story drift ratio produced by the Loma Prieta earthquake is much smaller than the ratio (=0.5%) recommended for moderate design earthquakes.

(5) If the walls were to remain elastic during the Loma Prieta earthquake, the elastic overturning moments at the second floor would have been 1.3 times the wall flexural strength.

(6) Since shear walls are cracked in the N-S direction, nonlinear behavior has to be considered in estimating realistic internal forces. The results of nonlinear analyses indicate that the wall moments produced by the Loma Prieta earthquake do not exceed the wall flexural capacities.

Chapter 6
San Jose 10-story Commercial Building

6.1. Building Description

The 10-story Commercial Building Building (see Fig. 6.1) is located in the City of San Jose, California. The building was designed in 1964 and constructed in 1967. This building, which is designated as CSMIP355, is a 10-story office building with a rectangular plan (see Fig. 6.2). The vertical-load-carrying system consists of reinforced concrete one-way slabs supported by concrete pan joists and reinforced concrete frames. In the transverse (E-W) direction, the lateral-force-resisting system of the structure consists of two exterior reinforced concrete shear walls and six interior reinforced concrete frames. In the longitudinal (N-S) direction, the lateral-force-resisting system is composed of two exterior and two interior reinforced concrete frames. The building is found on alluvial soil with a base dimensions of 190 by 96 square ft. The foundations of the structure is a 5-foot mat at one story level below grade. The materials used for construction of the building are: light-weight concrete for the slabs, and 5,000 psi normal-weight concrete for the walls and frames. The steel reinforcement varies from Grade 40 in the upper stories to Grade 60 in the lower stories.

6.2. UBC Seismic Lateral Forces

6.2.1. Building Reactive Weight

The reactive weight of the building includes all the dead load of the slabs, walls, as well as additional 15 pounds per square foot for partitions, ceiling, or anything else that might be tied down to the floors. The reactive weights for the typical floors and roof are 2,500 and 2,200 kips, respectively. The reactive weight of the building, W, was estimated to be 24,500 kips.

6.2.2. 1964 UBC Design Base Shear

According to the 1964 UBC, the minimum design base shear V was calculated by the following formula:

$$V = ZKCW \tag{6.1}$$

where Z (= 1.0) is the zone factor and K (= 1.0) is the building system coefficient. The factor C was calculated by the following formula:

$$C = \frac{0.05}{T^{1/3}} \tag{6.2}$$

The period T of the building was calculated as

$$T = \frac{0.05h_n}{D^{1/2}} \tag{6.3}$$

The periods computed from Eq. (6.3) are equal to 0.68 and 0.45 seconds in the E-W and N-S directions, respectively. The design base shears are equal to 1,394 and 1,594 kips in the E-W and N-S directions, respectively. The design base shear ratios in the E-W and N-S directions are 5.7% and 6.5%, respectively. Because the reactive weight used in the original calculation of the design base shear was 32,800 kips (8), assuming normal-weight concrete floors, the design base shears were 1,857 and 2,146 kips in the E-W and N-S directions, respectively. Since light-weight concrete floors were actually used in the construction, the actual design base shear ratios were 7.6% and 8.7% in the E-W and N-S directions, respectively.

6.2.3. 1991 UBC Design Base Shear

According to the 1991 UBC, the minimum design base shear V is calculated by the following formula:

$$V = \frac{ZIC}{R_w} W \tag{6.4}$$

where Z (= 0.4) is the zone factor. The building could be classified as a dual system in the E-W direction (R_w = 12). In the N-S direction, the building is classified as a reinforced concrete moment resisting frame (R_w = 12). The factor C was calculated by the following formula:

$$C = \frac{1.25S}{T^{2/3}} \tag{6.5}$$

where S (= 1.5) is the soil factor (alluvial soil). The fundamental period T of the building in the E-W direction was calculated as

$$T = 0.02(h_n)^{3/4} = 0.74 \text{ seconds} \tag{6.6}$$

If the 1991 UBC formula (34-4) was used, the period in the E-W direction (the shear wall direction) would be 0.36 seconds. The period from the mathematical model of the building (to be discussed later) in the E-W direction is 0.44 seconds. Using either of the last two estimates for the period, the design base shear in the E-W direction is 2,250 kips.

In the N-S direction, the period is calculated as

$$T = 0.03(h_n)^{3/4} = 1.11 \text{ seconds} \tag{6.7}$$

The design base shear in the N-S direction is estimated to be 1,428 kips. The 1991 UBC design base shear ratios are estimated to be 9.2% and 5.8% in the E-W and N-S directions, respectively.

6.3. Review of the 1991 UBC Seismic Design

6.3.1. Mathematical Model of the Building

Based on the design drawings of the building a three-dimensional elastic model was established. It was assumed that the floors are rigid in their own plane. The columns were assumed to be fixed at the base. The modulus of elasticity of concrete was taken as 4,000 psi.

6.3.2. Story Drifts and Member Forces

An elastic structural analysis was carried out by the ETABS computer program. The factored 1991 UBC lateral seismic loads together with the factored gravity loads were applied to the mathematical model of the structure. A 40 pounds per square foot live load was applied to floors, and 5% accidental torsion was considered in the analysis.

Figure 6.3 shows the calculated story drift ratios. The results indicate that the maximum drift ratio is 0.11% for moment frames in the N-S direction. According to the 1991 UBC, the allowable drift ratio for this frame is equal to 0.25%. The maximum drift ratio obtained from the analysis was only 44% of the UBC drift limit.

Using the ACI strength design of reinforced concrete structures (4), the member capacity ratios were calculated. The capacity ratio for a given cross section is defined as the ratio between the moment produced by the design loads and the design moment capacity at the same axial load. Figure 6.4 shows the capacity ratios of some selected cross sections of an interior frame in the N-S direction. These ratios should be no larger than 1.0 for the design to be acceptable. The capacity ratio of the critical beam is about 1.0, while the columns' capacity ratios are low. The contribution of gravity loads in the capacity ratios of the beams are very significant (see Fig. 6.5); the ratios in some beams are as high as 0.64. Moment ratios of the E-W frames and the exterior N-S frames were generally less than those of the interior N-S frames.

It is concluded that this structure conforms with the 1991 UBC seismic design requirements for member strengths and story drifts. The design of this structure is governed by the strength of the beams in the N-S direction.

6.4. Analysis of the Recorded Response

6.4.1. Effective Peak Acceleration

Under the California Strong Motion Instrumentation Program (CSMIP) the building has been instrumented with 13 sensors at 3 different floors (see Fig. 6.2). Figure 6.6 shows the acceleration time history of each sensor. The peak ground acceleration recorded at the base of the building was 0.10 g in the E-W direction and 0.09 g in the N-S direction. The recorded peak accelerations at the roof level were 0.37 g and 0.25 g in the E-W and N-S directions, respectively.

The effective peak accelerations (EPA) in the E-W and N-S directions were calculated from the elastic response spectra (see Fig. 6.7) of the base acceleration records. The EPA was found to be about 0.08 g, i.e., one-fifth that of the 1991 UBC severe design earthquake (0.4 g). The spectral acceleration in the N-S direction at about one second (the measured fundamental period, as will be shown later) was 0.11 g. The spectral acceleration of the 1991 UBC-implied moderate design earthquake at one second is equal to 0.131 g, which is 1.19 times that calculated from the

Loma Prieta record.

6.4.2. Measured Natural Periods

In order to identify natural periods from the records, transfer functions between the base and roof accelerations were computed (see Fig. 6.8).

N-S direction — The transfer function between A_{13} and A_5 indicates that the fundamental period was 0.96 seconds (or 1.04 Hz). The natural periods obtained from the response of the 1984 Morgan Hill earthquake were reported by Papageorgiou and Lin (21); the reported natural periods varied from 0.82 to 0.91 seconds in the N-S direction (see Table 6.1).

E-W direction — The transfer function was computed from (A_{11} + A_{12}) and (A_3 + A_4). The identified fundamental period was 0.70 seconds (or 1.43 Hz). The reported period obtained from the Morgan Hill earthquake was 0.59-0.64 seconds.

Torsional direction — The transfer function was computed from (A_{11} - A_{12}) and (A_3 - A_4). The identified fundamental period was 0.45 seconds (or 2.20 Hz), which again is larger than the report period (0.37-0.39 seconds) from the Morgan Hill earthquake.

6.4.3. Relative Displacement Response

The relative displacements were calculated at six locations by subtracting the base displacements from the corresponding absolute displacement record. Because a low frequency noise was observed in the relative displacement time histories, frequency contents up to 0.6 Hz have been filtered numerically. Figure 6.9 shows the average relative displacement records at the center of mass. The peak response during the Loma Prieta earthquake occurred at 12.04 and 18.50 seconds from the beginning of the earthquake in the E-W and N-S directions, respectively.

6.4.4. Rocking and Torsion Response

Significant rocking motion was observed by Bard in the E-W (shear wall) direction during the 1984 Morgan Hill earthquake (2). Because sensor 2, which measures the vertical acceleration at the base (see Fig. 6.2), malfunctioned during the Loma Prieta earthquake, it is not possible to calculate the rocking contribution to the lateral displacements in the E-W direction. If the rigid-body component due to rocking is subtracted from the relative displacements in the E-W direction, the "net" relative displacements will be significantly reduced. Because of the uncertainty in estimating the rocking motion, it was decided to limit the structural analysis of the building to the N-S (moment frame) direction.

The torsional vibration was examined to quantify the torsional component in the relative displacement records. The displacements due to torsion were calculated by multiplying the torsional angle of the floor by the perpendicular distance from the center of mass to the sensor. These "torsional" components were compared with the relative displacements. Figure 6.10 shows that the torsional vibration during the Loma Prieta earthquake is insignificant.

6.5. Building Response during the 1989 Loma Prieta Earthquake

6.5.1. Method of Analysis

A three-dimensional mathematical model was used to calculate the member forces and story drifts that developed during the 1989 Loma Prieta earthquake. A linear structural analysis using the ETABS computer program was carried out to calculate the member forces at the peak response in the N-S direction. Gravity loads (dead loads and 50% of the live load) were first applied and then the three components (two translational and one torsional) of the relative displacements at the center of mass of each floor were imposed to the mathematical model. The relative displacements of the floors that were not instrumented were estimated by the modal combination technique described below.

First, the dynamic characteristics (mode shapes and natural periods) of the model were computed; gross-sectional member stiffness values were used. The periods of the model were compared with those obtained from the records during the earthquake (see Table 6.1). Since the periods of this elastic model are significantly shorter than those identified from the records, the gross-sectional stiffness values were reduced by 25% to account for the loss of stiffness due to cracking. Table 6.1 shows that the period of the cracked model in the N-S direction is very close to the measured period. Table 6.2 shows the sequence of the mode shapes and the corresponding periods. The first three modes are mainly translational while the fourth mode is mainly torsional.

The periods of the translational modes in the E-W and N-S directions are well separated.

Following the modal combination technique described in Chapter 2, and using the mode shapes computed from the cracked model, the relative displacements at the center of mass of the two instrumented floors were used to calculate the lateral displacements at the center of mass of the floors that were not instrumented. In each direction, the modal amplitudes C_i for the first two modes were solved from the lateral displacements at the two instrumented floors by the following equation:

$$\sum_{i=1}^{2} C_i \{\phi_i\} = \{d\} \tag{6.8}$$

where $\{\phi_i\}$ is the i-th mode shape and $\{d\}$ is the relative displacement. Figure 6.11 shows the relative displacement profile at the 18.50 second mark in the N-S direction. The contribution of each mode is also shown. The figure shows that the contribution of the second mode is minimal. These displacements were then used to calculate the story drift ratios.

6.5.2. Story Drift Ratios

Figure 6.12 shows that the maximum story drift ratio was 0.17%. This drift ratio is about 1.5 times that produced by the 1991 UBC seismic lateral loads. Since the calculated story drift ratios are much less than 0.5%, it is expected that little damage to nonstructural components was experienced during the Loma Prieta earthquake. This is mainly due to the large lateral stiffness of this type of reinforced concrete structures.

6.5.3. Member Forces and Moment Ratios

Member forces computed from the structural analysis were used to calculate member capacity ratios. The resulting capacity ratios indicate that members of an interior frame are more critical. Figure 6.13 shows the capacity ratios in some selected members of the structure. The results indicate that the capacity ratios of the columns were low (≤ 0.71) while some beams have exceeded 0.9. The yield moments of the beams were also calculated; the yield moment is defined as the moment which corresponds to the first yielding of steel reinforcements. Many beams have exceeded the yield moments. The ratio between the moments produced by the Loma Prieta earthquake and the yield moment of the beams was as high as 1.37.

Figure 6.14 shows the ratios between the moments produced by the earthquake and the UBC required strength. The figure shows that this ratio has reached 1.05 in the beams and 1.7 in the columns. Significant structural yielding might have occurred had these members been proportioned to just satisfy the UBC strength requirement.

6.6. Design Implications of UBC Serviceability Requirements

As demonstrated in Chapter 2, the EPA of the 1991 UBC "moderate" design earthquake is about 0.07 g. At this level of earthquake excitation, the elastic spectral acceleration for a structure with a period of about 1.0 second (see Fig. 6.7) and soil type S_3 is 0.13 g. Examining the elastic response spectra of the base acceleration, it was found that the spectral acceleration corresponding to the period of the building was 0.11 g, i.e., 85% the spectral acceleration of the 1991 UBC-implied moderate earthquake. Scaling the maximum story drift ratio (= 0.17%) produced by the earthquake by a factor of 1.19 (= 0.13/0.11) and taking into account the fact that the design story drift ratio was 44% of the allowable ratio, then the maximum story drift ratio corresponding to an EPA equal to 0.07 g is 0.46% (= $0.17\% \times 1.19/0.44$). Although this ratio is still not excessive (< 0.5%), it should be noted that the large lateral stiffness of this reinforced concrete structure, not the UBC drift limits, is the main contributing factor for this satisfactory response.

If the capacity ratios which were as high as 0.95 were scaled by the same manner, the maximum capacity ratio at an EPA of 0.07 g would be equal to 1.13 (= 0.95×1.19). This indicates that some members will just reach their ultimate moment capacities. It should be kept in mind that the live load was reduced by 50% in computing the moments during the earthquake; this reduced live load helped to keep the capacity ratio of the beams lower. It has been shown that the UBC-implied nominal design strength, $M_n^{(es)}$, at the "moderate" design earthquake level is (34):

$$\frac{M_n^{(es)}}{M_n} = \left[\frac{R_w}{1.4 R_{ser}} + \frac{(1.4 + 1.4\,r)G}{(1.4 + 1.7\,r)} \left(1 - \frac{R_w}{1.4 R_{ser}} \right) \right] \tag{6.9}$$

where r is the ratio between live load moment and dead load moment (= 0.25) and G is the ratio between factored gravity load moment and design moment. Figure 6.5 shows that G was as high as 0.64. From Eq. 6.9, the ratio between the moments produced by the moderate earthquake

(R_{ser} = 6) and the design moment capacity can be as high as 1.17, which is close to the ratio obtained by scaling the Loma Prieta results (= 1. 13).

6.7. Conclusions

Based on a detailed study of the response of building CSMIP355 during the Loma Prieta earthquake and the UBC design review, the following conclusions can be made.

(1) The EPA of the base acceleration recorded during the 1989 Loma Prieta earthquake is about the same as that of the UBC-implied moderate earthquake.

(2) The CSMIP355 building satisfies the 1991 UBC; the design is governed by the strength requirements.

(3) A comparison of the natural periods obtained from the 1984 Morgan Hill and 1989 Loma Prieta indicates that the fundamental periods in the N-S and N-W directions have elongated by 11% and 14%, respectively.

(4) The maximum story drift ratio produced by the Loma Prieta earthquake was only 0.17% in the moment frame (N-S) direction. It indicates that nonstructural damage was minimal. Many beams have exceeded their yield moments, although the ultimate moment capacities have not been reached. It is not a desirable performance from the viewpoint of serviceability because a structure of this kind may be subjected to this low level of ground excitation several times during its service life.

(5) The large lateral stiffness of this type of reinforced concrete buildings and the significant effect of gravity loads have helped keeping the capacity ratios within an acceptable limit.

Chapter 7
Summary, Conclusions, and Recommendations

7.1. Summary

Significant number of seismic records in extensively instrumented buildings have been collected by CDMG during the Loma Prieta earthquake, and the recorded peak ground motions at the base of many buildings fall in the range 0.06-0.15 g, which is representative of "moderate" design earthquakes implicitly used by UBC. Four medium-rise buildings (6- to 13-story high), one steel and three reinforced concrete buildings, have been selected for this study. These buildings were reviewed by the 1991 UBC seismic provisions. System identification was performed to obtain natural periods from recorded responses; these periods were compared with those obtained from the 1984 Morgan Hill earthquake. A three-dimensional finite element model for each building was established; natural periods and mode shapes were computed by using the computer program ETABS. The analytically predicted natural periods were then correlated with those identified from the recorded responses. Lateral displacements at the floors that were not instrumented were computed by a modal superposition technique. Static structural analyses at some selected peak responses were performed by imposing relative floor displacements (two translational and one torsional displacements) on the mathematical models; realistic gravity loads were also included in the analyses. The member stress ratios (or capacity ratios for reinforced concrete structures) and story drift ratios were then computed and compared with serviceability requirements.

CSMIP357 (San Jose 13-story Government Office Building)

(1) The UBC design review indicates that the building satisfies the 1991 UBC. The design stress ratios are generally low and the design is governed by the UBC story drift requirement.

(2) The natural periods identified from the building response during the 1984 Morgan Hill earthquake in the E-W, N-S, and torsional directions were 2.19, 2.06, and 1.63 seconds,

respectively; these periods have changed to 2.18, 2.23, and 1.69 seconds during the Loma Prieta earthquake.

(3) The story drift ratio produced by the Loma Prieta earthquake is as high as 0.97%, which is about twice the 0.5% limit commonly used to control nonstructural damage for moderate earthquakes. Based on the elastic structural analyses, stress ratios as high as 1.41 may have been reached if the structure were to respond elastically during the earthquake.

CSMIP462 (Hayward 6-story Office Building)

(1) The building is torsionally irregular in plan. Although the original design satisfies the 1964 UBC, it does not satisfy the 1991 UBC; the design is governed by the wall capacity ratio, which is as high as 3.0. Because the UBC amplification factor for accidental torsion is equal to 2, a 10% accidental eccentricity has to be used in the 1991 UBC design.

(2) The natural periods of the first three modes identified from the building response recorded during the Loma Prieta earthquake have lengthened from 0.60, 0.60, and 0.55 seconds, to 0.95, 0.85, and 0.68 seconds in the E-W, N-S, and torsional directions, respectively. Except for the second mode, which is predominantly moving in the N-S direction, the other two modes are strongly coupled in the E-W and torsional directions. The identified mode shapes are consistent with those predicted analytically.

(3) Although significant torsional response is observed during the Loma Prieta earthquake, the maximum story drift ratio is only 0.41%. Therefore, it is expected that nonstructural damage was minimal. As the wall capacity ratio may be as high as 3.4 if the structure were to respond elastically during the Loma Prieta earthquake, wall yielding must have occurred.

CSMIP356 (San Jose 10-story Residential Building)

(1) The CSMIP356 building satisfies the 1991 UBC strength requirements in the E-W direction. But the wall flexural capacities in the N-S direction are not sufficient.

(2) The natural periods identified from the building response recorded during the 1984 Morgan Hill earthquake in the E-W, N-S, and torsional directions are 0.43, 0.64, and 0.39 seconds, respectively; these periods have lengthened to 0.43, 0.78, and 0.38 seconds during the Loma Prieta earthquake.

(3) Because of the large lateral stiffness of this shear wall building, the maximum story drift ratio produced by the Loma Prieta earthquake is only 0.19%. If the walls were to remain elastic during the Loma Prieta earthquake, the elastic overturning moments at the second floor level would have been 1.3 times the wall flexural strength. Since shear walls were cracked in the N-S direction, nonlinear behavior had to be considered in estimating realistic internal forces. The results of nonlinear analyses indicate that the wall moments produced by the Loma Prieta earthquake do not exceed the wall flexural capacities.

CSMIP355 (San Jose 10-story Commercial Building)

(1) The SMIP355 building satisfies the 1991 UBC; the design is governed by the strength requirements.

(2) The natural periods identified from the building response recorded during the 1984 Morgan Hill earthquake in the E-W, N-S, and torsional directions are 0.64, 0.91 and 0.39 seconds, respectively; these periods have lengthened to 0.70, 0.96, and 0.45 seconds during the Loma Prieta earthquake.

(3) During the Loma Prieta earthquake, the maximum story drift ratio is only 0.17% in the moment frame (N-S) direction; it indicates that nonstructural damage is minimal. Many beams have exceeded their yield moments, although the ultimate moment capacities have not been reached. Scaling the results of the building response to the UBC-implied moderate earthquake has shown that the moment ratio can be as high as 1.13.

7.2. Conclusions

Based on a review of the UBC design, a detailed study of the recorded response of four medium-rise buildings that were excited during the Loma Prieta earthquake, and a correlation of the calculated response with the available observed damage, the following conclusions can be made.

(1) The effective peak ground accelerations of the recorded base accelerations of the four buildings are about the same as that of the UBC-implied moderate design earthquake.

(2) Although the effective peak accelerations of the base acceleration are about the same as that of the UBC-implied moderate earthquake, unusual high response amplification is observed in the elastic response spectra of the base acceleration records, especially in the steel building CSMIP357.

(3) A comparison of natural periods identified from the records of the 1984 Morgan Hill and the 1988 Loma Prieta earthquakes indicates that the natural periods have generally lengthened. This observation is an indication of the stiffness loss resulting from member yielding and/or cracking.

(4) In computing lateral displacements of the floors that are not instrumented, higher modes of vibration cannot be ignored. Furthermore, assuming a constant story drift ratio between two instrumented floors that are not adjacent to each other may significantly underestimate actual story drift ratios.

(5) If nonlinear behavior due to concrete cracking is not taken in consideration in the structural analysis, imposing measured lateral displacements on elastic model of reinforced concrete structures may overestimate actual member forces.

(6) During the Loma Prieta earthquake, the computed story drift ratio in the steel building CSMIP357 is as high as 0.97%, which is about twice the 0.5% story drift limit commonly used to control nonstructural damage for moderate level earthquakes. This high drift ratio indicates that the building must have suffered nonstructural damage. The damage to nonstructural elements as predicted by the computed story drift ratios and floor accelerations

correlates well with the observed damage reported by Rihal (26). As the design of this building is governed by the drift limit, it appears that the UBC story drift limit for steel frame buildings is too high (i.e., nonconservative).

(7) For the three reinforced concrete buildings selected for this study, the story drift ratios developed are less than 0.5%. Therefore damage to nonstructural elements in these building is limited. The design of these buildings is governed by strength requirements, not story drift limits. In fact, the design story drift ratios of these buildings are generally much smaller than the UBC limit. The large lateral stiffness of these reinforced concrete buildings, not the UBC drift limits, is the main reason for the limited nonstructural damage.

(8) Based on elastic structural analyses of the CSMIP357 steel building, stress ratios as high as 1.41 may have developed if the structure were to respond elastically during the earthquake. This high stress ratio indicates that member yielding must have occurred. The observed lengthening of the natural period is also an indication of stiffness loss due to yielding.

(9) The design of the three reinforced concrete buildings is governed by the UBC strength requirements. Two buildings (CSMIP355 and CSMIP462) have shown that yielding in moderate earthquakes, like the Loma Prieta earthquake, can occur in buildings designed with $R_w \geq 8$ or higher. It is not a desirable performance from the viewpoint of serviceability because a structure of this kind may be subjected to this low level of excitation several times during its service life. The gravity load effect also helps to reduce the capacity ratios that are developed during the Loma Prieta earthquake.

7.3. Recommendations

It has been demonstrated from the viewpoint of the seismic limit state design philosophy that a two-phase design procedure has to be adopted in seismic provisions (34, 35). The need for such a design procedure has been confirmed from the case study of four multistory buildings. An attempt to "fix" the serviceability aspect of the Uniform Building Code in its existing format will be awkward, if not impossible, and less transparent to designers. It is highly recommended that the serviceability limit state be considered by: (1) specifying the level of moderate design earthquakes explicitly; (2) specifying story drift limits, which should be independent of the force reduction factor, to avoid nonstructural damage; and (3) specifying allowable stress or design strength to avoid structural damage.

REFERENCES

1. *Allowable Stress Design (ASD) Manual of Steel Construction,* Amer. Inst. of Steel Constr., Chicago, Ill., 1989.

2. Bard, P., "The Importance of Rocking in Building Motion: An Experimental Evidence," *Proc. 9th World Conf. Earthquake Engrg.*, vol. VIII, pp. 333-338, Int. Assoc. for Earthquake Engrg., Tokyo, Japan, 1988.

3. Bertero, V. V., "Evaluation of Response Reduction Factors Recommended by ATC and SEAOC," *Proc. 3rd U.S. Nat. Conf. Earthquake Engrg.*, pp. 1663-1673, Earthquake Engrg. Res. Inst., Charleston, South Carolina, 1986.

4. "Building Code Requirements for Reinforced Concrete," *ACI 318-89*, Amer. Concr. Inst., Detroit, Mich., 1989.

5. Degenkolb, H. J., Chmn., "Basic Design Criteria of the Recommended Lateral Force Requirements and Commentary," *J. Struct. Div.*, vol. 98, no. ST9, pp. 1913-1922, ASCE, 1972.

6. *Earthquake Resistant Regulations - A World List,* Int. Assoc. for Earthquake Engrg., Tsukuba, Japan, 1988.

7. "An Evaluation of a Response Spectrum Approach to Seismic Design of Buildings," *ATC-2*, Applied Technology Council, Palo Alto, Calif., 1974.

8. *An Evaluation of a Response Spectrum Approach to Seismic Design of Buildings,* ATC-2, Berkeley, Calif., September, 1974.

9. Ferritto, J. M., "Economics of Seismic Design for New Buildings," *J. Struct. Engrg.*, pp. 2925-2938, ASCE, 1984.

10. Housner, G. W., Chmn., *Competing Against Time,* California Governor's Board of Inquiry on the 1989 Loma Prieta Earthquake, Calif., 1990.

11. Huang, M. J., et al., "Processed Data from the Strong-Motion Records of the Morgan Hill Earthquake of 24 April 1984," *Reprt OSMS 85-05*, Calif. Strong Motion Instrumentation Program, Calif. Div. Mines Geology, Sacramento, Calif., 1985.

12. Kaba, S. A. and Mahin, S. A., "Interactive Computer Analysis Methods for Predicting the Inelastic Cyclic Behavior of Structural Sections," *Report No. UCB/EERC-83/18*, Earthquake Engrg. Res. Ctr., Univ. of California, Berkeley, 1983.

13. Kato, B., "Seismic Design Criteria for Steel Buildings," *Proc. Pacific Struct. Steel Conf.*, vol. 1, pp. 133-147, Auckland, New Zealand, 1986.

14. Kent, D., "Inelastic Behavior of Reinforced Concrete Members with Cyclic Loading," *Ph.D. Thesis*, Univ. of Canterbury, New Zealand, 1969.

15. Lin, B. C. and Papageorgiou, A. S., "Demonstration of Torsional Coupling Caused by Closely Spaced Periods - 1984 Morgan Hill Earthquake Response of the Santa Clara County Building," *Earthquake Spectra*, vol. 5, no. 3, pp. 539-556, Earthquake Engrg. Res. Inst., 1989.

16. "Loma Prieta Earthquake October 17, 1989," *Report No. 89-03*, Earthquake Engrg. Res. Inst., El Cerrito, Calif., 1989.

17. Mahin, S. A., Boroschek, R., and Zeris, C., "Engineering Interpretation of the Responses of Three Instrumented Buildings in San Jose," *Preprints*, SMIP89 Seminar, CDMG, Sacramento, Calif., 1989.

18. Maison, B. F. and Neuss, C. F., "SUPER-ETABS: An Enhanced Version of the ETABS Program," Technical Report to the National Science Foundation, J. G. Bouwkamp, Inc., Berkeley, Calif., 1983.

19. *NEHRP Recommended Provisions for the Development of Seismic Regulations for New Buildings*, Bldg. Seismic Safety Council, Washington, D.C., 1988.

20. *The October 17, 1989 Loma Prieta Earthquake: A Quick Look Report*, EQE Engr., San Francisco, Calif., 1989.

21. Papageorgiou, A. S. and Lin, B. C., "Influence of Lateral Load Resisting System on the Earthquake Response of Structures - A System Identification Study," *Earthquake Engrg. Struct. Dyn.*, vol. 18, pp. 799-814, 1989.

22. Park, R. and Paulay, T., *Reinforced Concrete Structures*, John Wiley & Sons, 1975.

23. "Performance of Structures During the Loma Prieta Earthquake of October 17, 1989," NIST Special Publication 778, Nat. Inst. Stand. Technol., Gaithersburg, MD, 1990.

24. "Preliminary Report on the Seismological and Engineering Aspects of the October 17, 1989 Santa Cruz (Loma Prieta) Earthquake," *Report No. UCB/EERC-89/14*, Earthquake Engrg. Res. Ctr., Univ. of California, Berkeley, Calif., 1989.

25. *Recommended Lateral Force Requirements and Commentary*, Struct. Engrs. Assoc. of Calif., San Francisco, Calif., 1990.

26. Rihal, S. S., "Correlation Between Recorded Building Data and Non-Structural Damage During the Loma Prieta Earthquake," *Preprint*, SMIP91 Seminar, CDMG, Sacramento, Calif., May, 1991.

27. Rojahn, C. and Hart, G. C., "U.S. Code Focusing on R-Factor of UBC, ATC-3 and NEHRP," *ATC-15-2*, pp. 41-48, Applied Technology Council, Palo Alto, Calif., 1989.

28. *Seismic Design Guidelines for Essential Buildings*, (Tri-Services Manual), Departments of the Army, the Navy, and the Air Force, Washington, D.C., 1986.

29. Shakal, A., et al., "CSMIP Strong-Motion Records of the Santa Cruz (Loma Prieta) California Earthquake of 17 October, 1989," *Reprt OSMS 89-06*, Calif. Strong Motion Instrumentation Program, Calif. Div. Mines Geology, Sacramento, Calif., 1989.

30. "Tentative Provisions for the Development of Seismic Regulations for Buildings," *ATC-3-06*, Applied Technology Council, Palo Alto, Calif., 1978.

31. Tsai, K.-C. and Popov, E. P., "Seismic Panel Zone Design Effect on Elastic Story Drift in Steel Frames," *J. Struct. Engrg.*, vol. 116, no. 12, pp. 3285-3301, ASCE, 1990.

32. Uang, C.-M., "A Comparison of Seismic Force Reduction Factors Used in U.S.A. and Japan," *Earthquake Engrg. Struct. Dyn.*, vol. 20, no. 4, pp. 389-397, 1991.

33. Uang, C.-M., "Establishing R (or R_w) and C_d Factors for Building Seismic Provisions," *J. Struct. Engrg.*, vol. 117, no. 1, pp. 19-28, ASCE, 1991.

34. Uang, C.-M., "Structural Overstrength and Limit State Philosophy in Seismic Design Provisions," *Report No. CE-91-1*, Final Report submitted to the NSF, Dept. of Civil Engr., Northeastern Univ., Boston, Mass., 1991.

35. Uang, C.-M. and Bertero, V. V., "UBC Seismic Serviceability Regulations: Critical Review," *J. Struct. Engrg.*, vol. 117, no. 7, pp. 2055-2068, ASCE, 1991.

36. *Uniform Building Code (UBC),* Int. Conf. of Bldg. Officials, Whittier, Calif., 1991.

37. Wilson, E. L., Der Kiureghian, A., and Bayo, E. P., "A Replacement for the SSRS Method is Seismic Analysis," *Earthquake Engrg. Struct. Dyn.*, vol. 9, pp. 187-194, 1981.

APPENDIX — NOTATION

The following symbols are used in this report:

A absolute acceleration;

a relative acceleration;

C_i i-th modal amplitude;

C_{es} elastic base shear ratio for the moderate design earthquake;

C_{eu} elastic base shear ratio for the severe design earthquake;

C_w UBC design base shear ratio;

D absolute displacement or plan dimension;

d relative displacement;

E_c concrete modulus of elasticity;

f'_c concrete compressive strength;

f_r concrete modulus of rupture;

$f^{(es)}$ member stress produced by the moderate design earthquake;

$f^{(g)}$ member stress produced by gravity loads;

$f^{(w)}$ member stress produced by the UBC design seismic forces;

$F_a^{(g)}$ UBC allowable stress for gravity load design;

$F_a^{(w)}$ UBC allowable stress for earthquake loading combinations [$= 4/3 \times F_a^{(g)}$];

$F_a^{(es)}$ UBC implied allowable stress for moderate earthquake loading combinations;

F_y specified yield stress of steel;

G ratio between gravity load effect and design strength;

h story height;

I importance factor;

K 1985 UBC structural system factor;

$M^{(es)}$ bending moment produced by the UBC design seismic forces;

M_n nominal design strength of AISC/LRFD and ACI;

$M_n^{(es)}$ UBC implied nominal design strength for the moderate design earthquake;

R_w 1988 UBC system modification factor;

R_{ser} ratio of elastic design base shears between severe and moderate earthquakes;

r ratio between live and dead load;

$\ddot{r}$ horizontal acceleration due to rocking:

S UBC site coefficient for soil;

T fundamental period of vibration;

V_c nominal shear strength;

W weight of reactive masses;

Z UBC seismic zone factor;

$\ddot{\alpha}$ rocking acceleration;

Δ story drift;

Δ_{es} story drift produced by the moderate design earthquake;

Δ_w UBC elastic design story drift produced by $C_w W$;

ϕ_i i-th modes shape;

$\ddot{\theta}$ torsional acceleration.

TABLES

Building Name	CDMG Station No.	Structural Type	Max. Horiz. Accel. (g)	
			Ground	Roof
Commercial Bldg. (San Jose)	57355	10-story concrete	0.11	0.38
Residential Bldg. (San Jose)	57356	10-story concrete	0.13	0.37
Office Building (San Jose)	57357	13-story steel	0.11	0.36
Office Building (Hayward)	58462	6-story concrete	0.12	0.45

Table 1.1 Buildings Selected for Study

Direction	Morgan Hill	Loma Prieta	Mathematical Model
N-S	2.06 (0.48)	2.23 (0.45)	2.11 (0.47)
E-W	2.19 (0.46)	2.18 (0.46)	2.11 (0.47)
Torsion	1.63 (0.61)	1.69 (0.59)	1.60 (0.62)

* period in seconds, frequency (listed in parentheses) in Hz.

Table 3.1 Comparison of Natural Periods (CSMIP 357)

Mode No.	Period (Frequency)	Main Direction
1	2.11 (0.47)	NE-SW
2	2.06 (0.49)	NW-SE
3	1.60 (0.62)	torsion
4	0.84 (1.19)	E-W
5	0.81 (1.23)	N-S
6	0.70 (1.43)	torsion
7	0.57 (1.73)	E-W
8	0.56 (1.79)	N-S
9	0.49 (2.04)	torsion
10	0.43 (2.30)	E-W
11	0.42 (2.36)	N-S
12	0.35 (2.86)	torsion

* period in seconds, frequency (listed in parentheses) in Hz.

Table 3.2 ETABS-Predicted Natural Periods (CSMIP 357)

Direction	Loma Prieta	Mathematical Model
N-S	0.85 (1.18)	0.74 (1.36)
E-W*	0.95 (1.05)	0.91 (1.10)
Torsion*	0.68 (1.47)	0.51 (1.98)

* both are coupled in the E-W and torsional directions.
** period in seconds, frequency (listed in parentheses) in Hz.

Table 4.1 Comparison of Natural Periods (CSMIP 462)

Direction	Morgan Hill	Loma Prieta	Mathematical Model
N-S	0.58 - 0.64 (1.72 - 1.56)	0.68 - 0.78 (1.47 - 1.28)	0.67 (1.49)
E-W*	0.42 - 0.43 (2.38 - 2.33)	0.42 - 0.43 (2.38 - 2.33)	0.44 (2.27)
Torsion*	0.38 - 0.39 (2.63 - 2.56)	0.36 - 0.38 (2.78 - 2.63)	0.39 (2.56)

* both are lightly-coupled in the E-W and torsional directions.
** period in seconds, frequency (listed in parentheses) in Hz.
*** Morgan Hill data from Ref. 21.

Table 5.1 Comparison of Natural Periods (CSMIP 356)

Direction	Morgan Hill	Loma Prieta	Elastic Model	Cracked Model
N-S	0.82 - 0.91 (1.22 - 1.10)	0.96 (1.04)	0.74 (1.35)	1.07 (0.93)
E-W	0.59 - 0.64 (1.69 - 1.56)	0.70 (1.43)	0.44 (2.27)	0.47 (2.13)
Torsion	0.37 - 0.39 (2.70 - 2.56)	0.45 (2.20)	0.28 (3.57)	0.29 (3.45)

* period in seconds, frequency (listed in parentheses) in Hz.
** Morgan Hill data from Ref. 21.

Table 6.1 Comparison of Natural Periods (CSMIP 355)

Mode No.	Period (Frequency)	Main Direction
1	1.07 (0.93)	N-S
2	0.47 (1.13)	E-W
3	0.33 (3.03)	N-S
4	0.29 (3.45)	torsion
5	0.17 (5.88)	E-W
6	0.12 (8.33)	N-S
7	0.11 (9.09)	E-W
8	0.07 (14.29)	torsion

* period in seconds, frequency (listed in parentheses) in Hz.

Table 6.2 ETABS-Predicted Natural Periods (CSMIP 355)

FIGURES

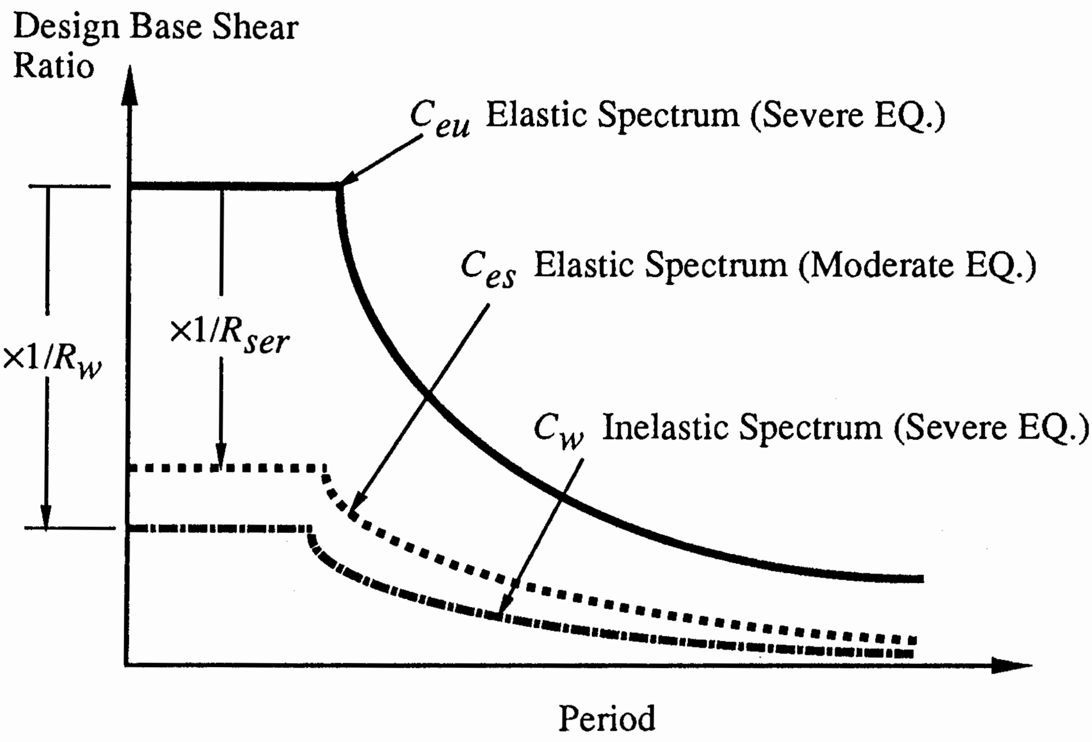

Fig. 2.1 UBC Design Spectra for Severe and Moderate Earthquakes

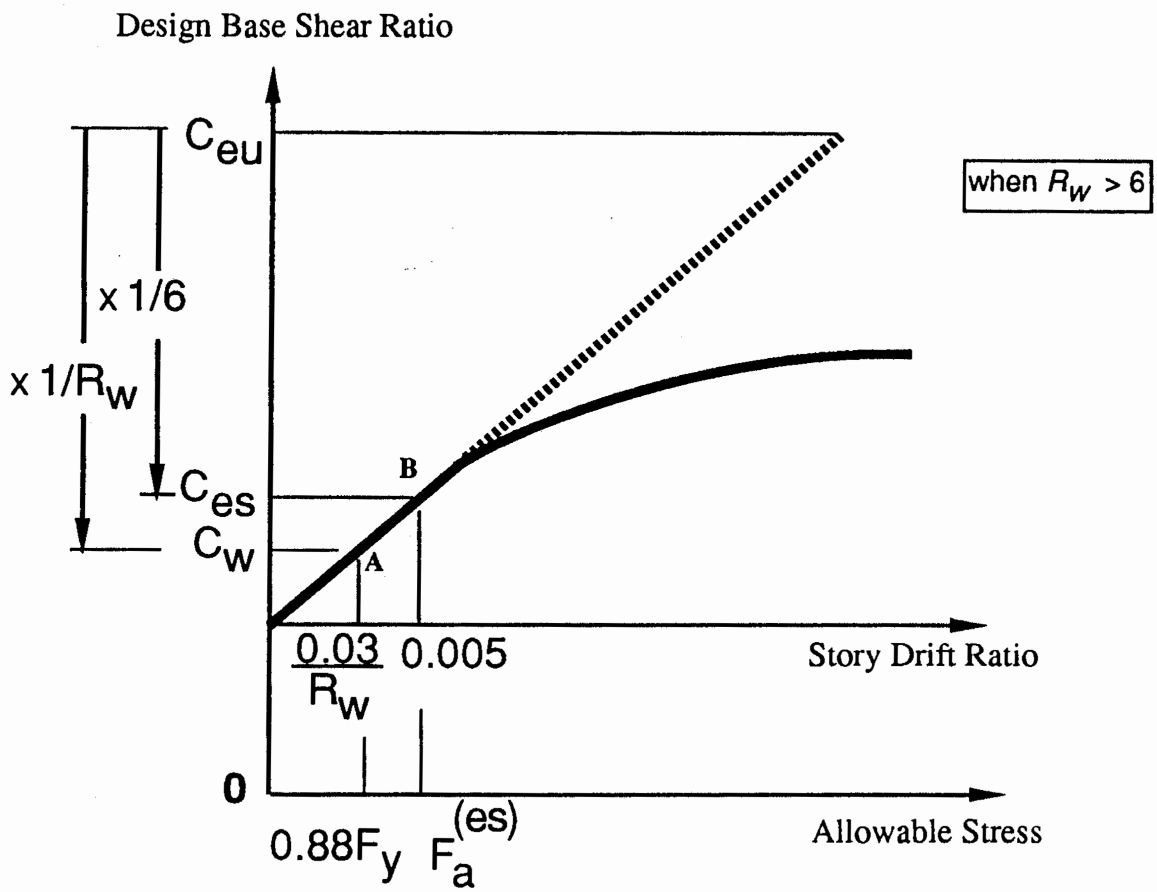

Fig. 2.2 UBC-Implied Serviceability Requirements for Moderate Design Earthquakes

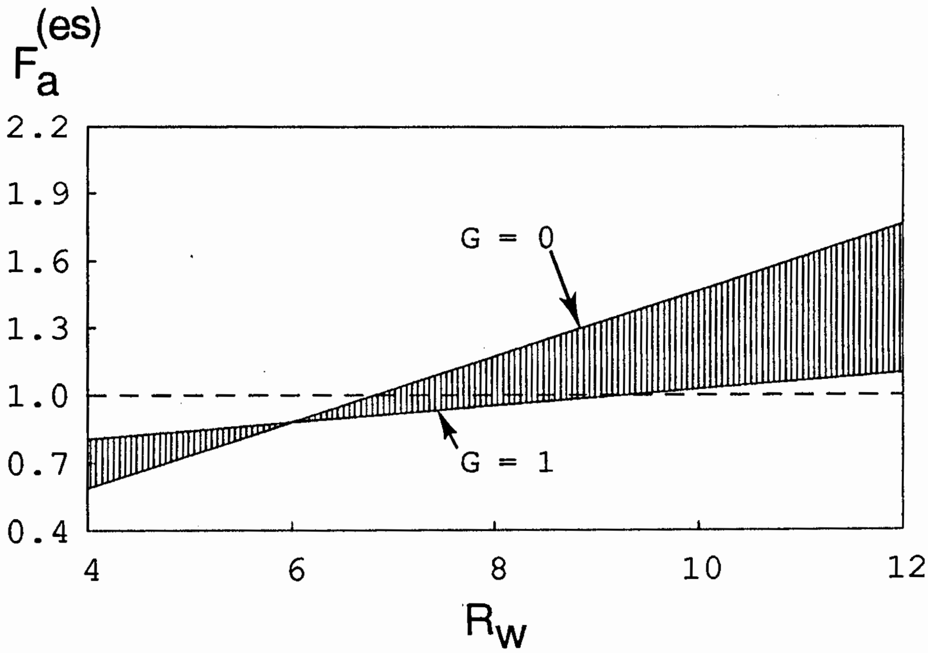

Fig. 2.3 Variations of $F_a^{(es)}$ with R_w Factor

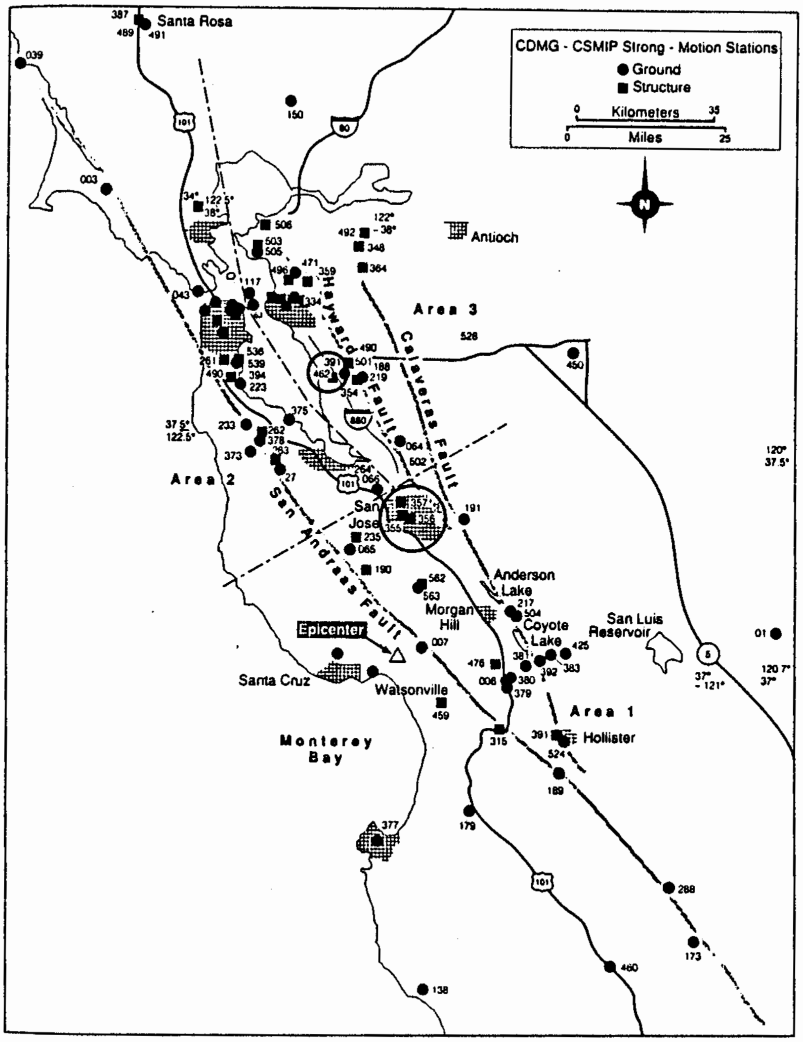

Fig. 2.4 Locations of CSMIP Stations (Shakal et. al 1989)

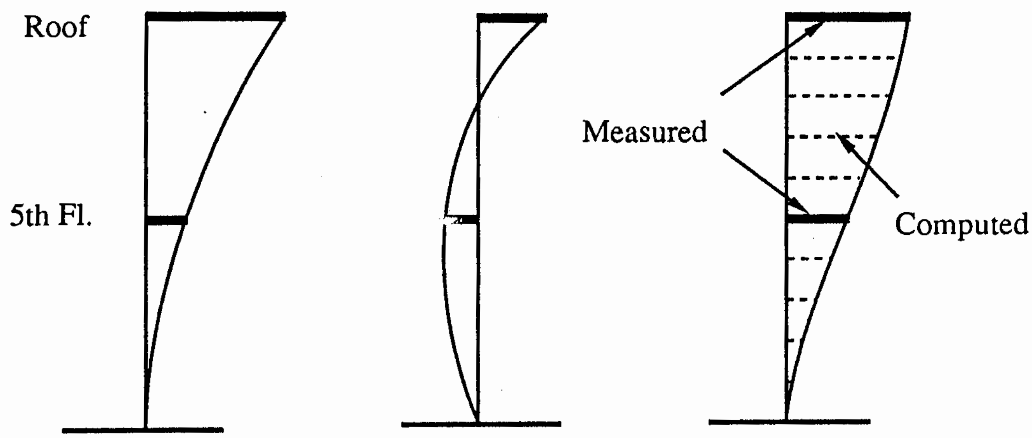

$$C_1 \times \{\phi_1\} + C_2 \times \{\phi_2\} = \{d\}$$

Fig. 2.5 Modal Superposition Method Used in This Study

San Jose - 13-story Government Office Bldg.

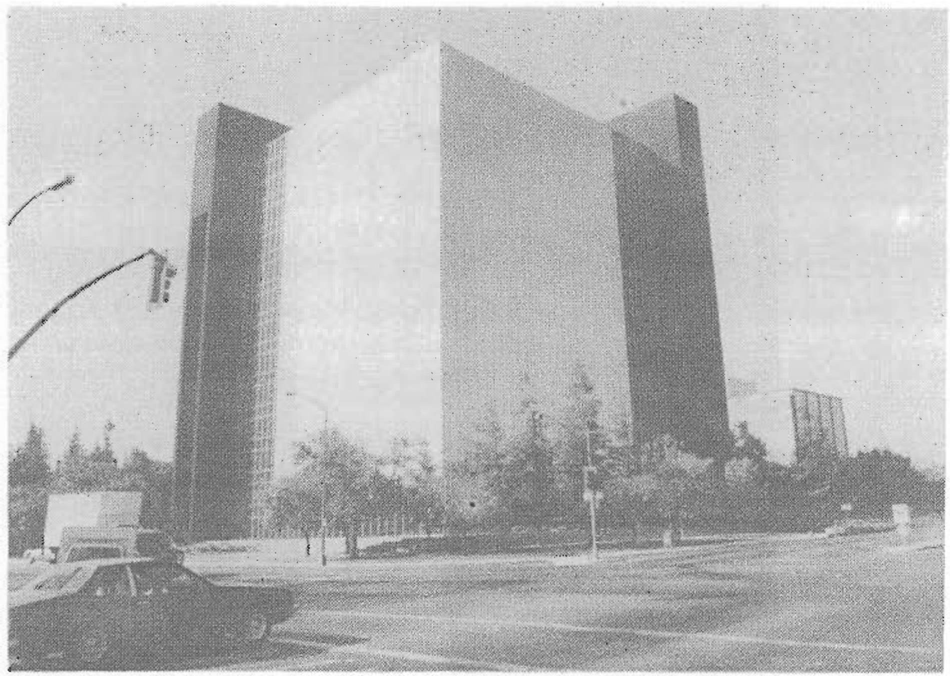

No. of Stories above/below ground: 13/0
Plan Shape: Rectangular
Base Dimensions: 173' x 167'
Typical Floor Dimensions: 167' x 167'
Design Date: 1972
Construction Date: 1975-76

Vertical Load Carrying System:
3.5" concrete slab on metal deck; steel columns, beams and joists.
Lateral Force Resisting System:
Moment-resistant steel frame.
Foundation Type:
Mat foundation.

Fig. 3.1 San Jose 13-story Government Office Building (CSMIP357, Shakal, et al., 1989)

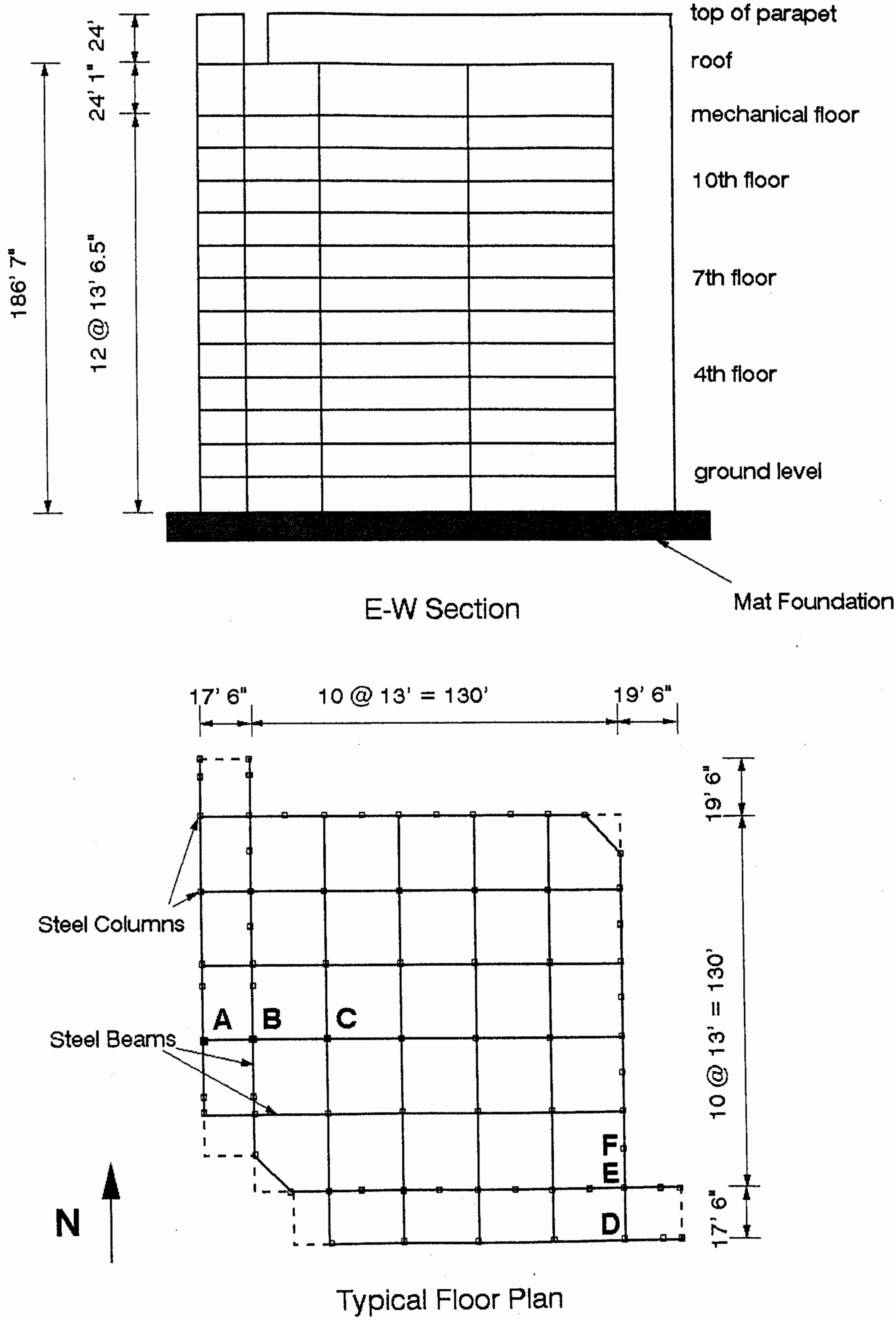

Fig. 3.2 General Layout of Building CSMIP357

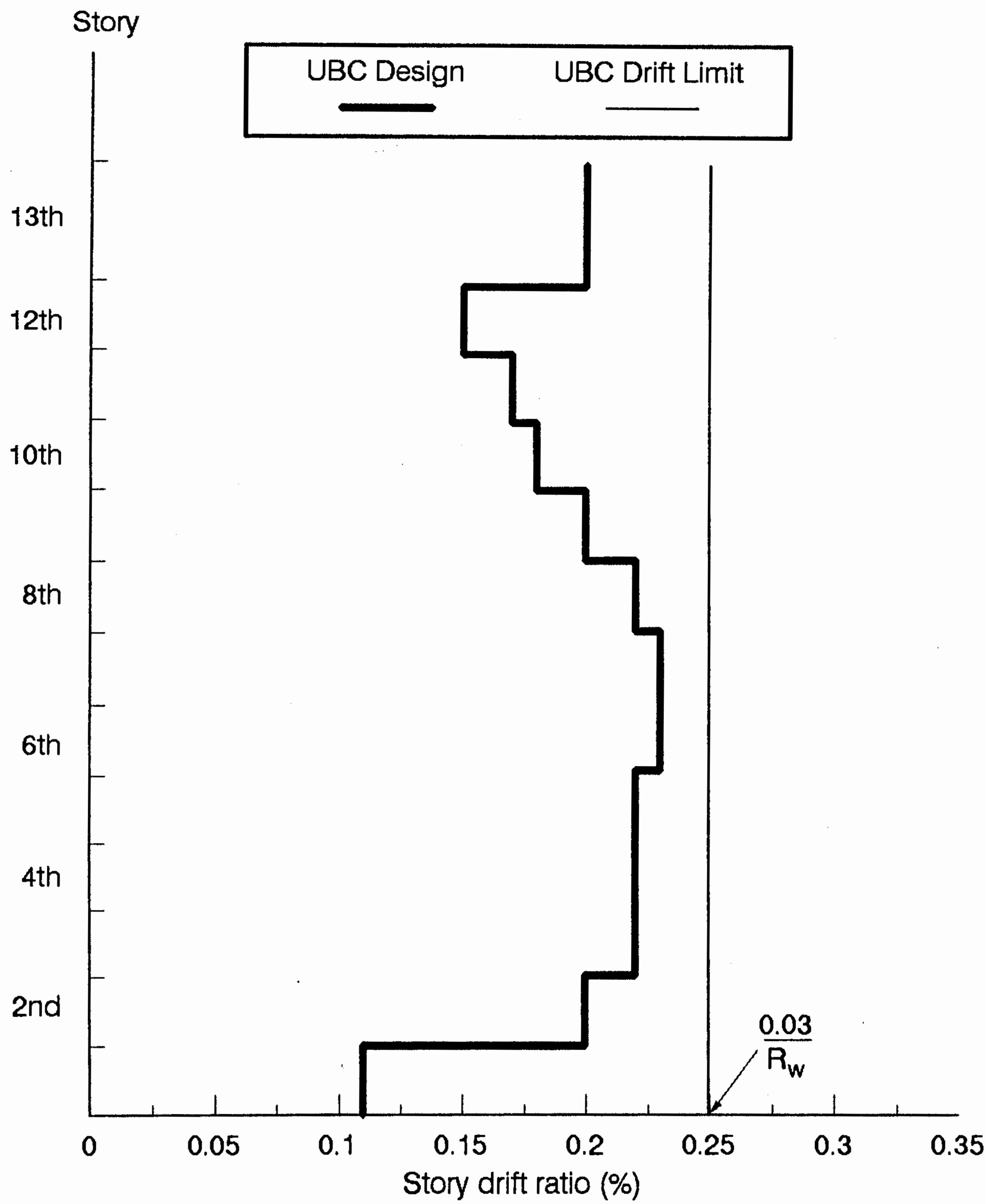

Fig. 3.3 Story Drift Ratios for the 1991 UBC Design

(CSMIP357, N-S)

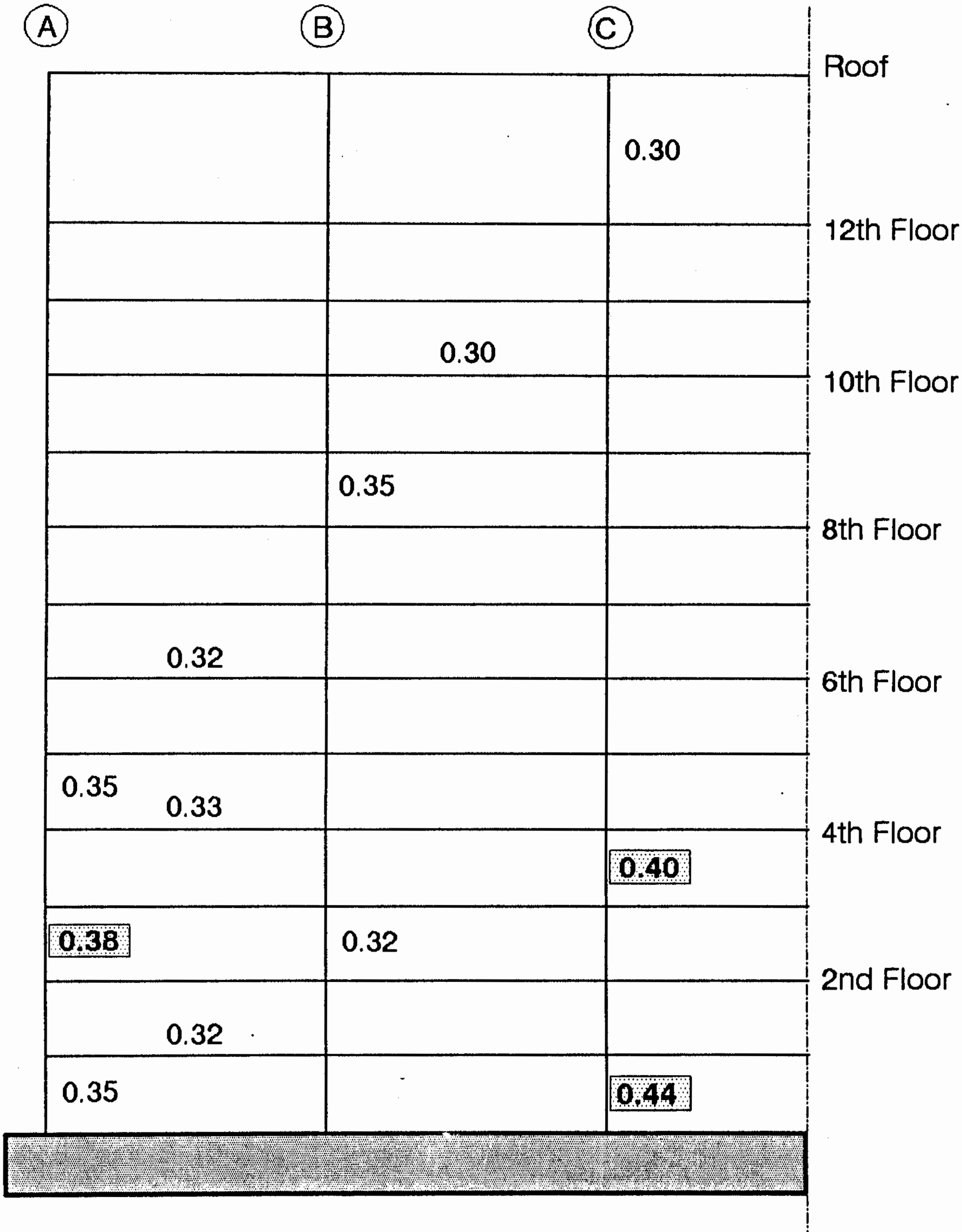

Fig. 3.4 Member Stress Ratios for the 1991 UBC Design

(CSMIP357, E-W)

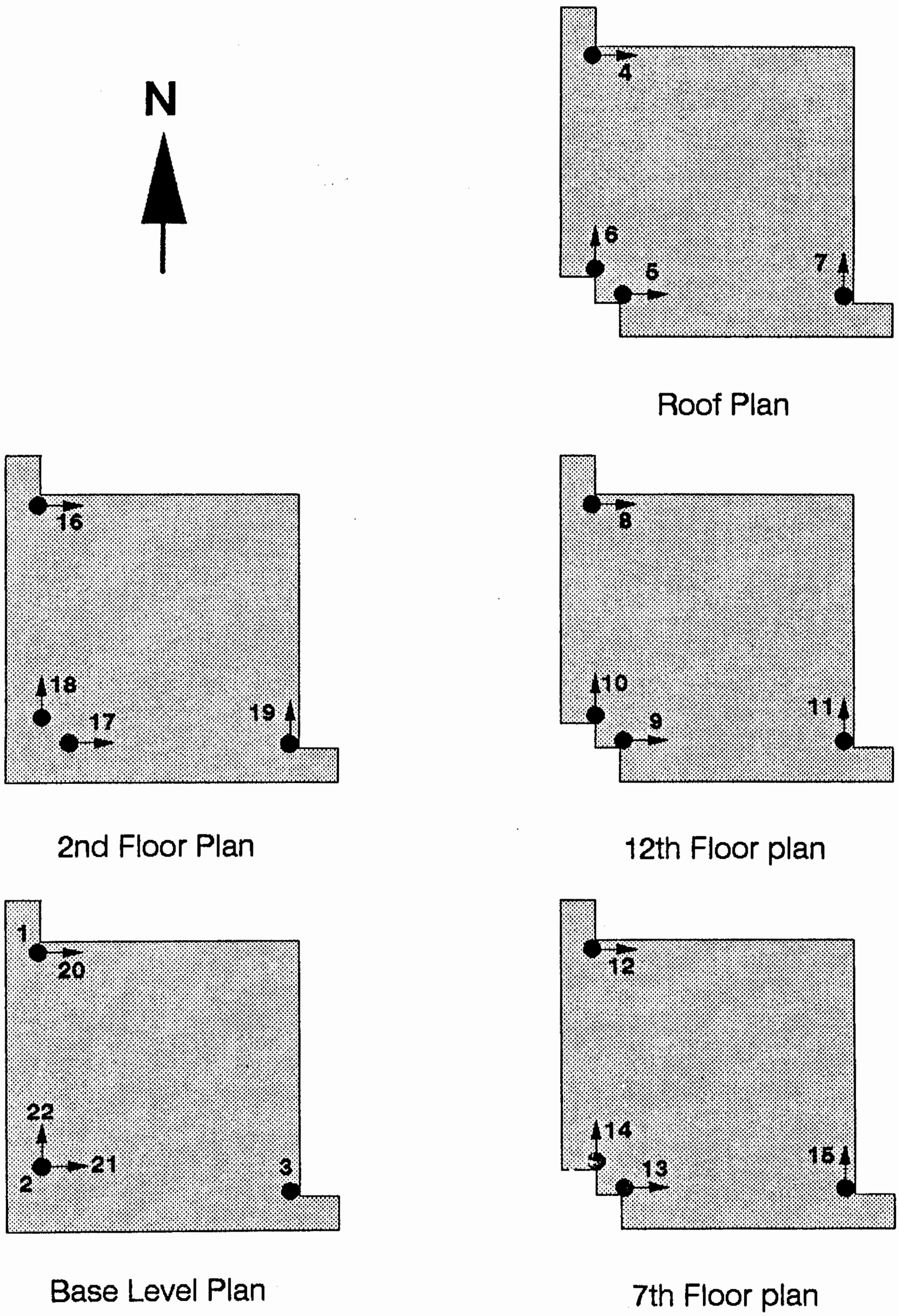

Fig. 3.5 Sensor Arrangement (CSMIP357)

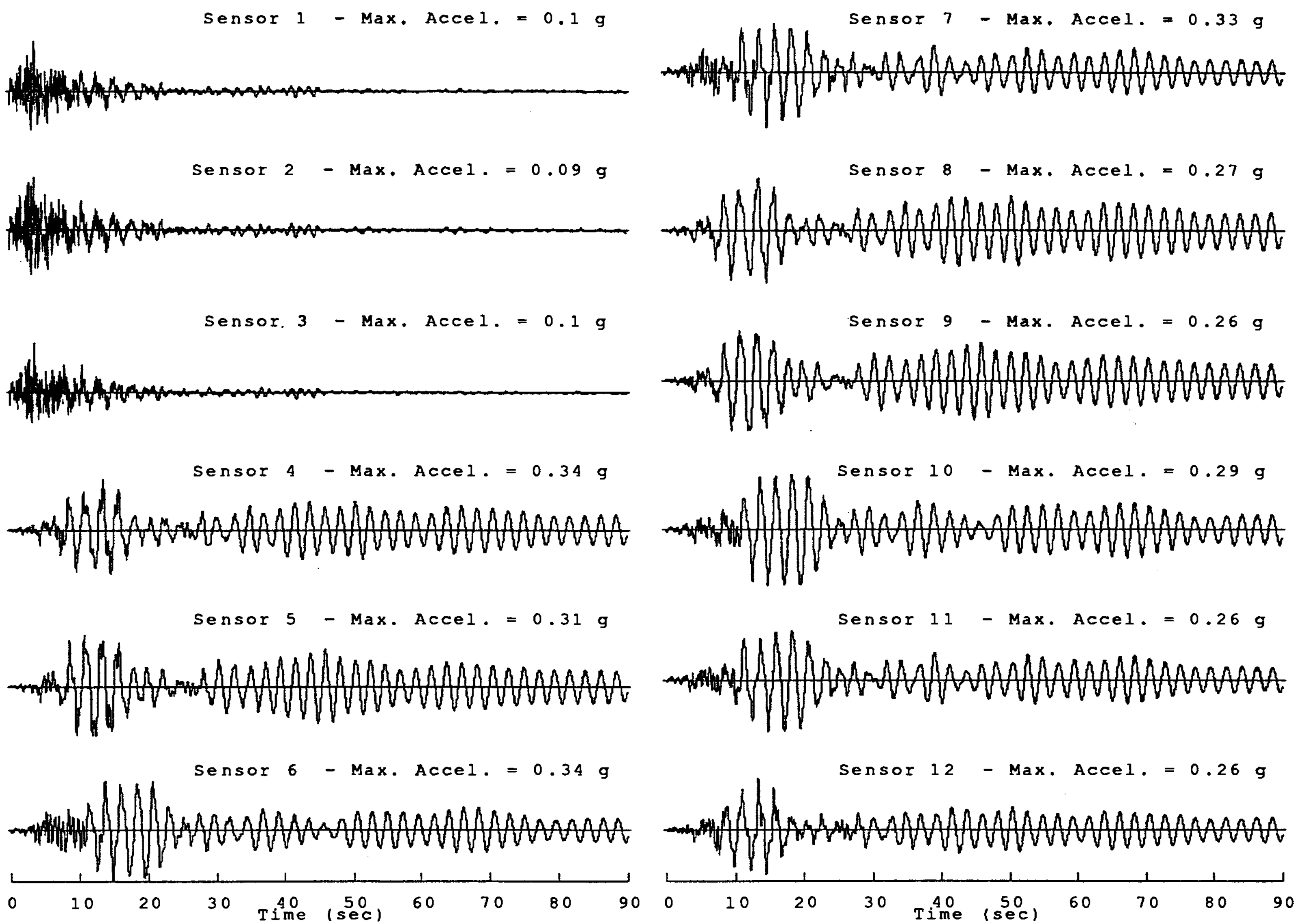

Fig. 3.6 Building CSMIP357 Acceleration Records

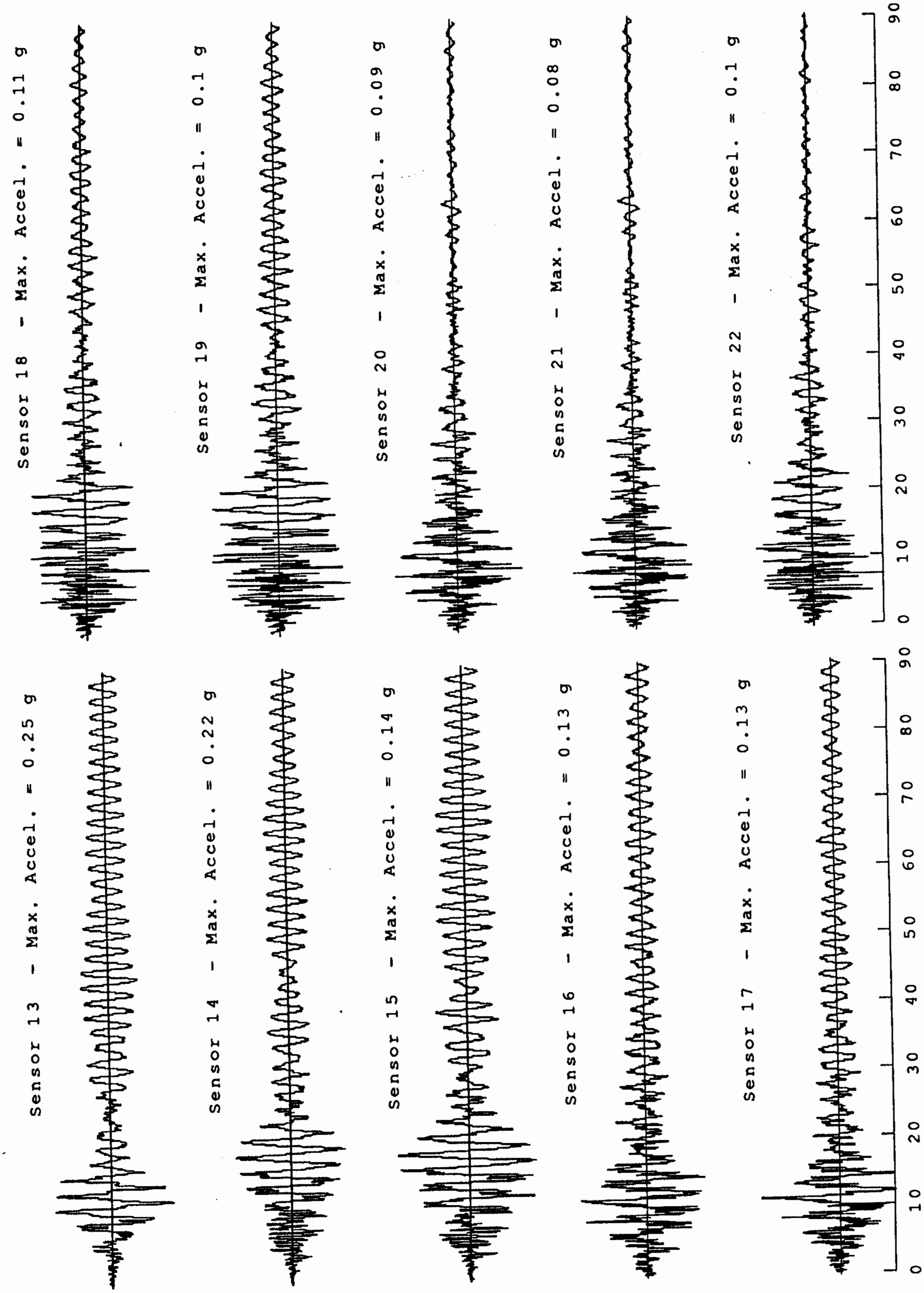

Fig. 3.6 (continued)

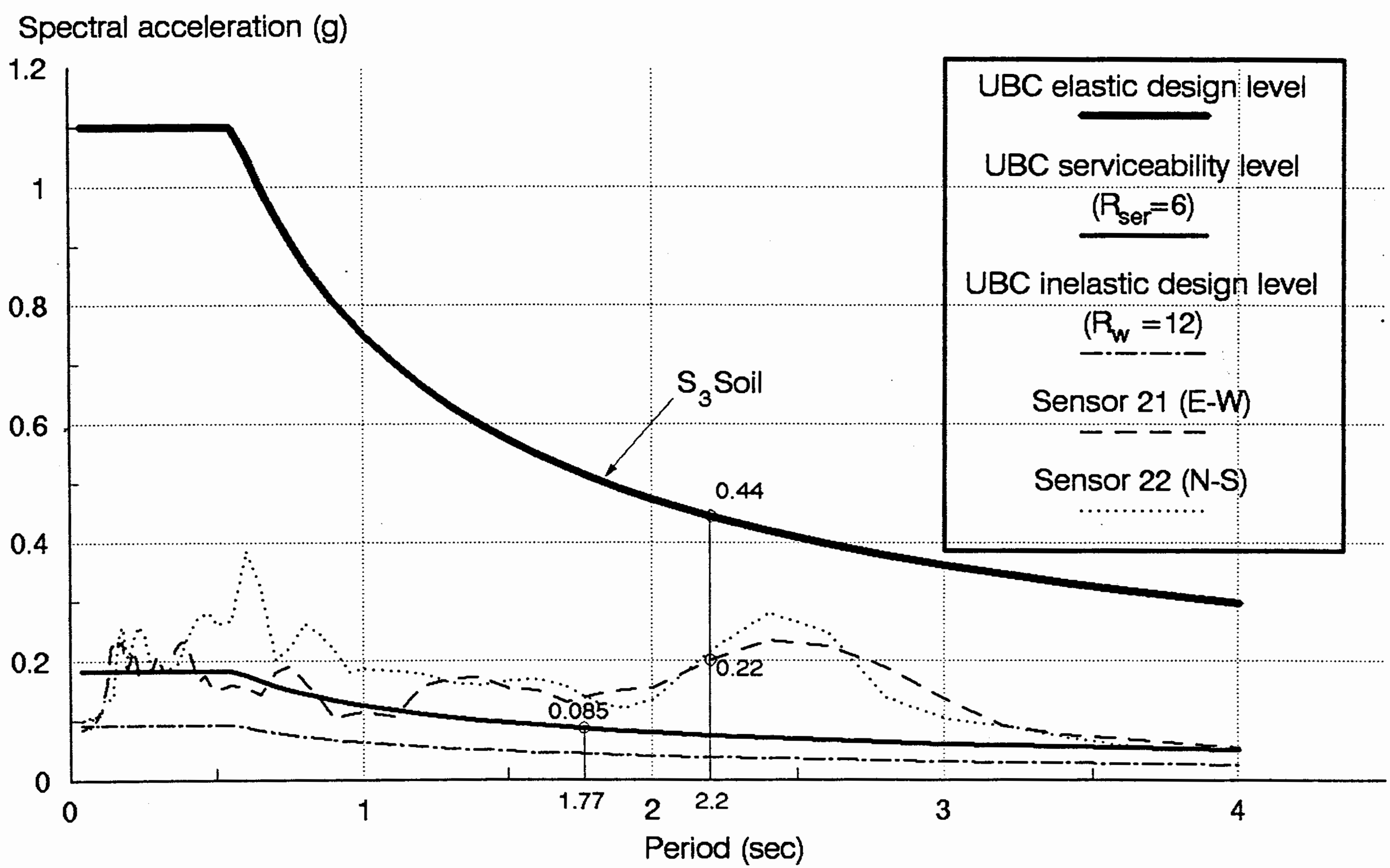

Fig. 3.7 UBC Design Spectra and the Elastic Response Spectra of the Base Acceleration Records (CSMIP357, 5% damping)

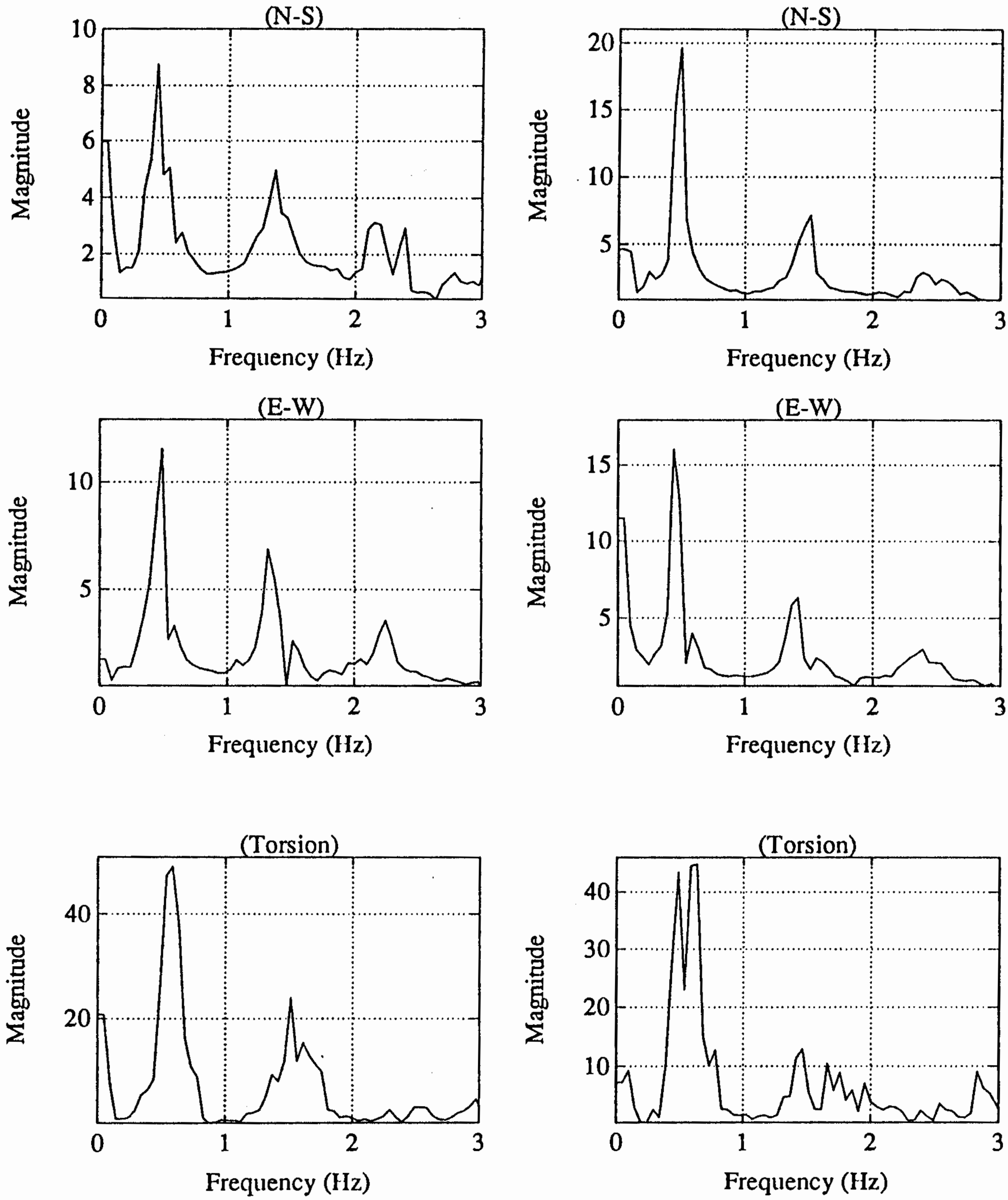

(a) Loma Prieta

(b) Morgan Hill

Fig. 3.8 Magnitude of Acceleration Transfer Functions between the Base and the Roof (CSMIP 357)

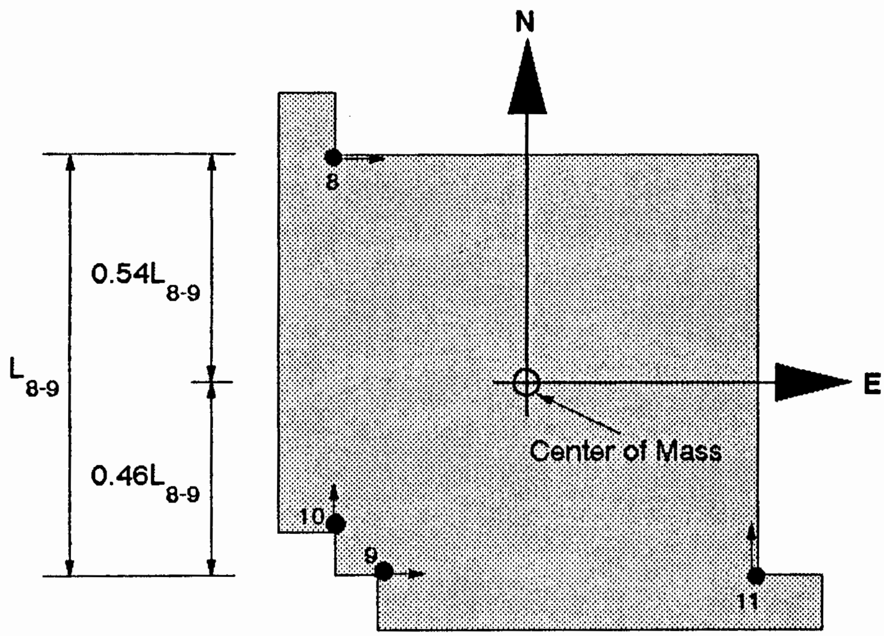

(a) Floor Geometry for Calculating E-W Displacment at Center of Mass

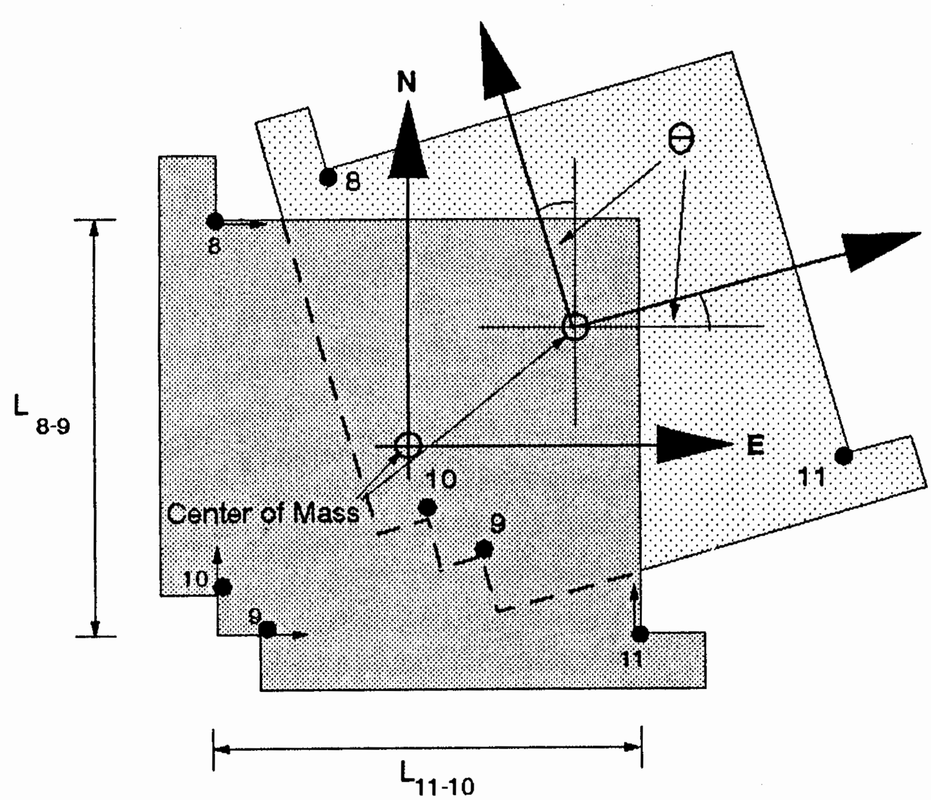

(b) Floor Geometry for Calculating Average Torsional Angle

Fig. 3.9 12th Floor Geometry (CSMIP357)

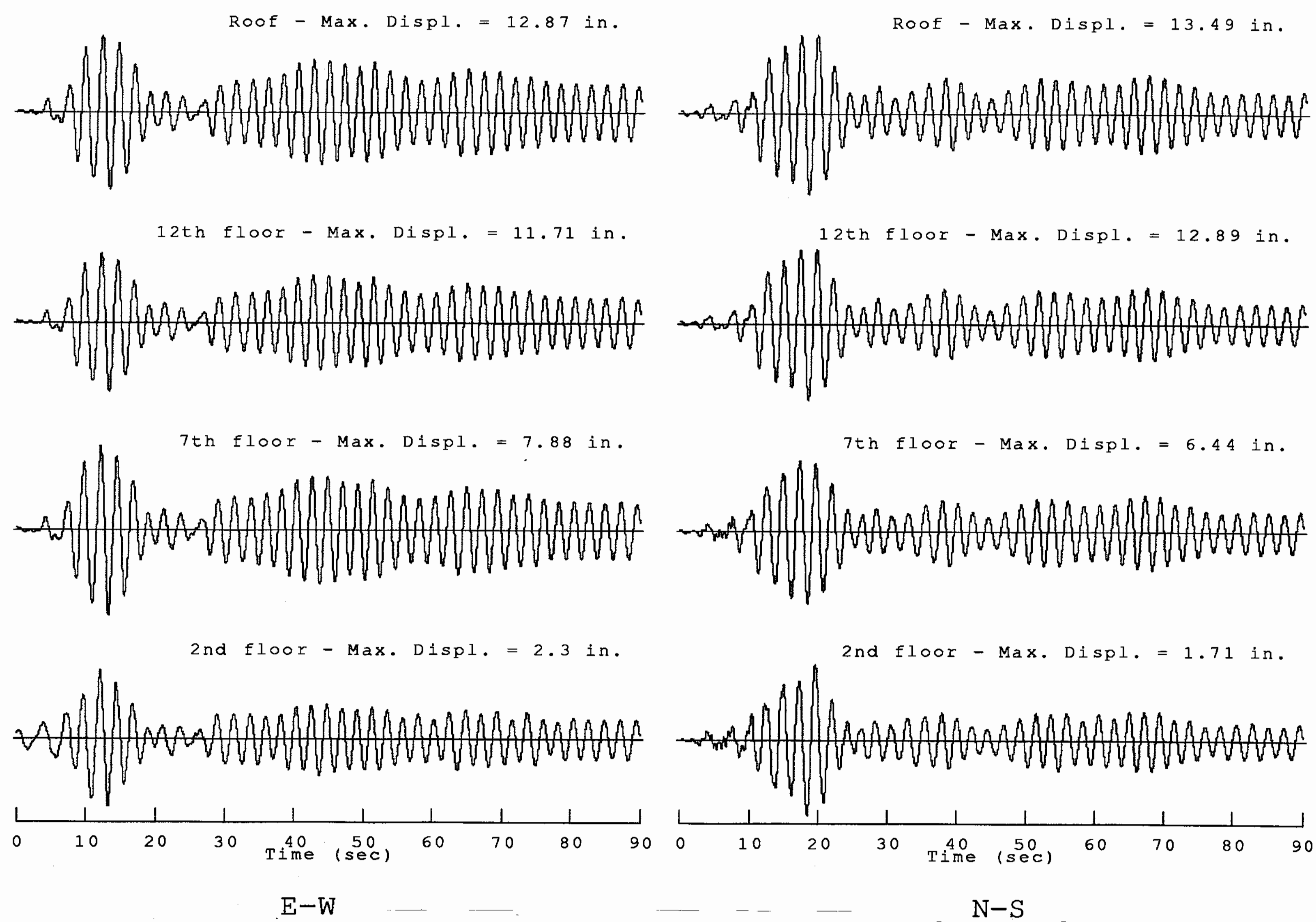

Fig. 3.10 Relative Displacement Time Histories at Center of Mass (CSMIP357)

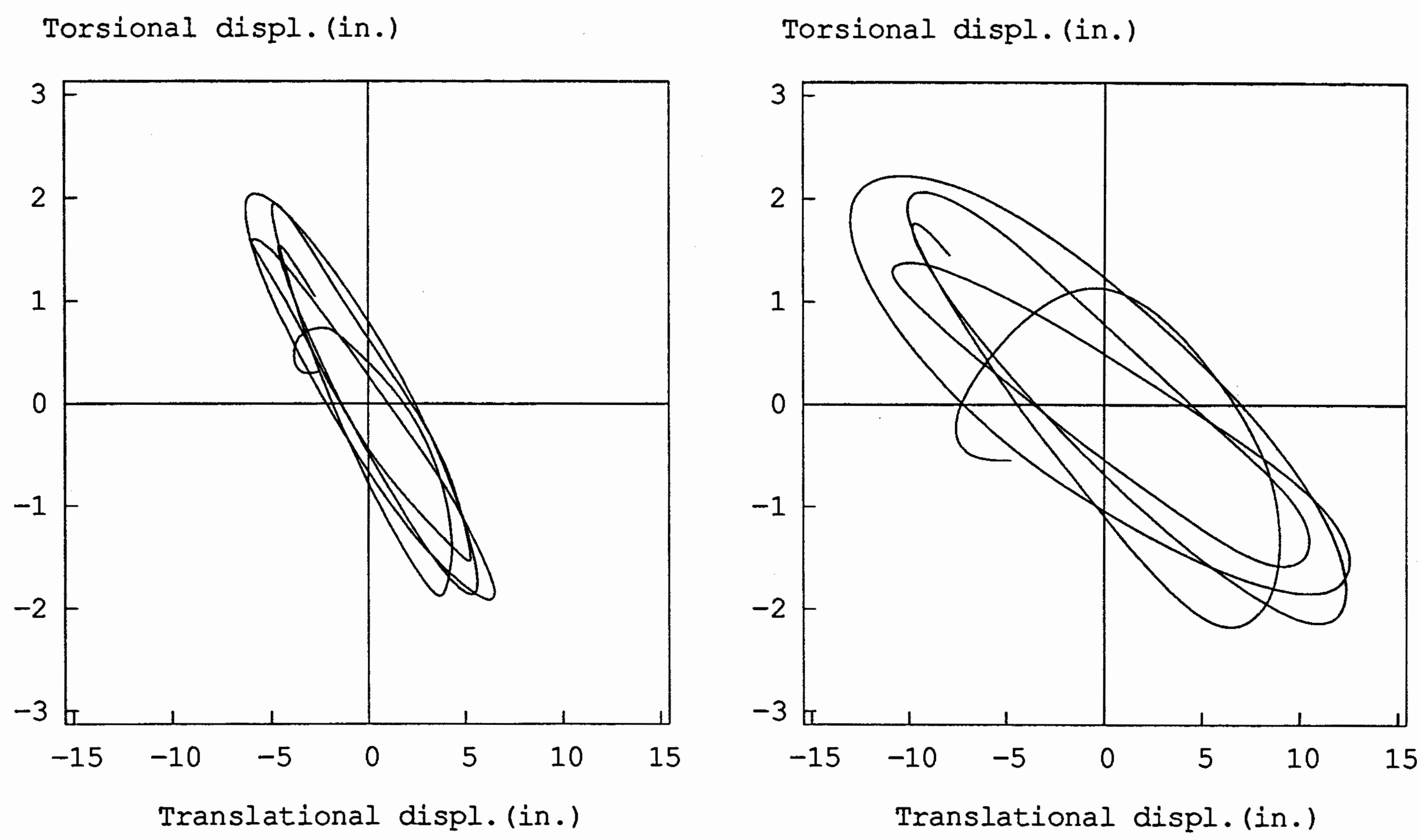

(a) Sensor 15 (7th floor)

(b) Sensor 11 (12th floor)

Fig. 3.11 Translational vs. Torsional Displacements (11-22 sec.)

(CSMIP357)

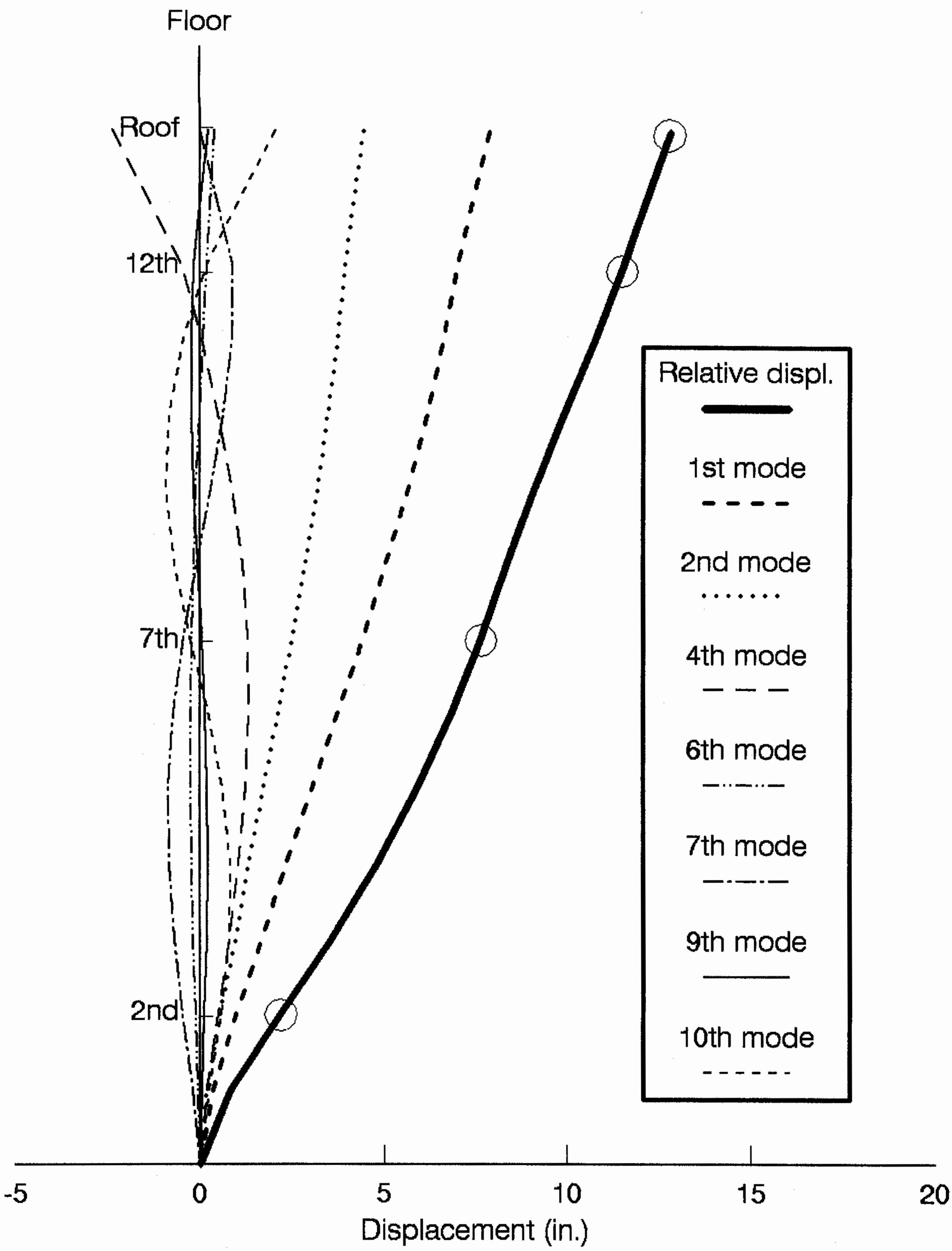

Fig. 3.12 Lateral Displacement Profile at 12.24 sec. of the Loma Prieta Earthquake (CSMIP357, E-W)

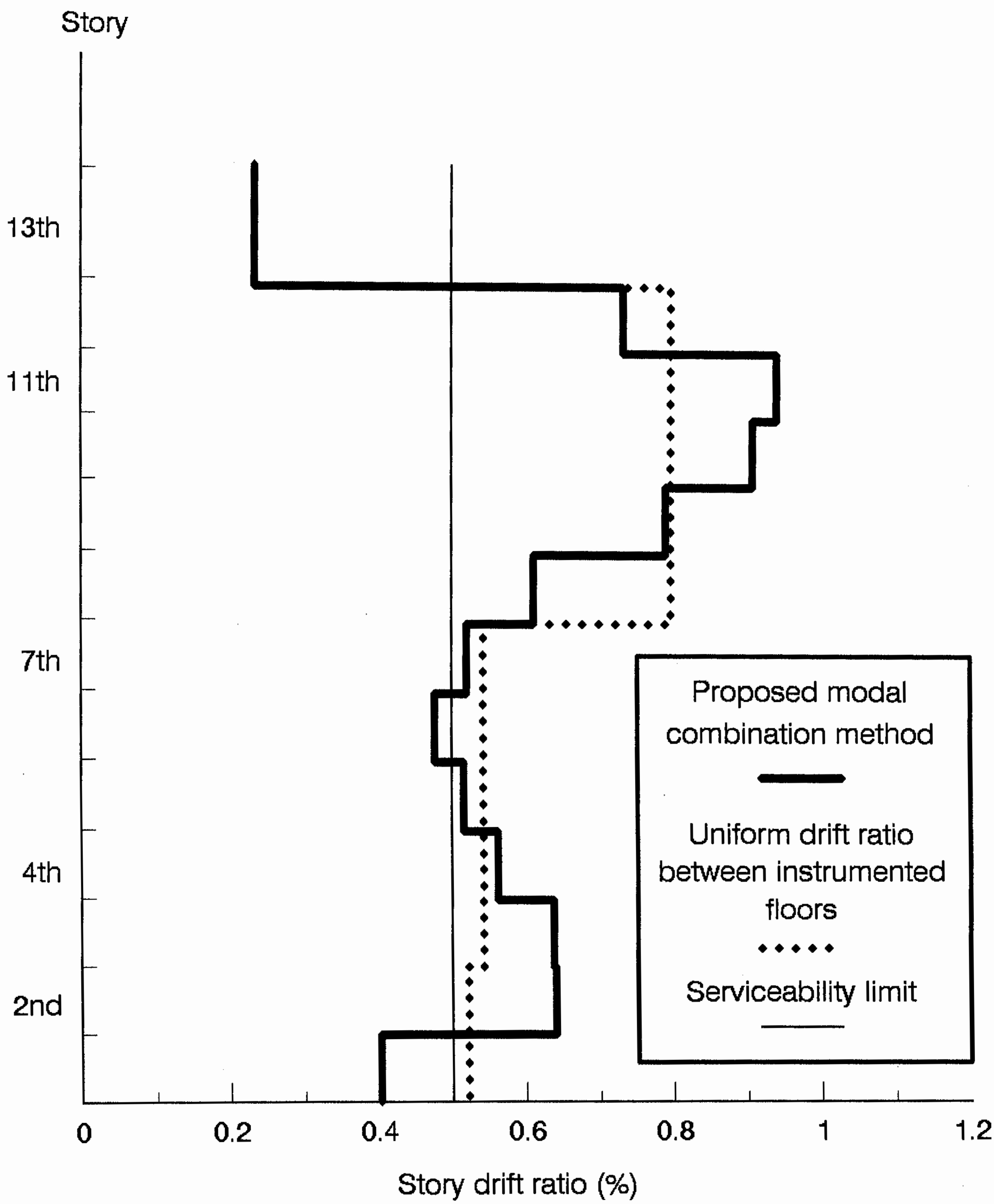

Fig. 3.13 Profile of Story Drift Ratios at Center of Mass (CSMIP357, N-S)

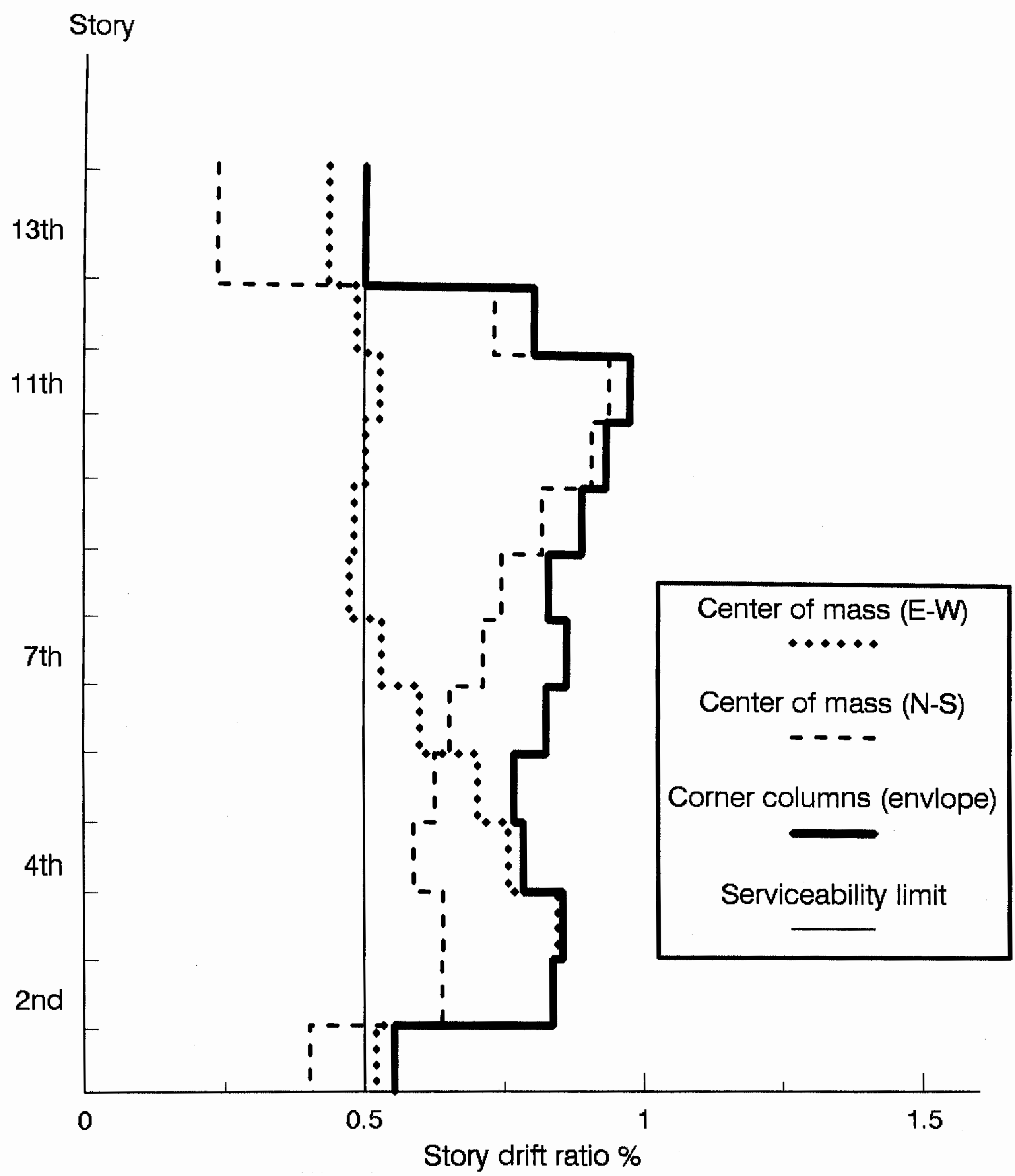

Fig. 3.14 Envelope of Story Drift Ratios

(CSMIP357)

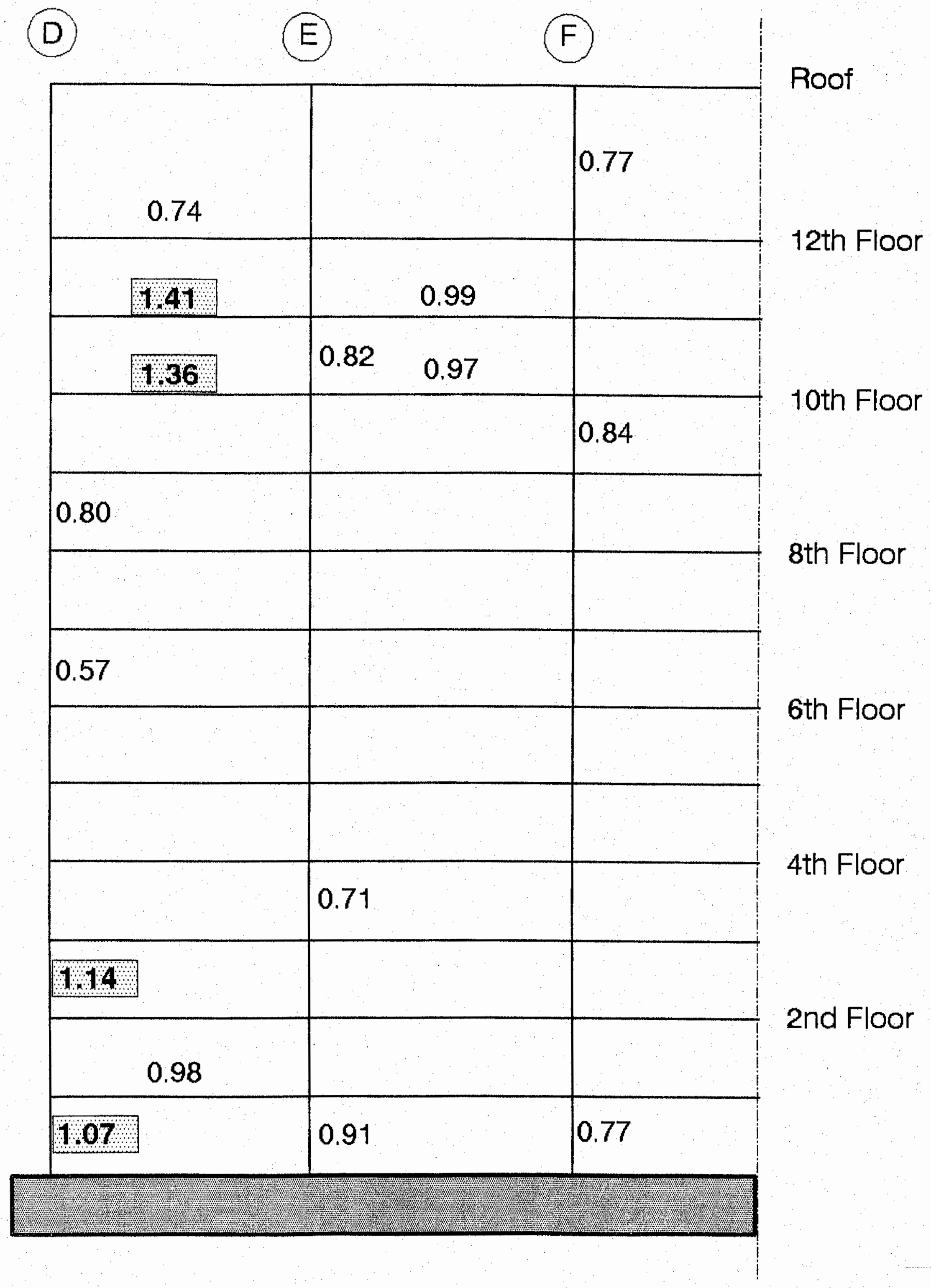

Fig. 3.15 Member Stress Ratios

(CSMIP357, N-S)

Hayward - 6-story Office Bldg.

No. of Stories above/below ground: 6/1
Plan Shape: Rectangular
Base Dimensions: 218' x 92'
Typical Floor Dimensions: 218' x 92'
Design Date: 1966
Construction Date: 1967

Vertical Load Carrying System:
Concrete waffle floors with 4" slabs and 10" deep two way joists; concrete columns.
Lateral Force Resisting System:
Concrete shear walls.
Foundation Type:
Spread footings under columns; combined footings under shear walls.

Fig. 4.1 Hayward 6-story Office Building (CSMIP462, Shakal, et al., 1989)

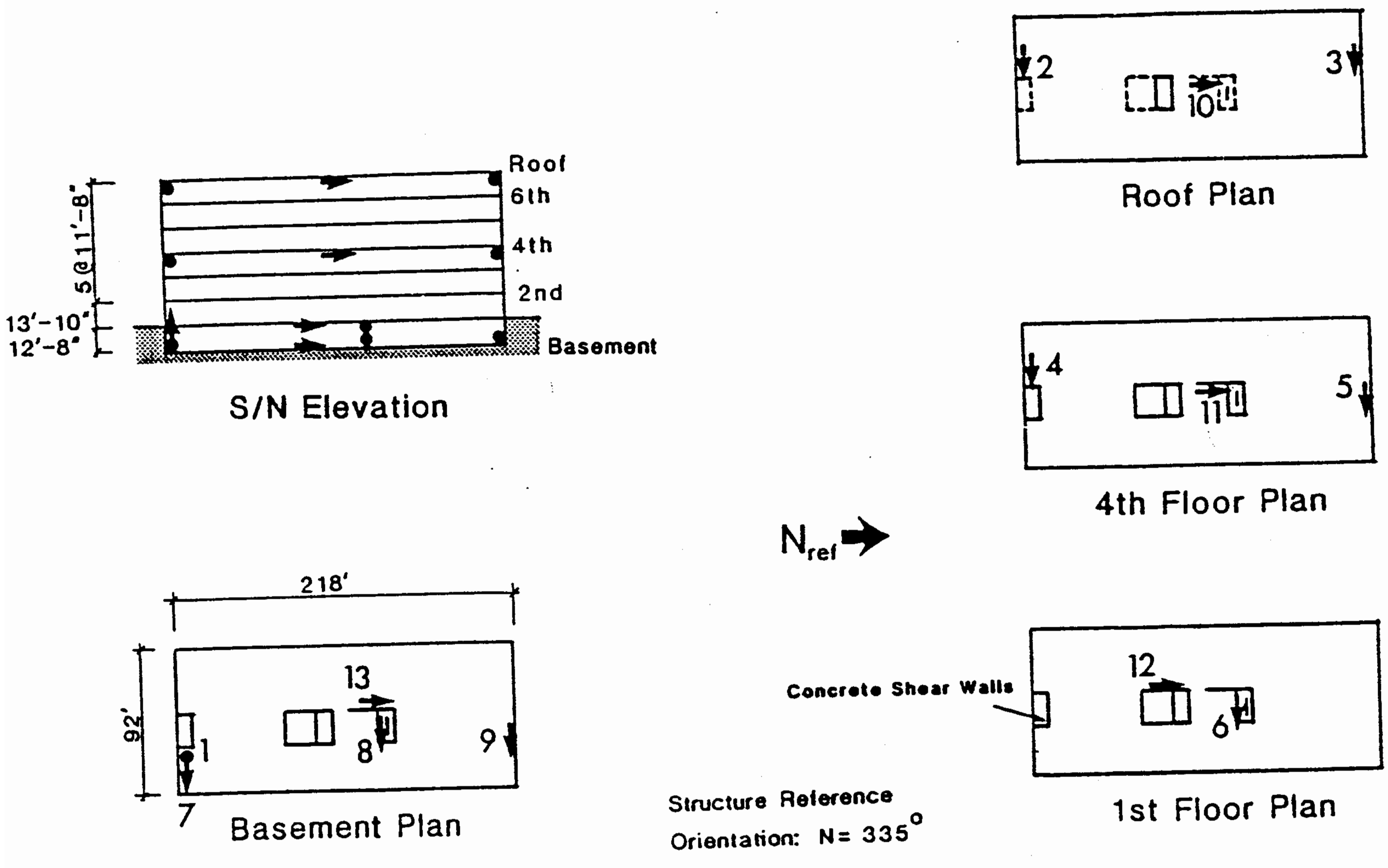

Fig. 4.2 General Layout of Building CSMIP462 (Shakal, et al., 1989)

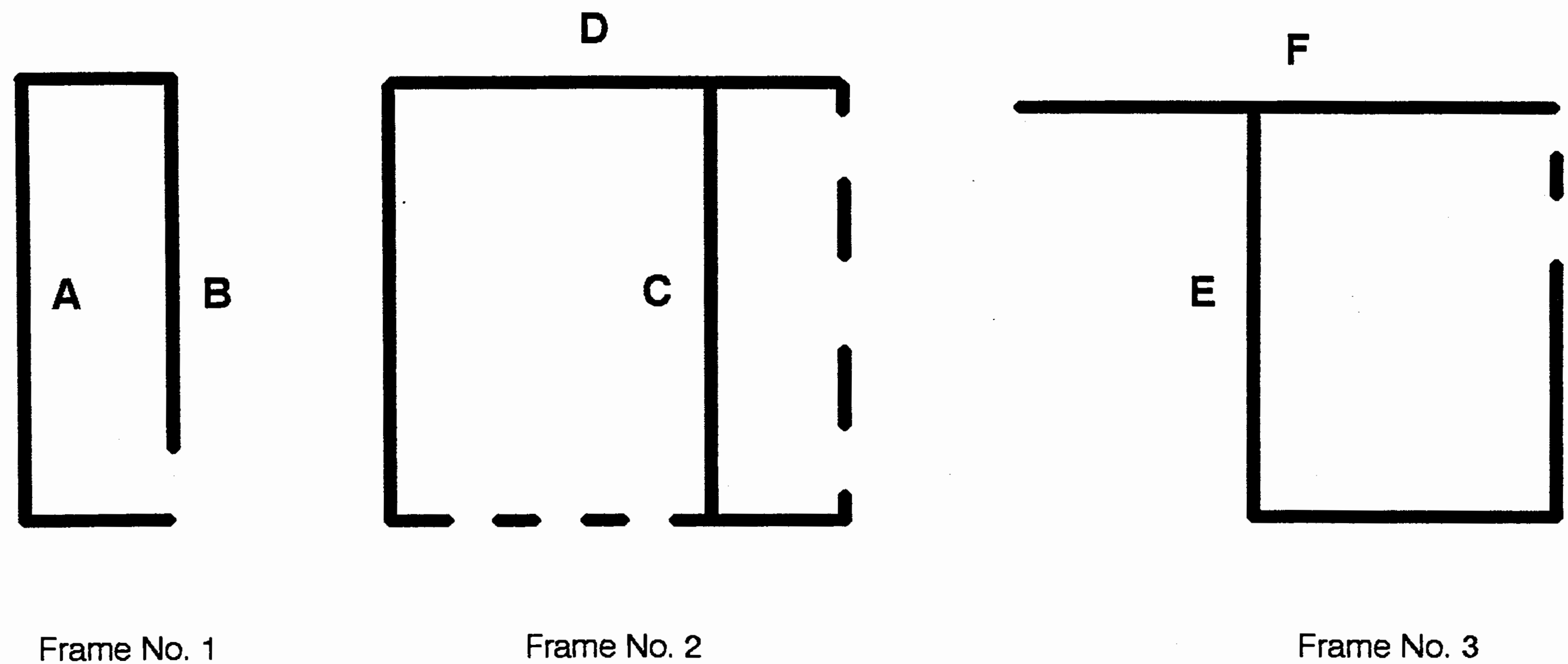

Fig. 4.3 Frame Plans and Selected Wall Arrangement

(CSMIP462)

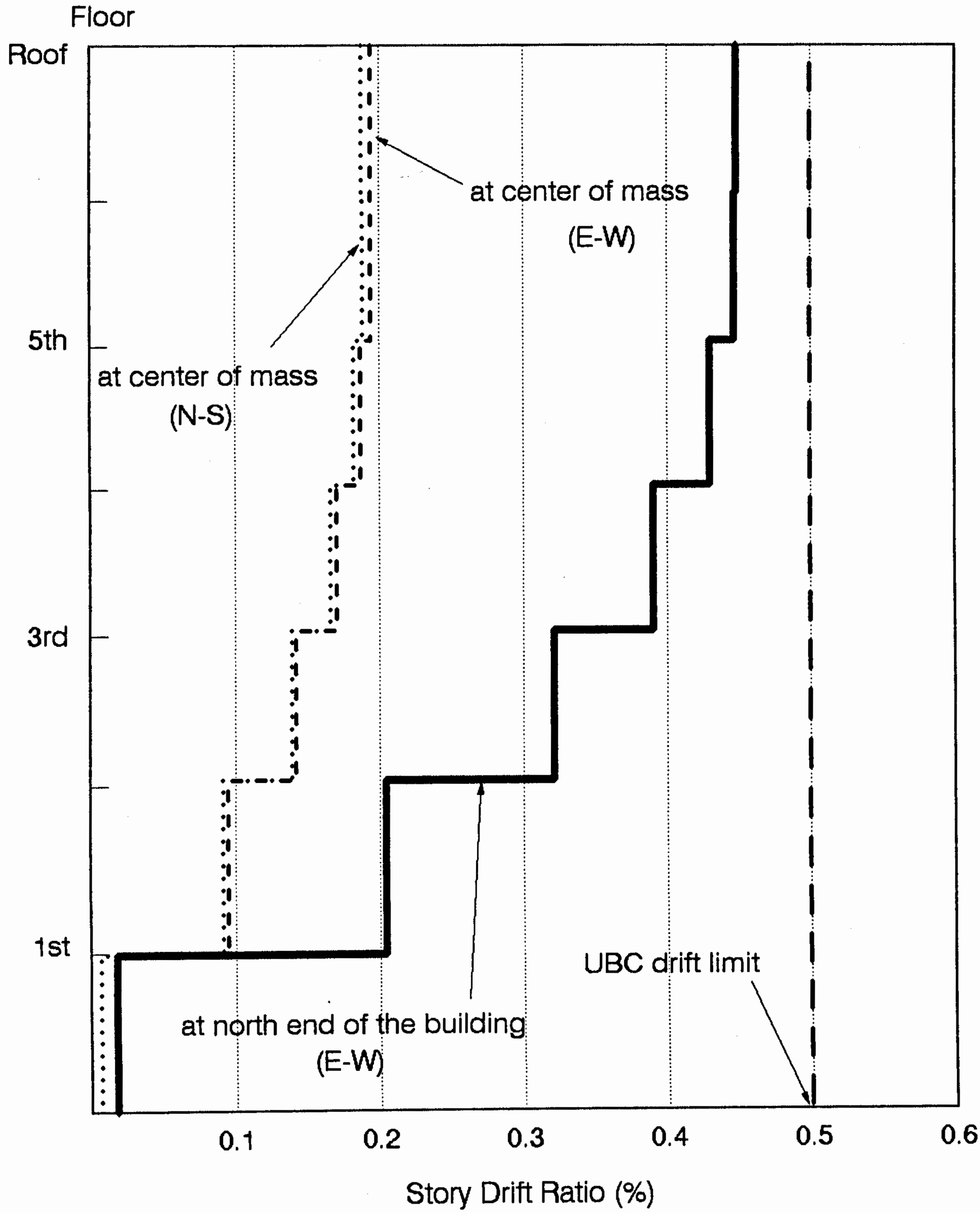

Fig. 4.4 Story Drift Ratios for the 1991 UBC Design

(CSMIP462)

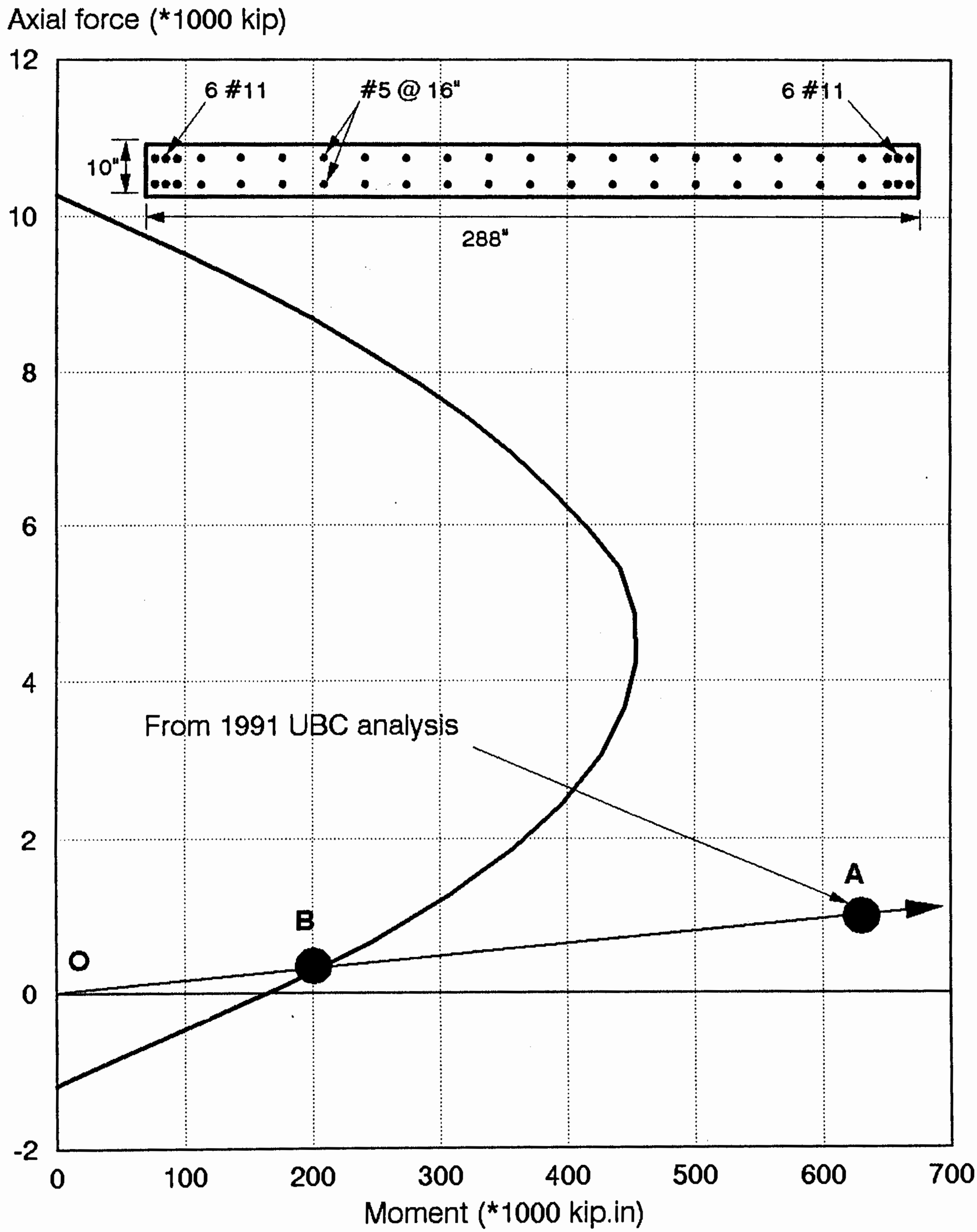

Fig. 4.5 Axial Force vs. Moment Interaction Diagram

(CSMIP462, Wall E, 2nd story)

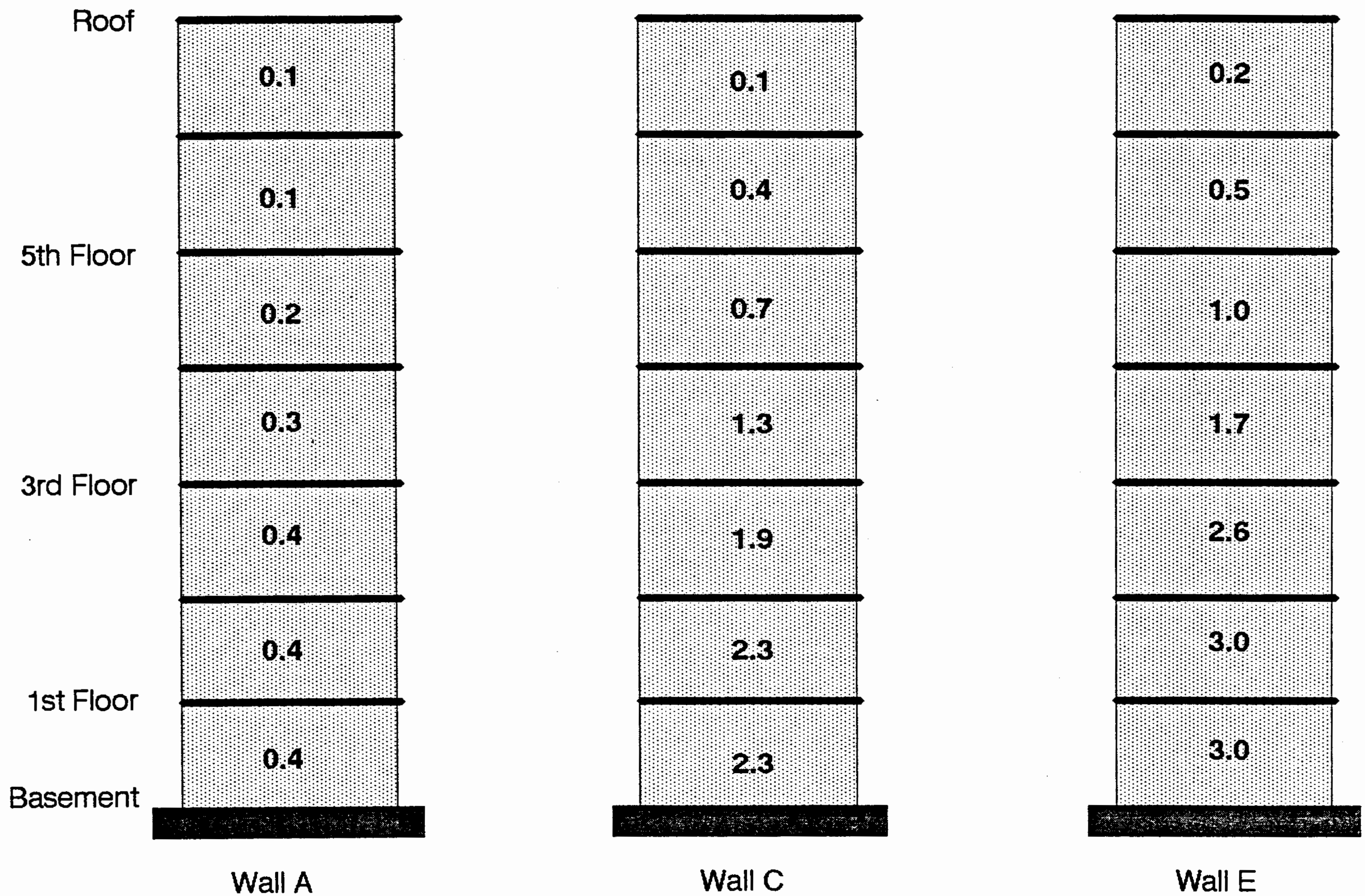

Fig. 4.6 1991 UBC Design Wall Capacity Ratios

(CSMIP462)

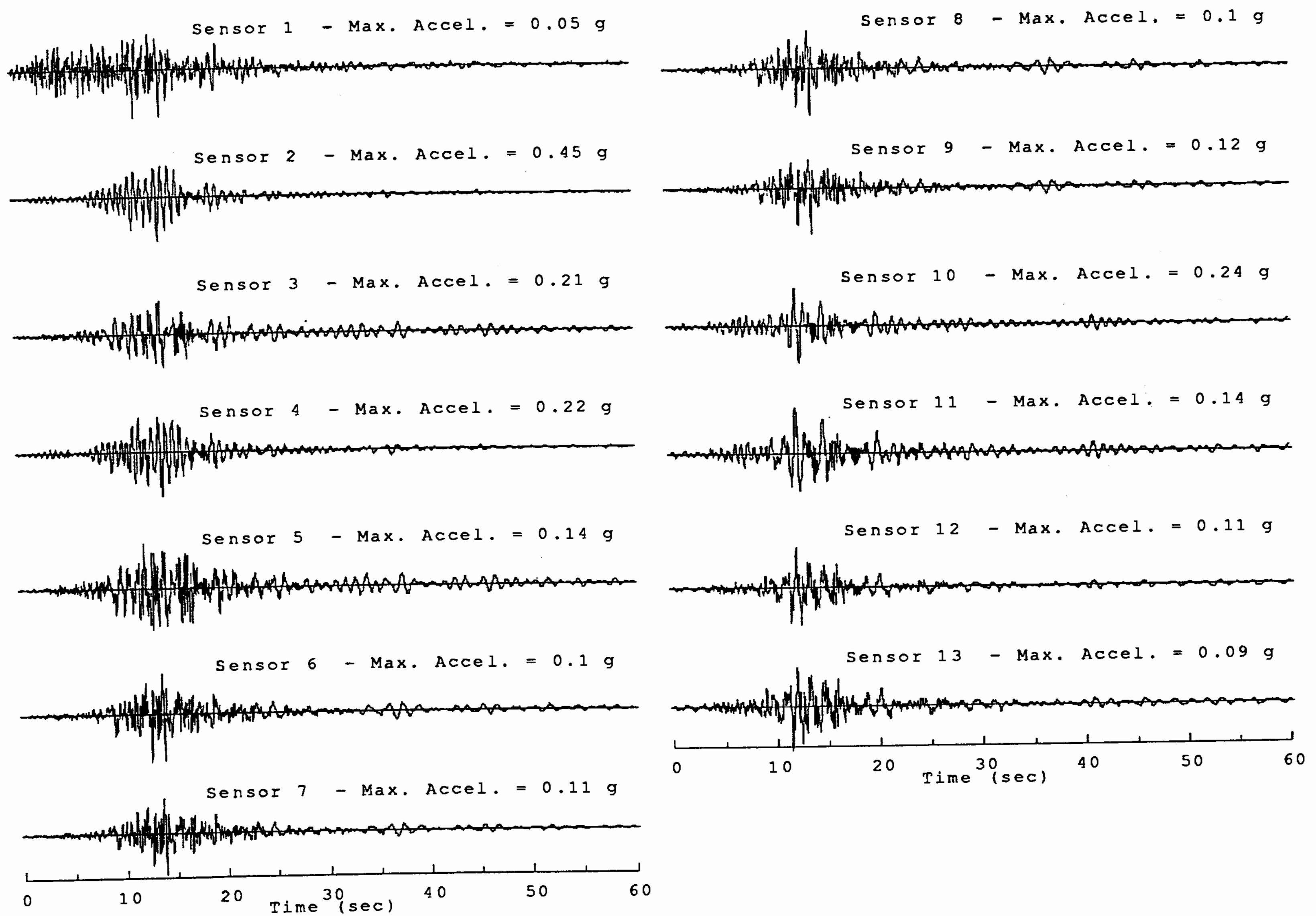

Fig. 4.7 Building CSMIP462 Acceleration Records

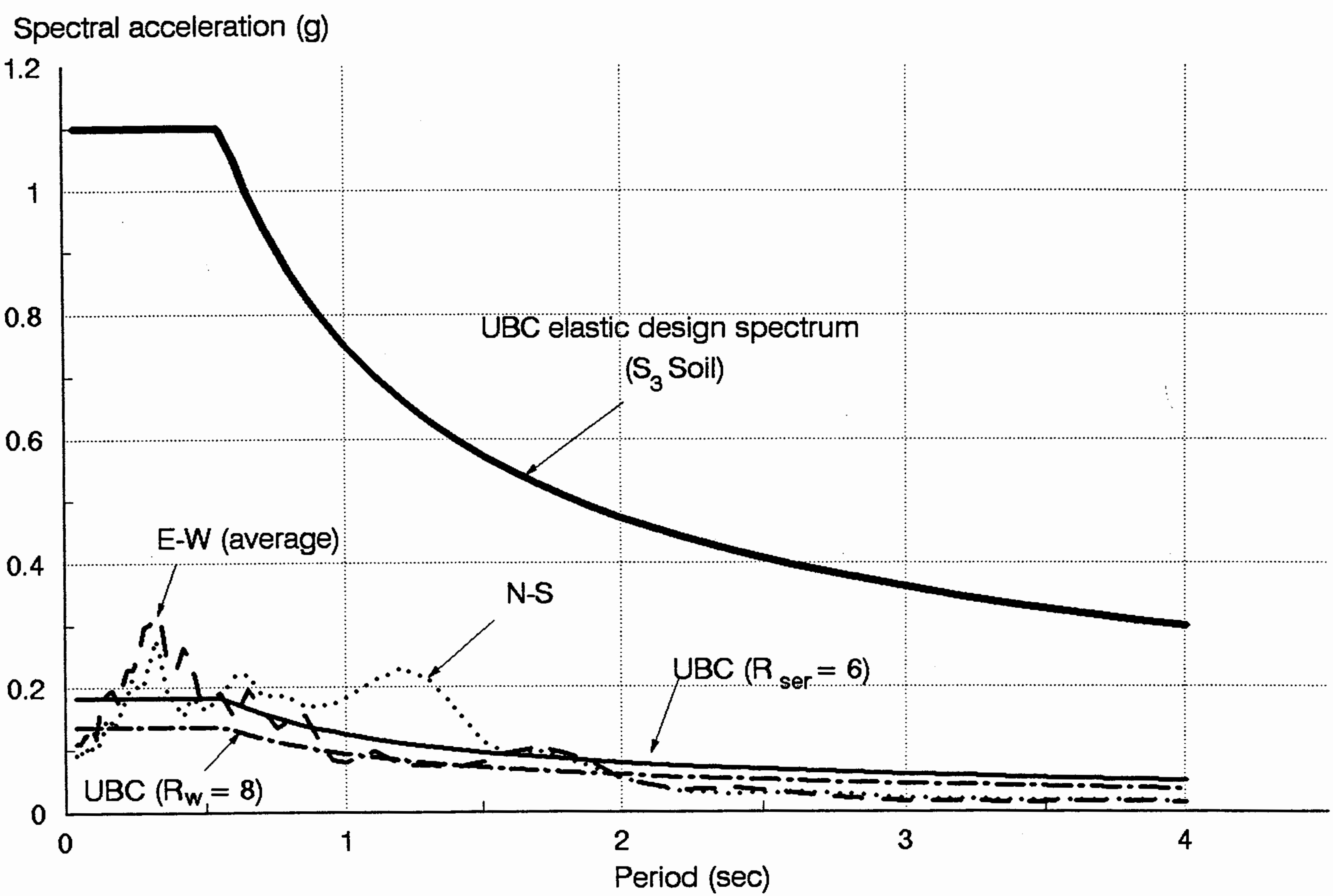

Fig. 4.8 UBC Design Spectra and the Elastic Response Spectra of the Base Acceleration Records (CSMIP462, 5% damping)

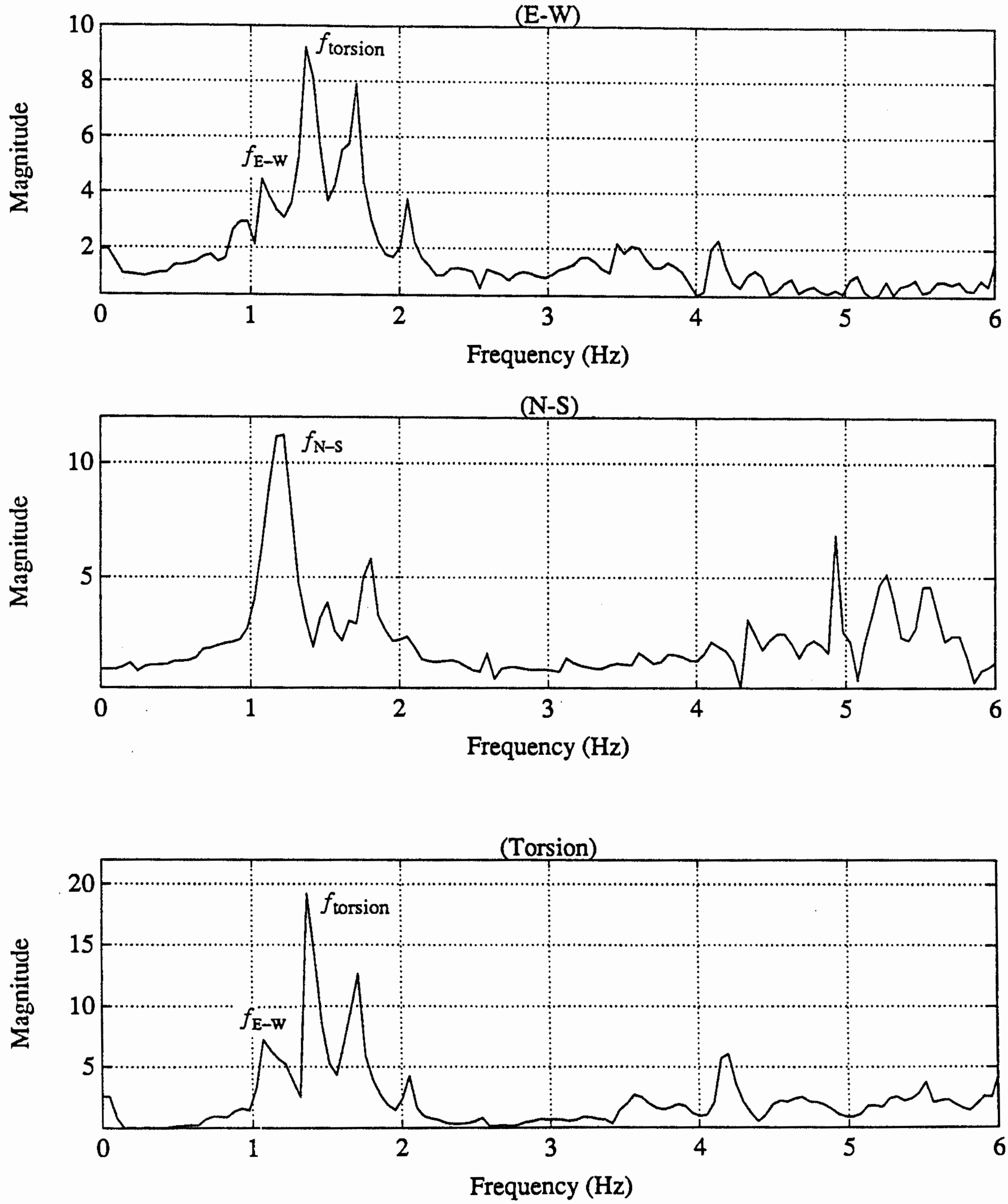

Fig. 4.9 Magnitude of Acceleration Transfer Functions between the Base and the Roof Floor (CSMIP 462)

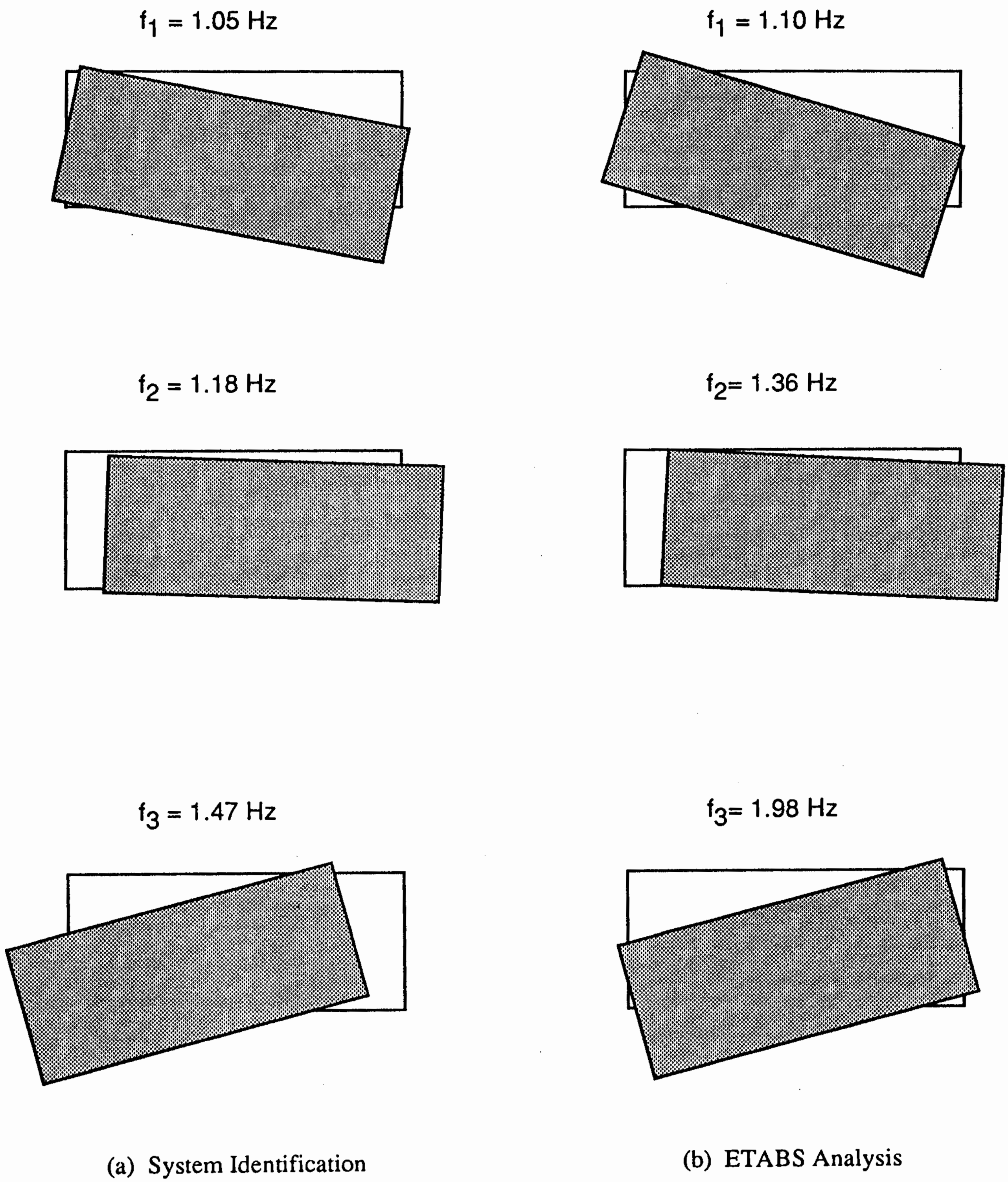

Fig. 4.10 Mode Shapes at Roof Level (CSMIP 462)

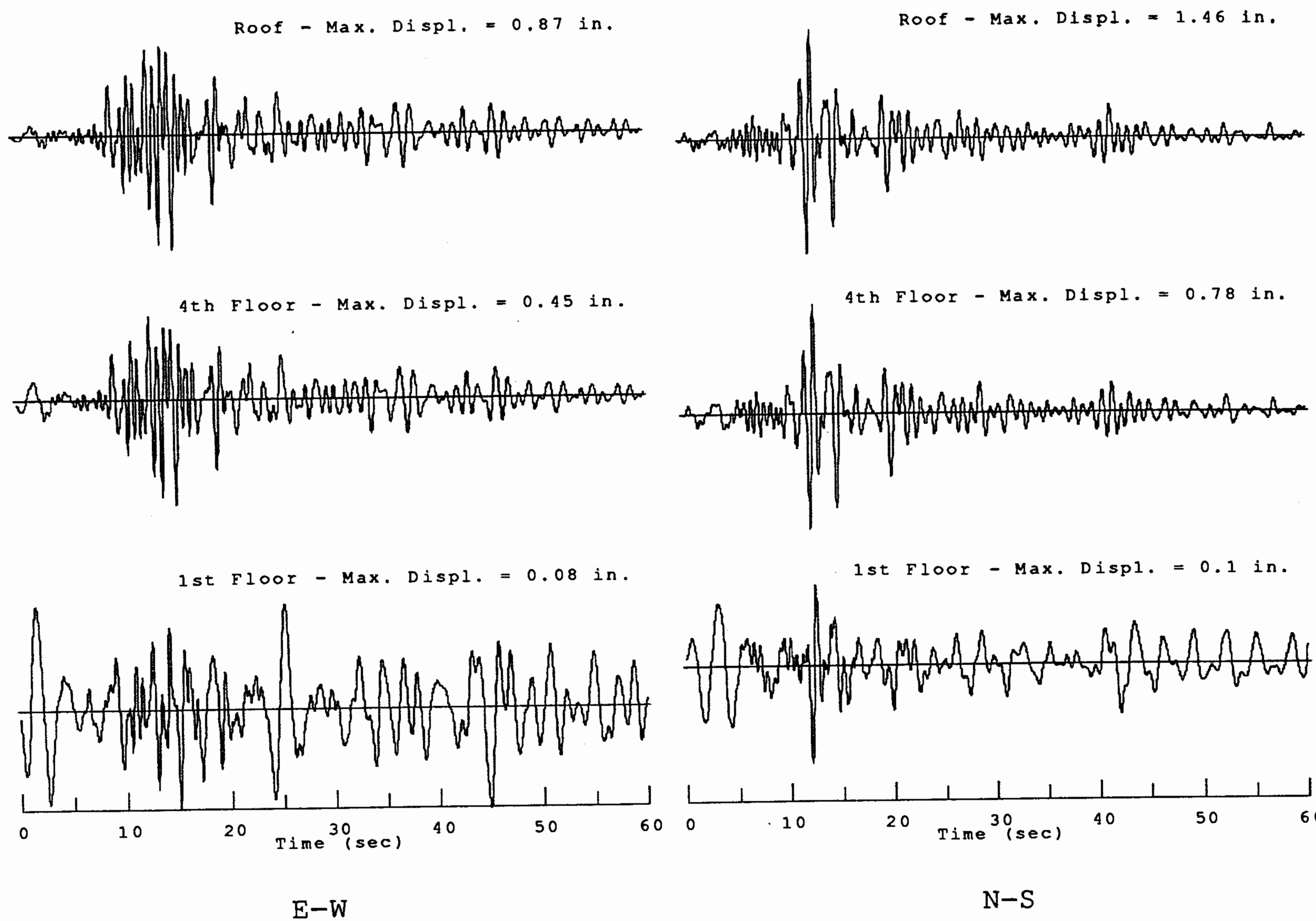

Fig. 4.11 Relative Displacement Time Histories at Center of Mass

(CSMIP462)

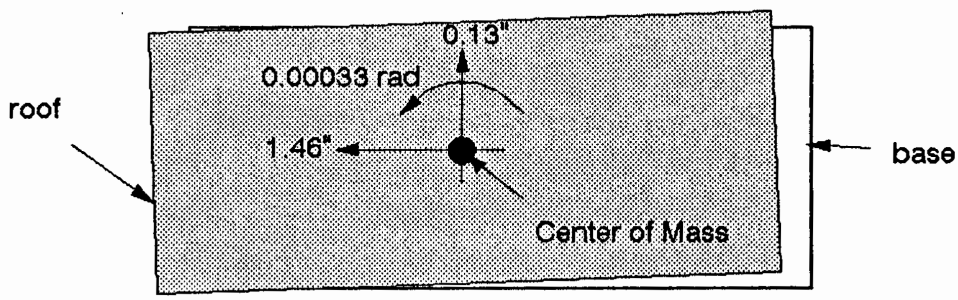

Case 1, t=12.08 sec

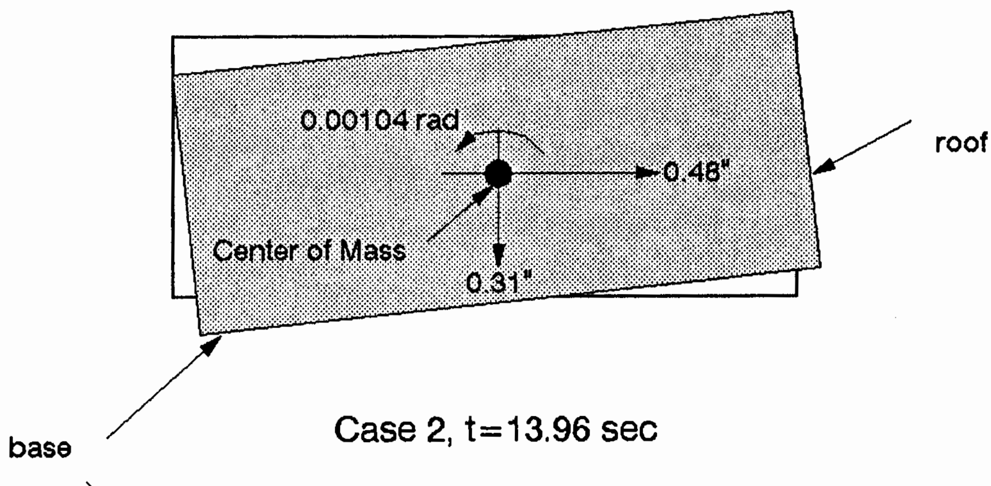

Case 2, t=13.96 sec

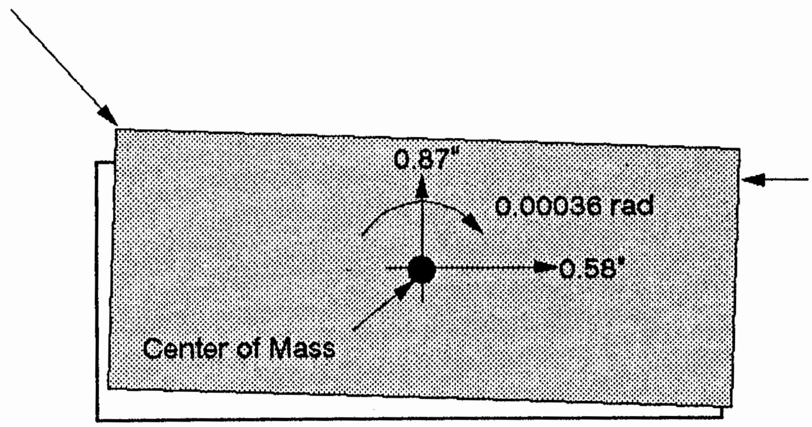

Case 3, t=15.04 sec

Fig. 4.12 Imposed Peak Responses at Roof Level (CSMIP462)

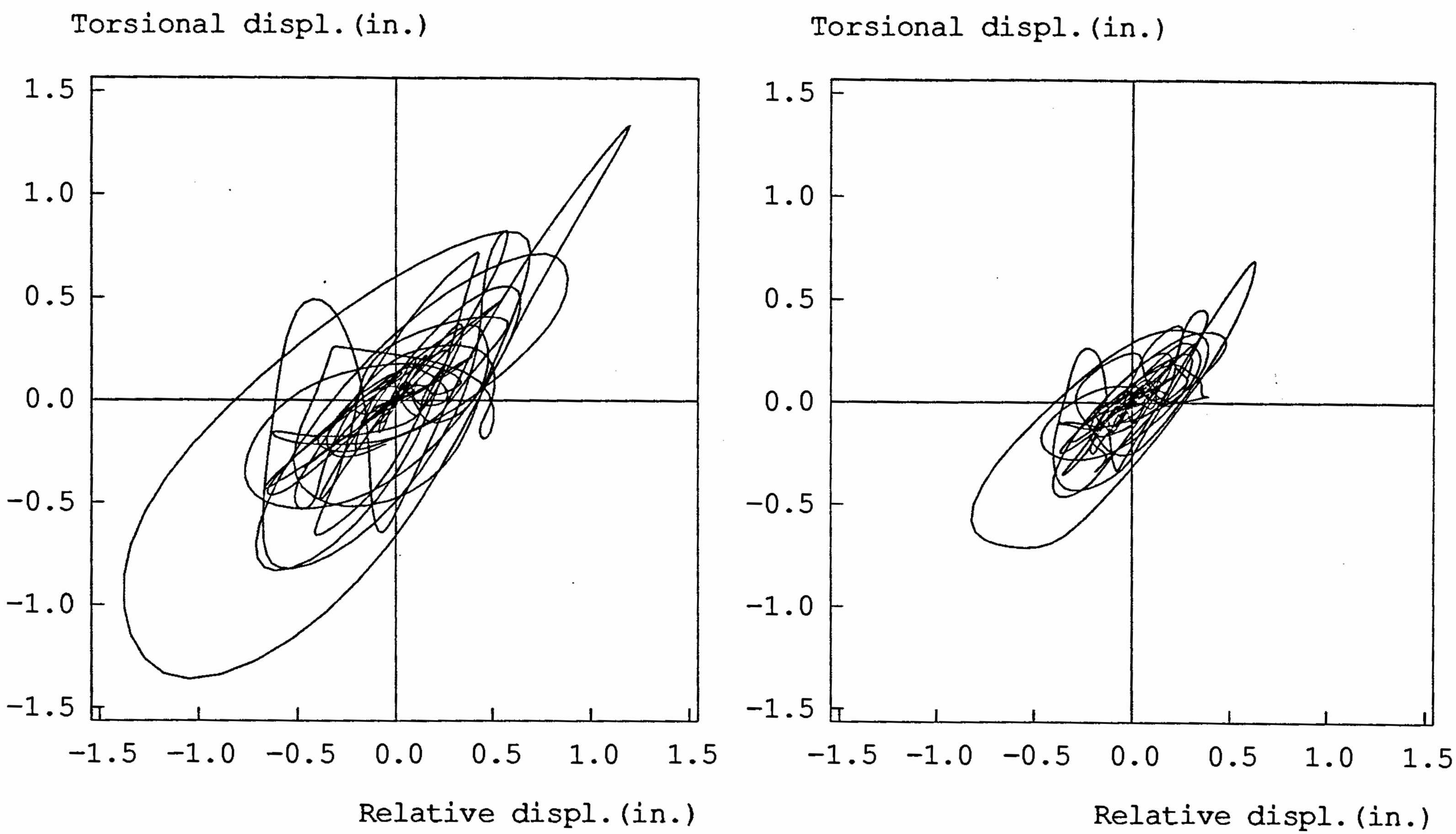

(a) Sensor 3 (Roof)

(b) Sensor 5 (4th floor)

Fig. 4.13 Relative vs. Torsional Displacements (5-25 sec.)

(CSMIP462)

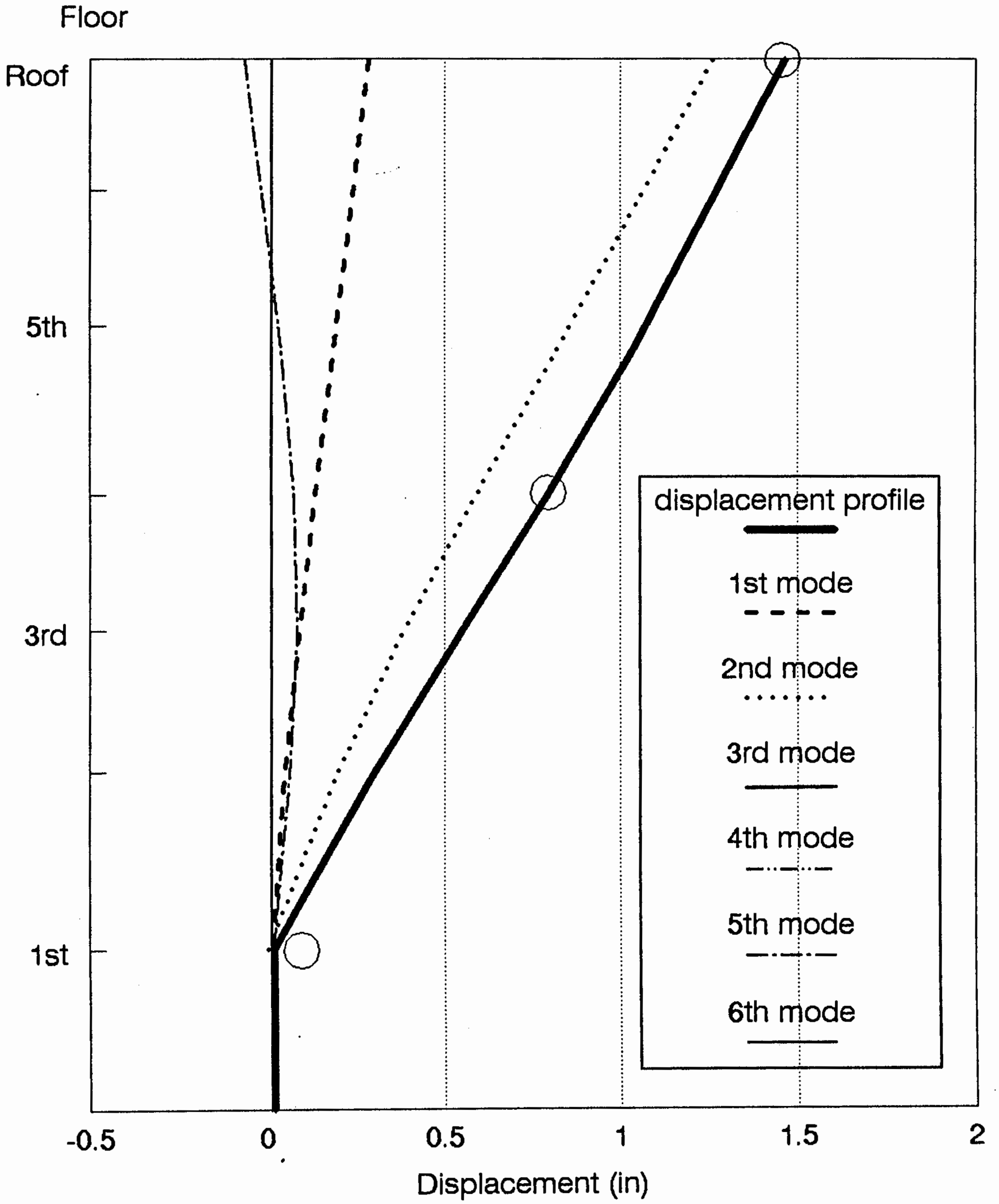

Fig. 4.14 Lateral Displacement Profile at Peak Response, Case 1

(CSMIP462, N-S)

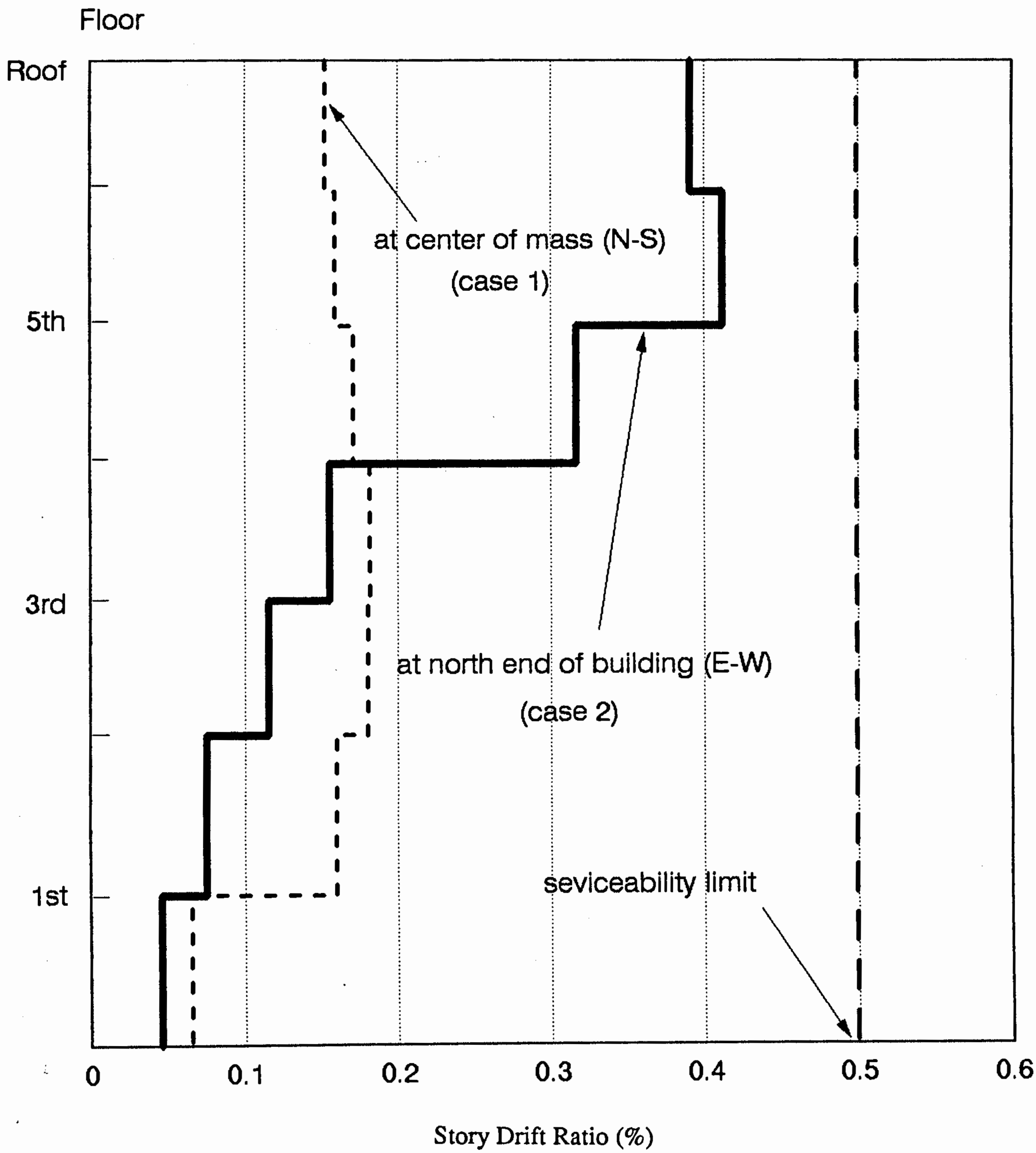

Fig. 4.15 Story Drift Ratios Produced by Loma Prieta Earthquake

(CSMIP462)

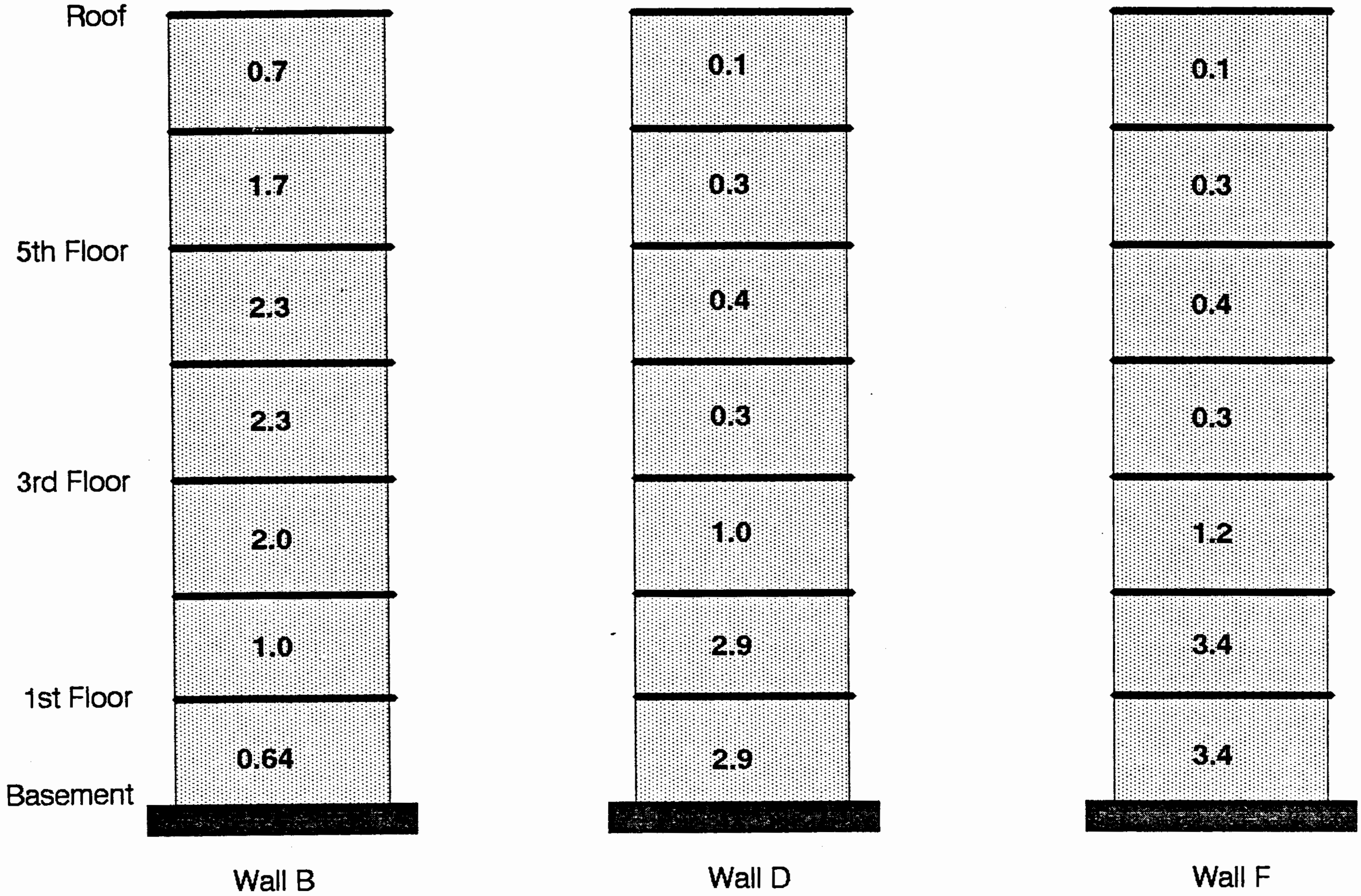

Fig. 4.16 Wall Capacity Ratios Produced by the Loma Prieta Earthquake

(CSMIP462)

San Jose - 10-story Residential Bldg.

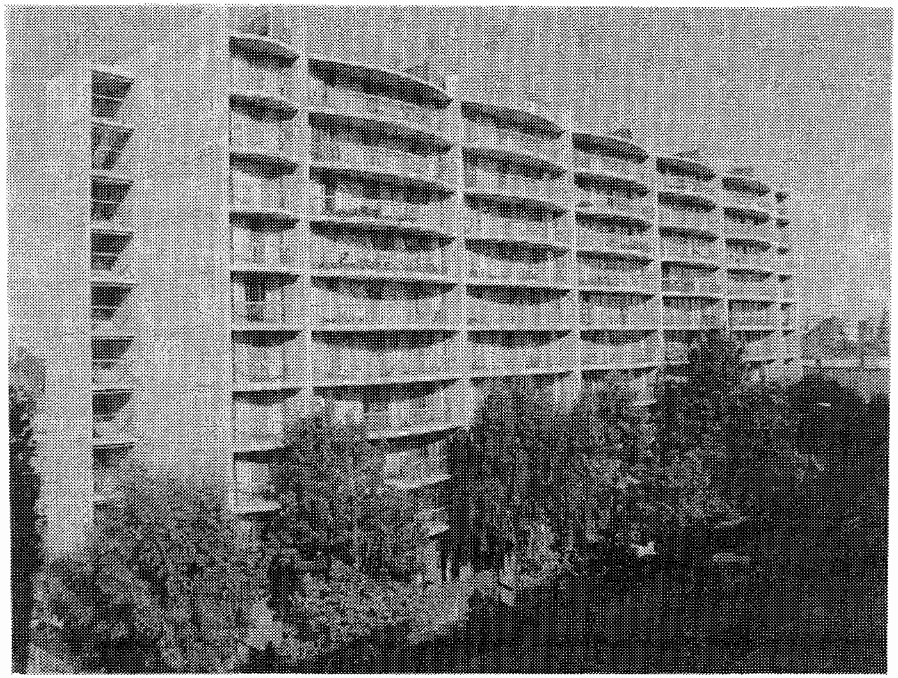

No. of Stories above/below ground: 10/0
Plan Shape: Rectangular
Base Dimensions: 210' x 64'
Typical Floor Dimensions: Same as base
Design Date: 1971
Construction Date: 1971-72

Vertical Load Carrying System:
One-way post-tensioned flat slabs on reinforced concrete bearing walls.
Lateral Force Resisting System:
Concrete shear walls at regular intervals in transverse direction, and along interior corridors in longitudinal direction.
Foundation Type:
Precast-prestressed concrete piles under all walls.

Fig. 5.1 San Jose 10-story Residential Building (CSMIP356, Shakal, et al., 1989)

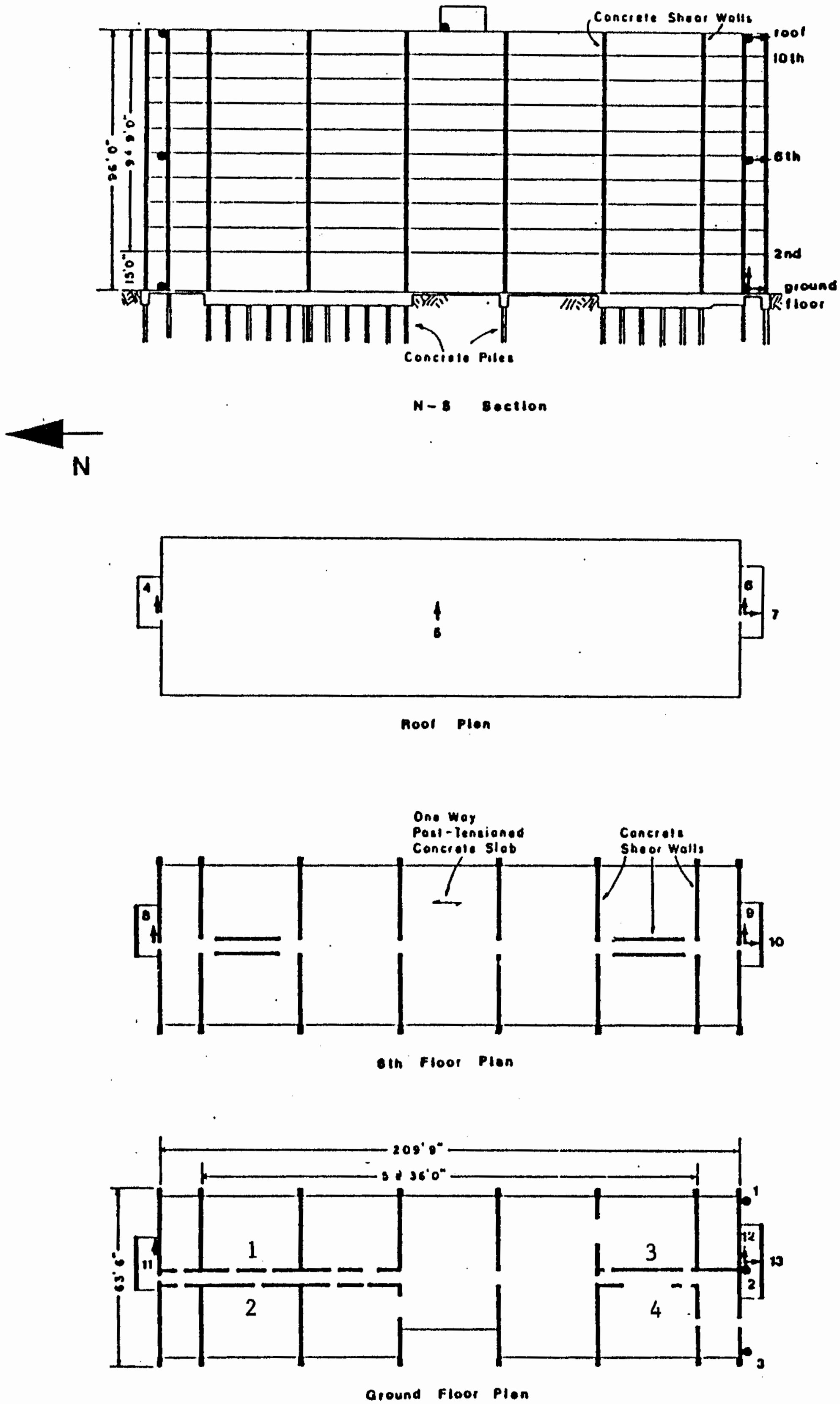

Fig. 5.2 General Layout of Building CSMIP356 (Shakal, et al., 1989)

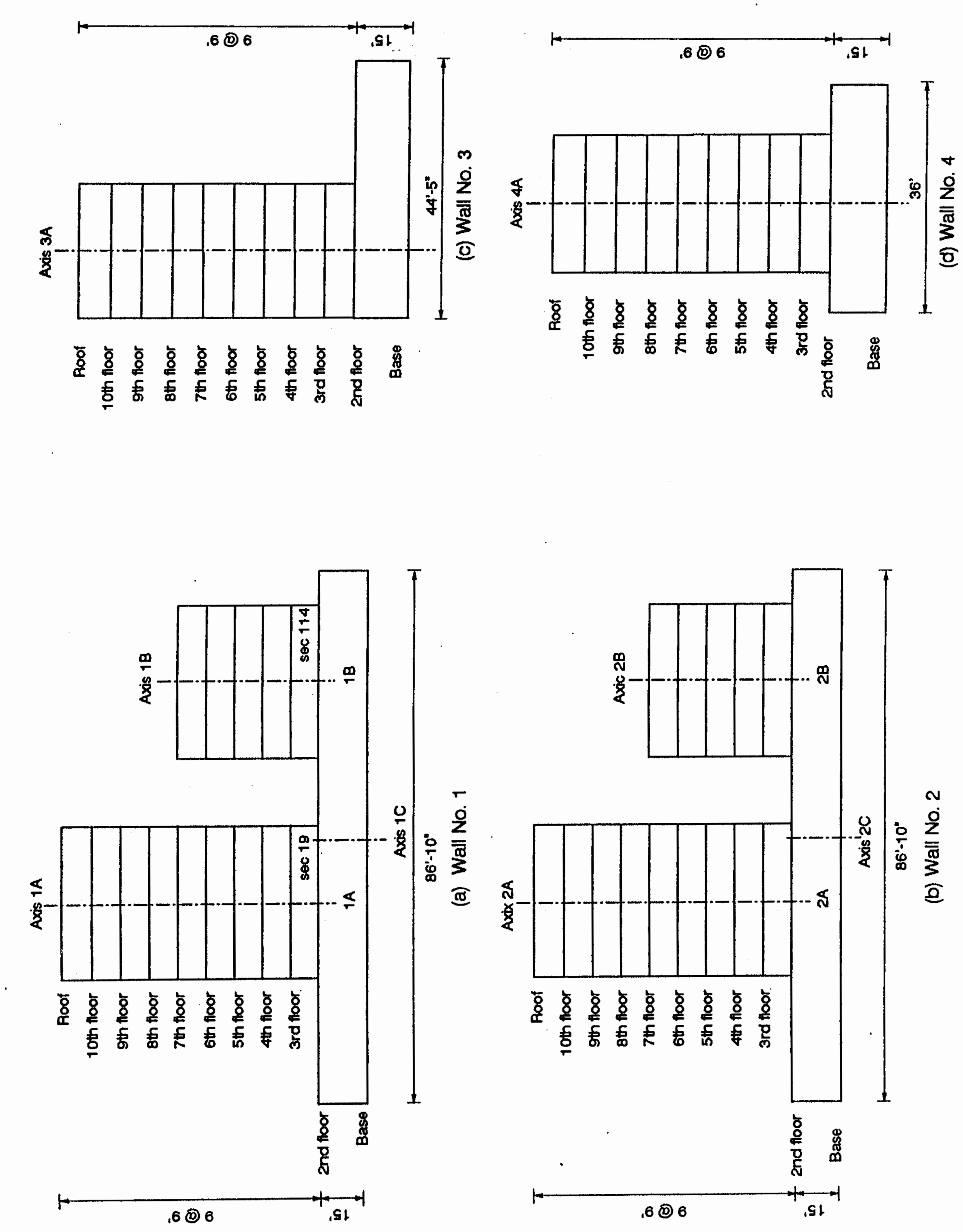

Fig. 5.3 Elevations of N-S Walls (CSMIP356)

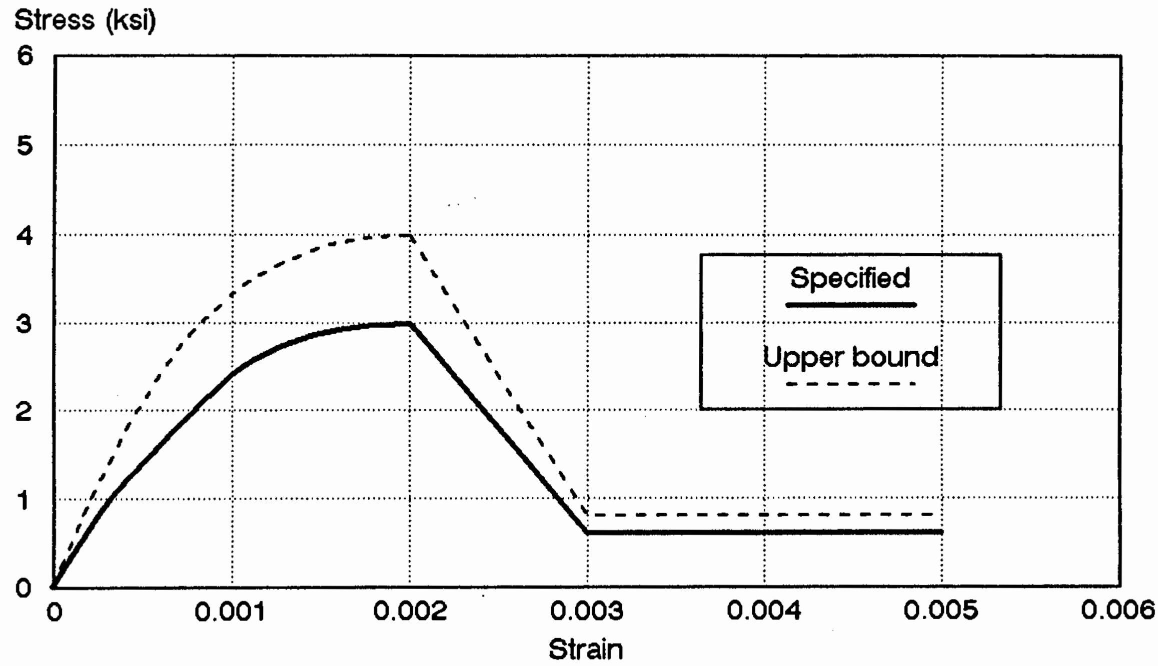

(a) Concrete

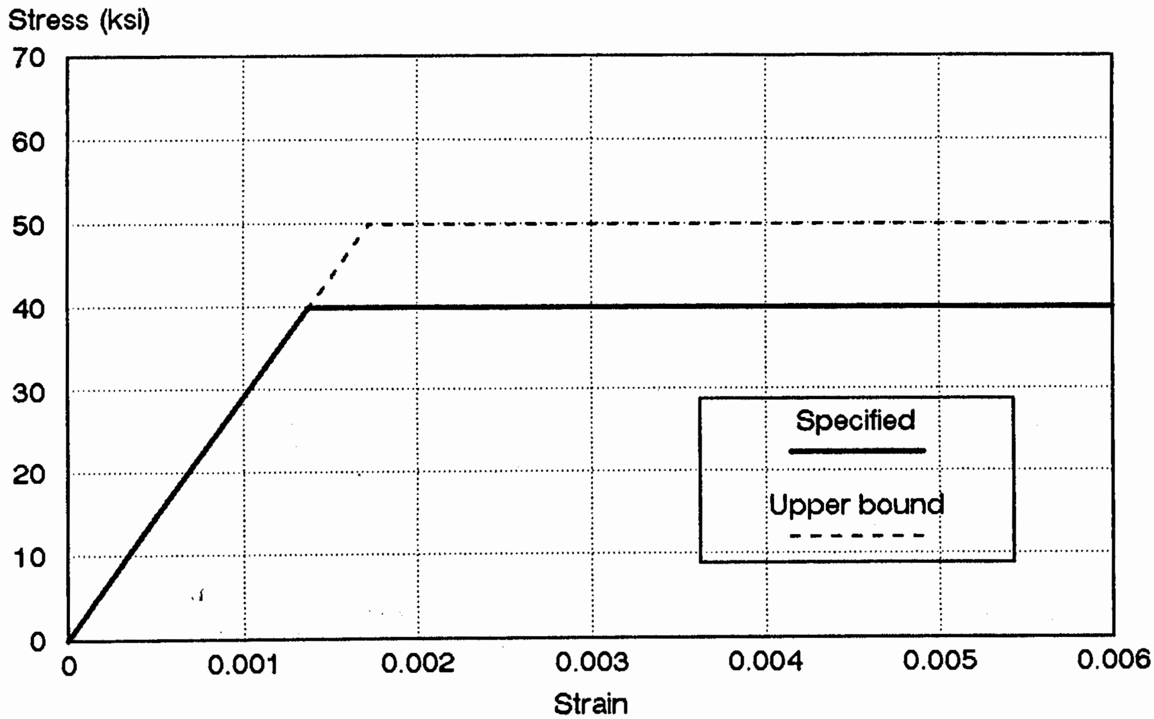

(b) Steel

Fig. 5.4 Concrete and Steel Stress-Strain Relationships

(CSMIP356)

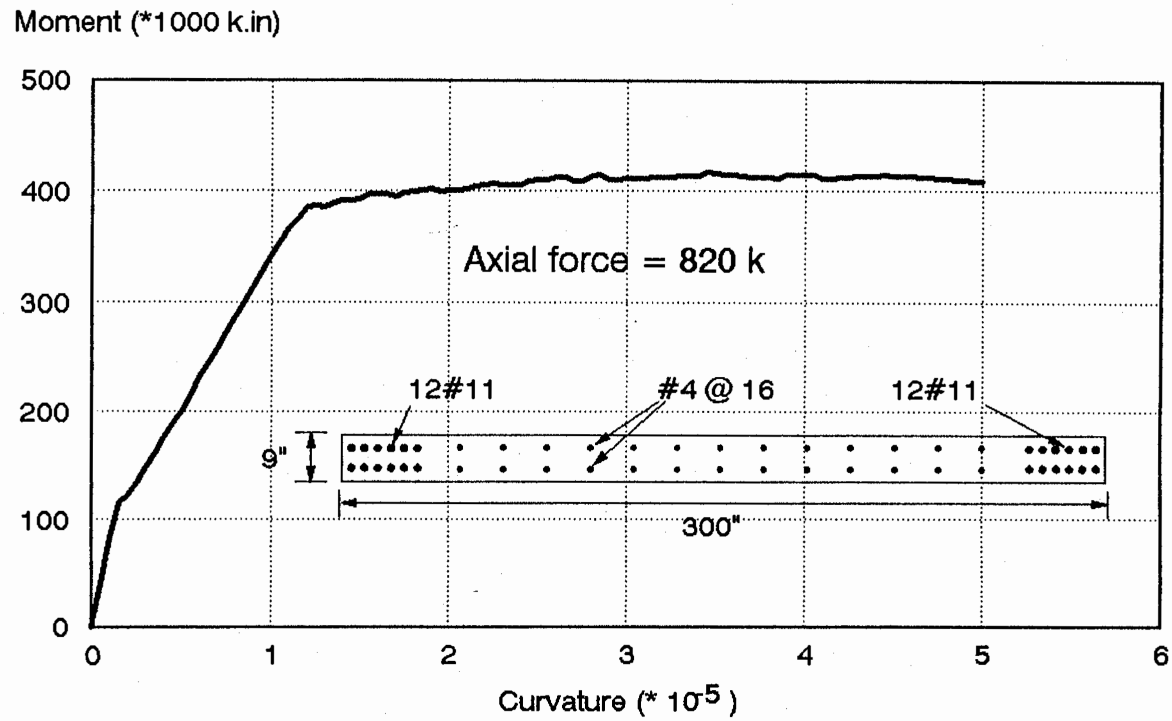

(a) Wall sec. 19

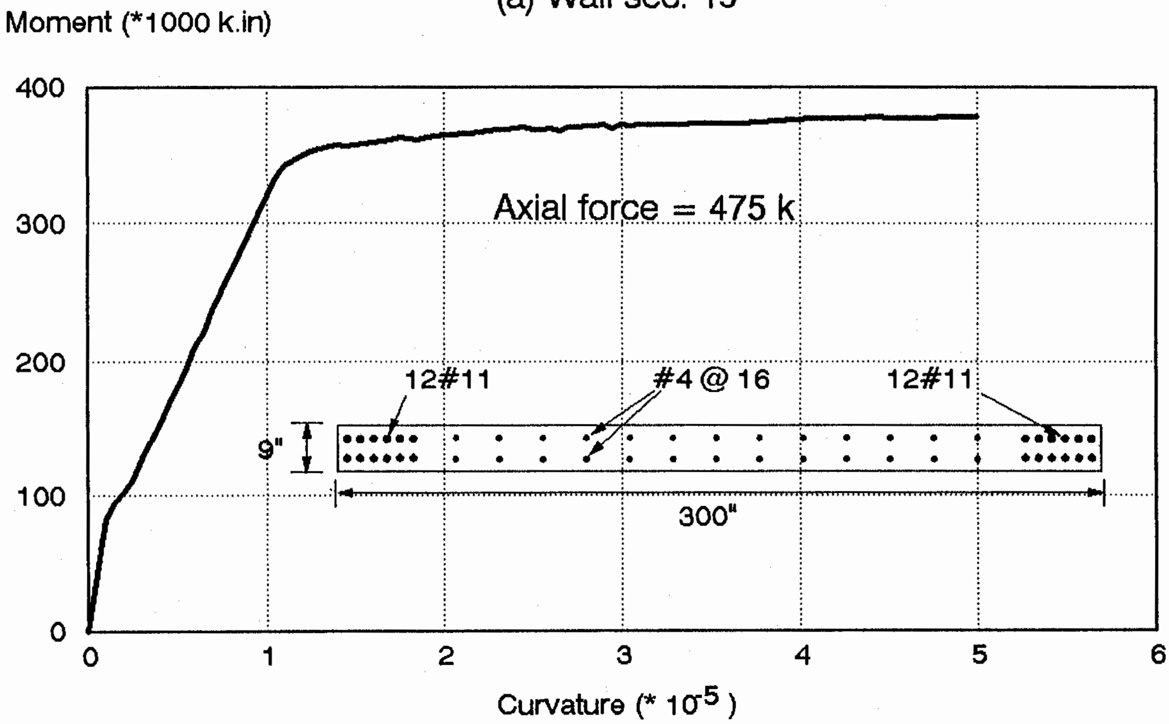

(b) Wall sec. 114

Fig. 5.5 Typical Moment-Curvature Diagram for Walls (CSMIP356)

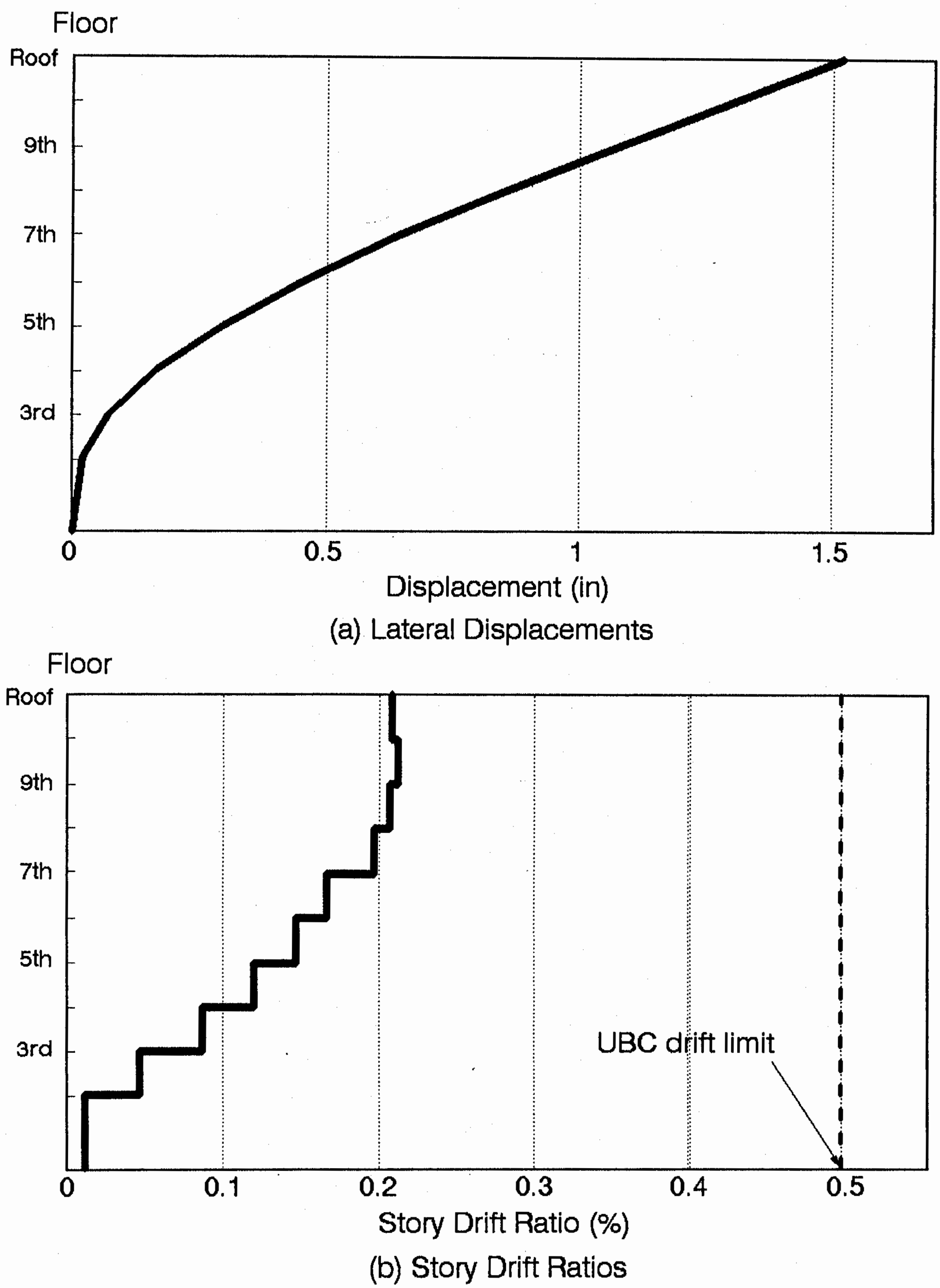

Fig. 5.6 Lateral Displacements and Story Drift Ratios Produced by

the 1991 UBC Seismic Forces (CSMIP356, N-S)

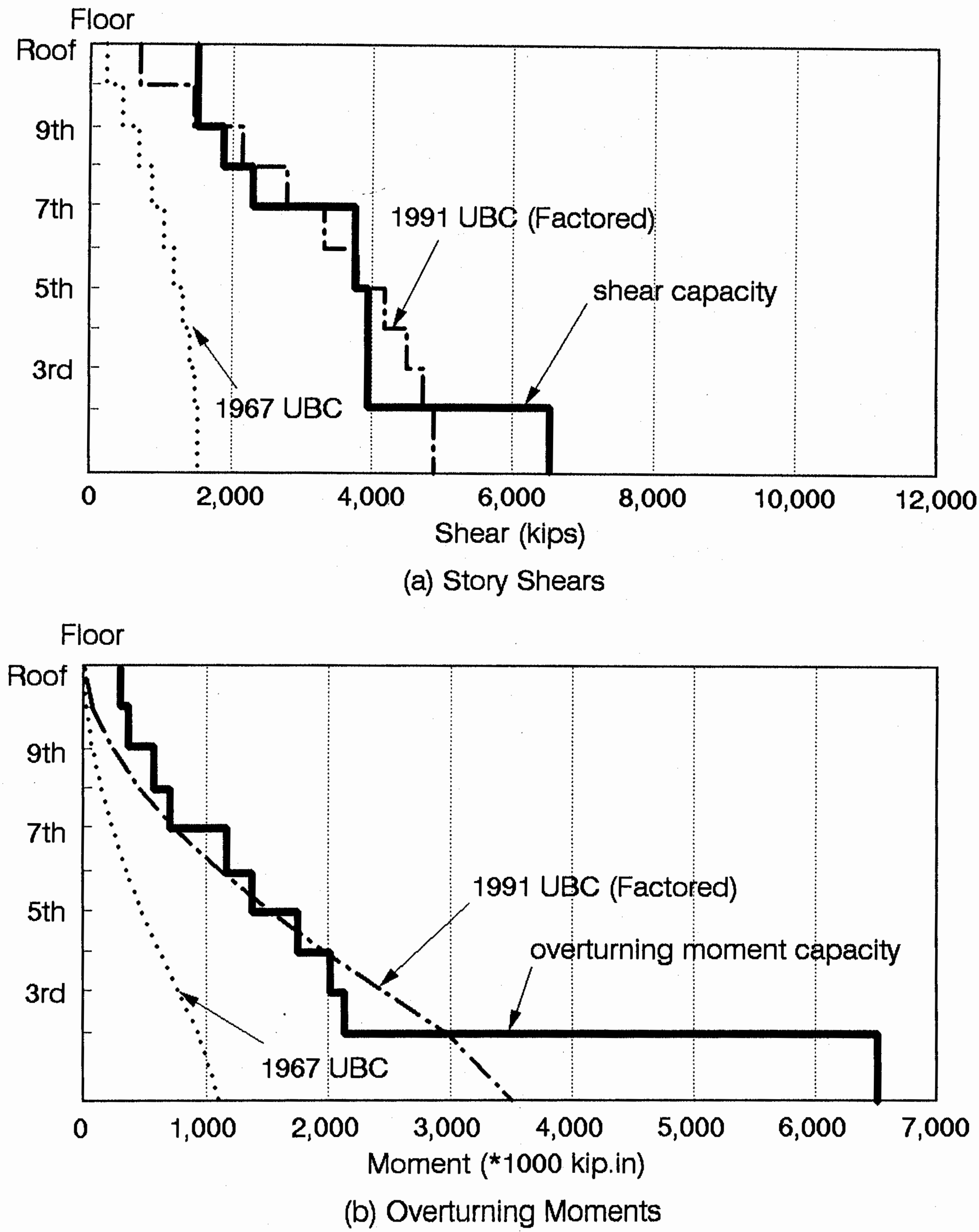

Fig. 5.7 Comparison of Story Shears and Overturning Moments

(CSMIP356, N-S)

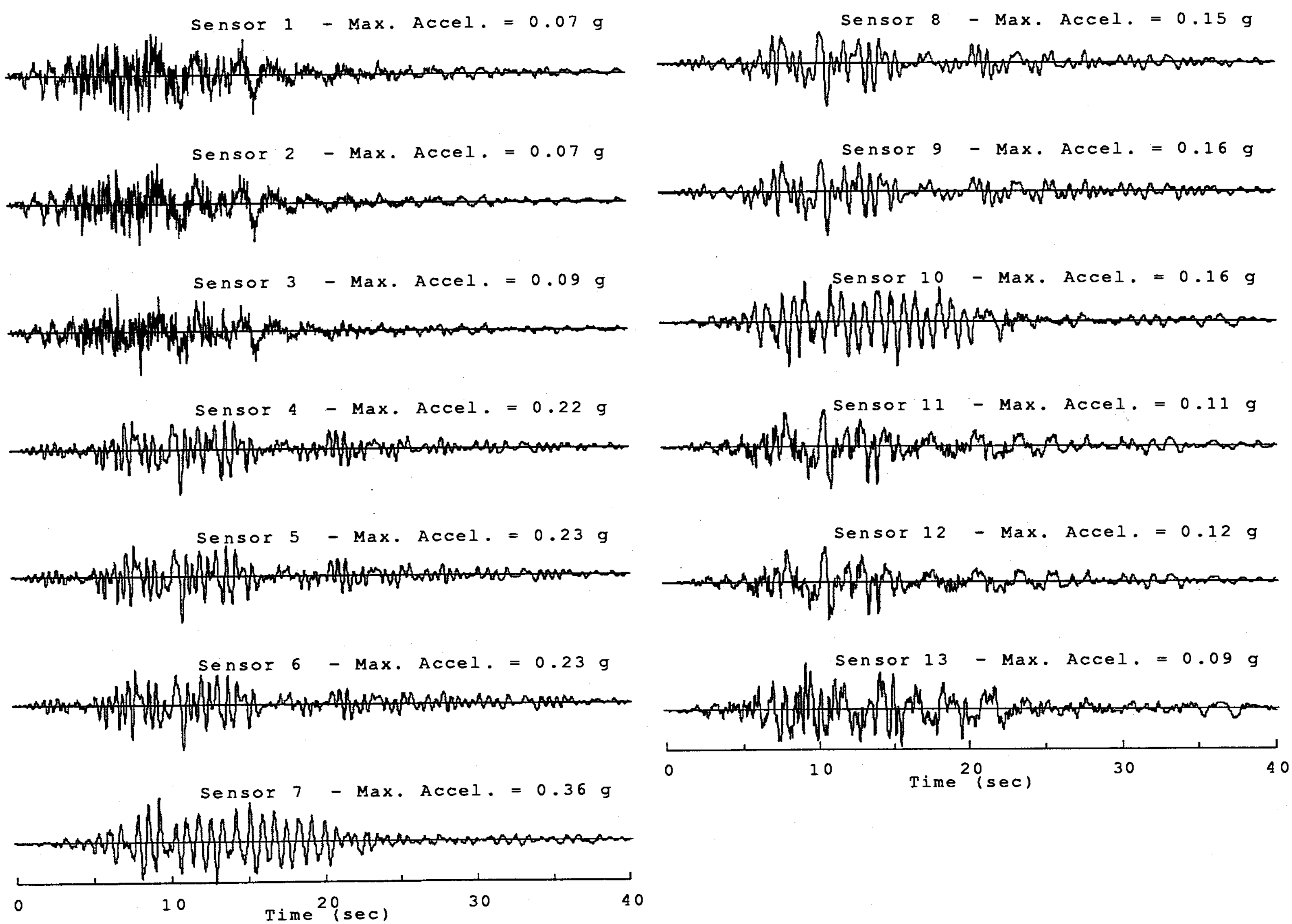

Fig. 5.8 Building CSMIP356 Acceleration Records

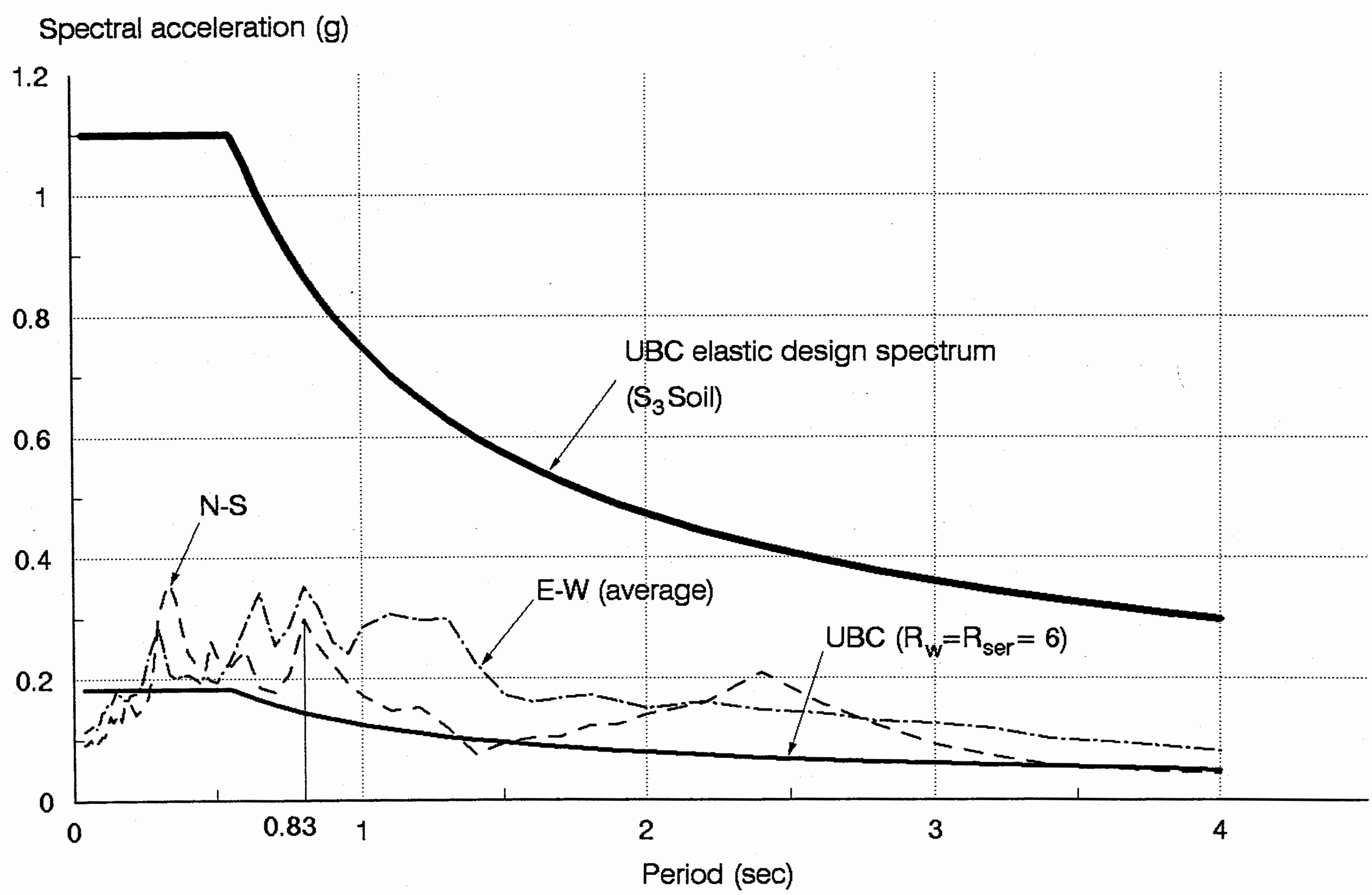

Fig. 5.9 UBC Design Spectra and the Elastic Response Spectra of the Base Acceleration Records (CSMIP356, 5% damping)

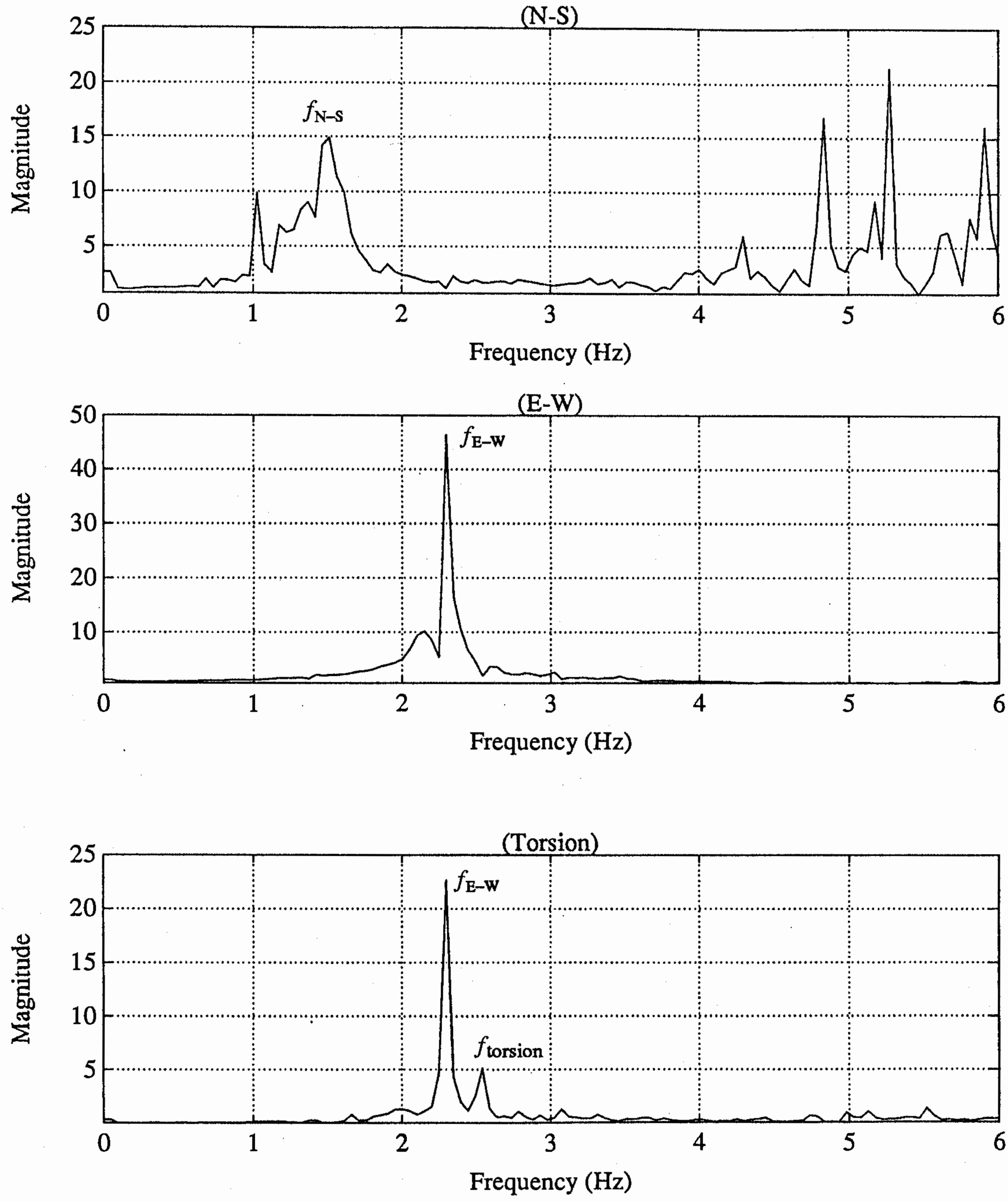

Fig. 5.10 Magnitude of Acceleration Transfer Functions between the Base and the Roof (CSMIP 356)

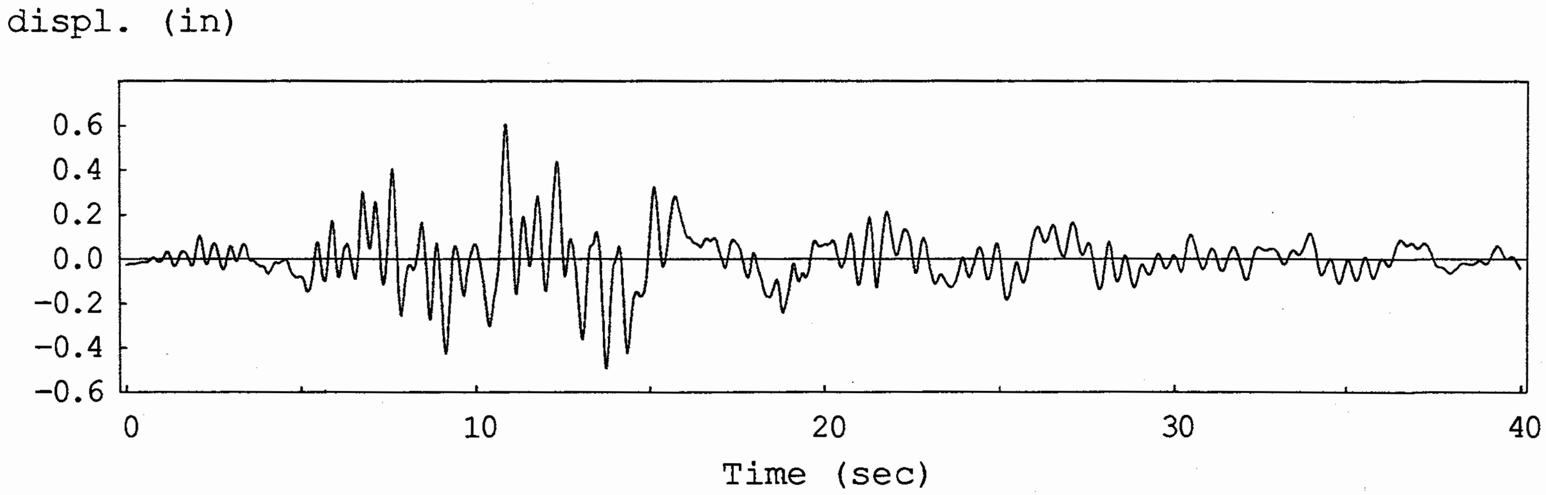

(a) Original relative displacement

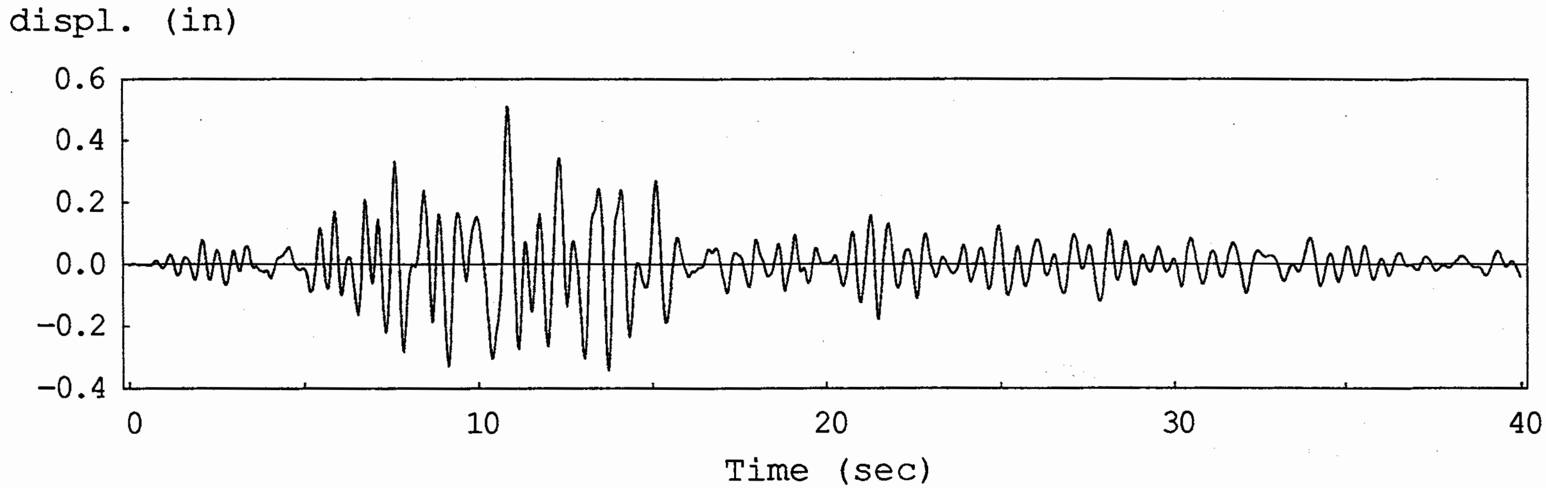

(b) Filtered relative displacement (cut-ff freq. = 0.6 Hz)

Fig. 5.11 Relative Displacement Time History at Sensor 6

(CSMIP356, E-W)

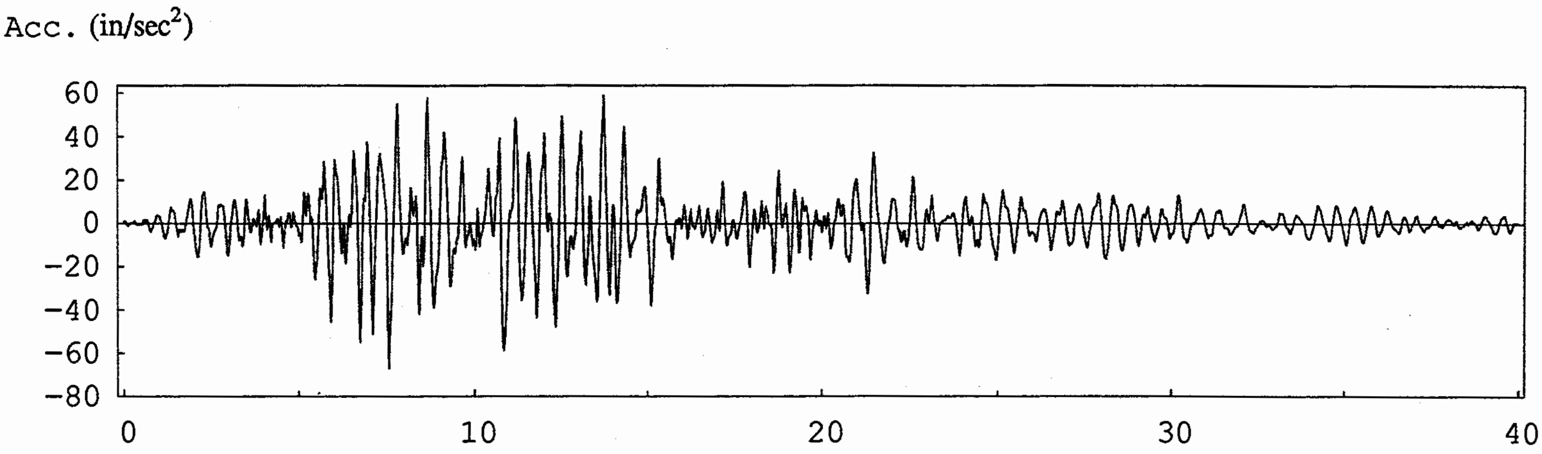

(a) Relative acceleration

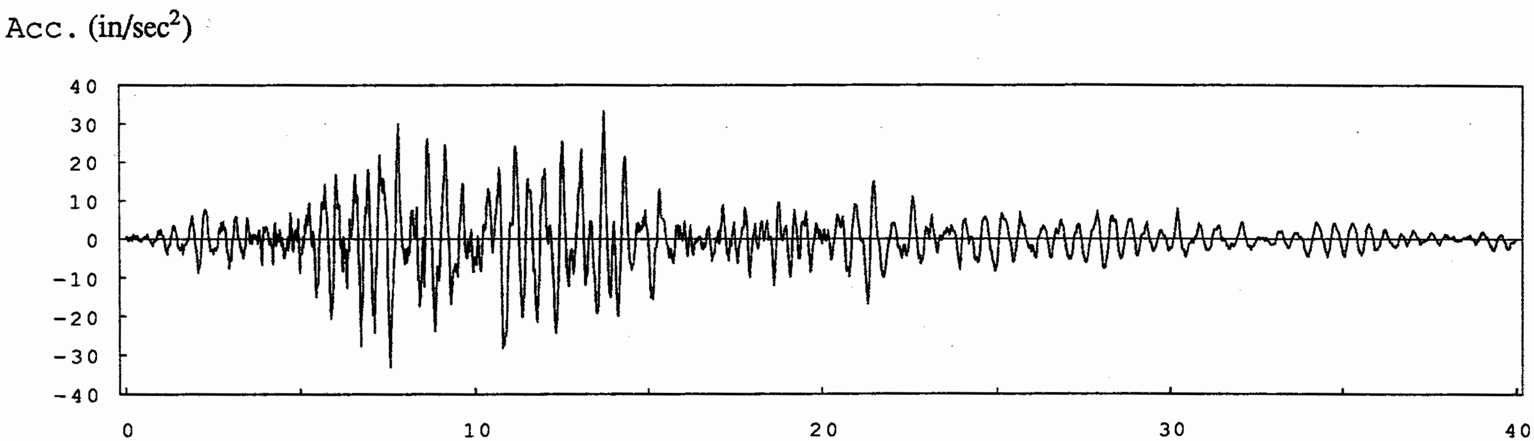

(b) Rocking acceleration

Fig. 5.12 Comparison of Relative and Rocking Acceleration in the Roof

(CSMIP356, E-W, Sensor 6)

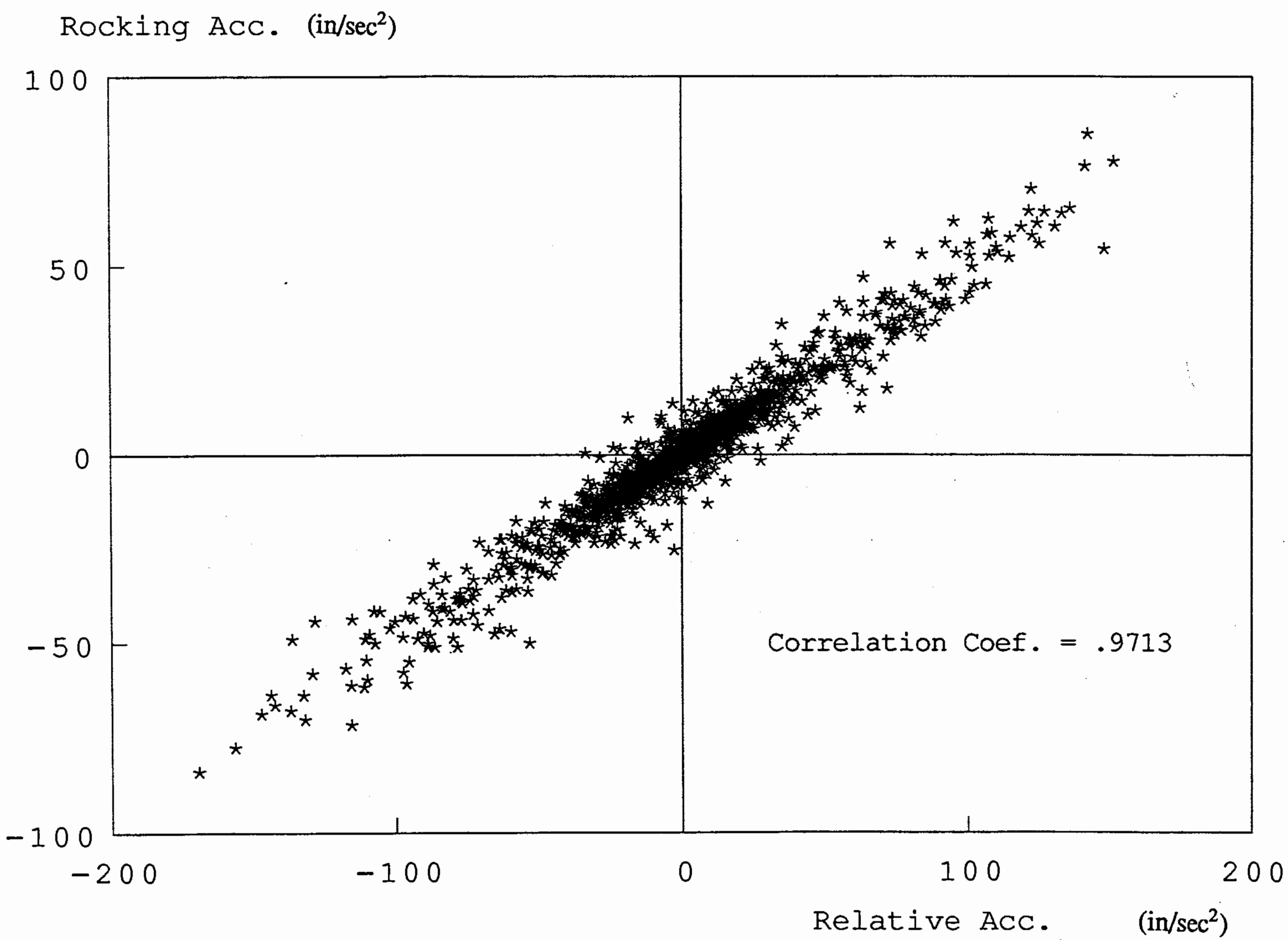

Fig. 5.13 Relationship between Relative and Rocking Acceleration at the Roof

(CSMIP356, E-W, Sensor 6)

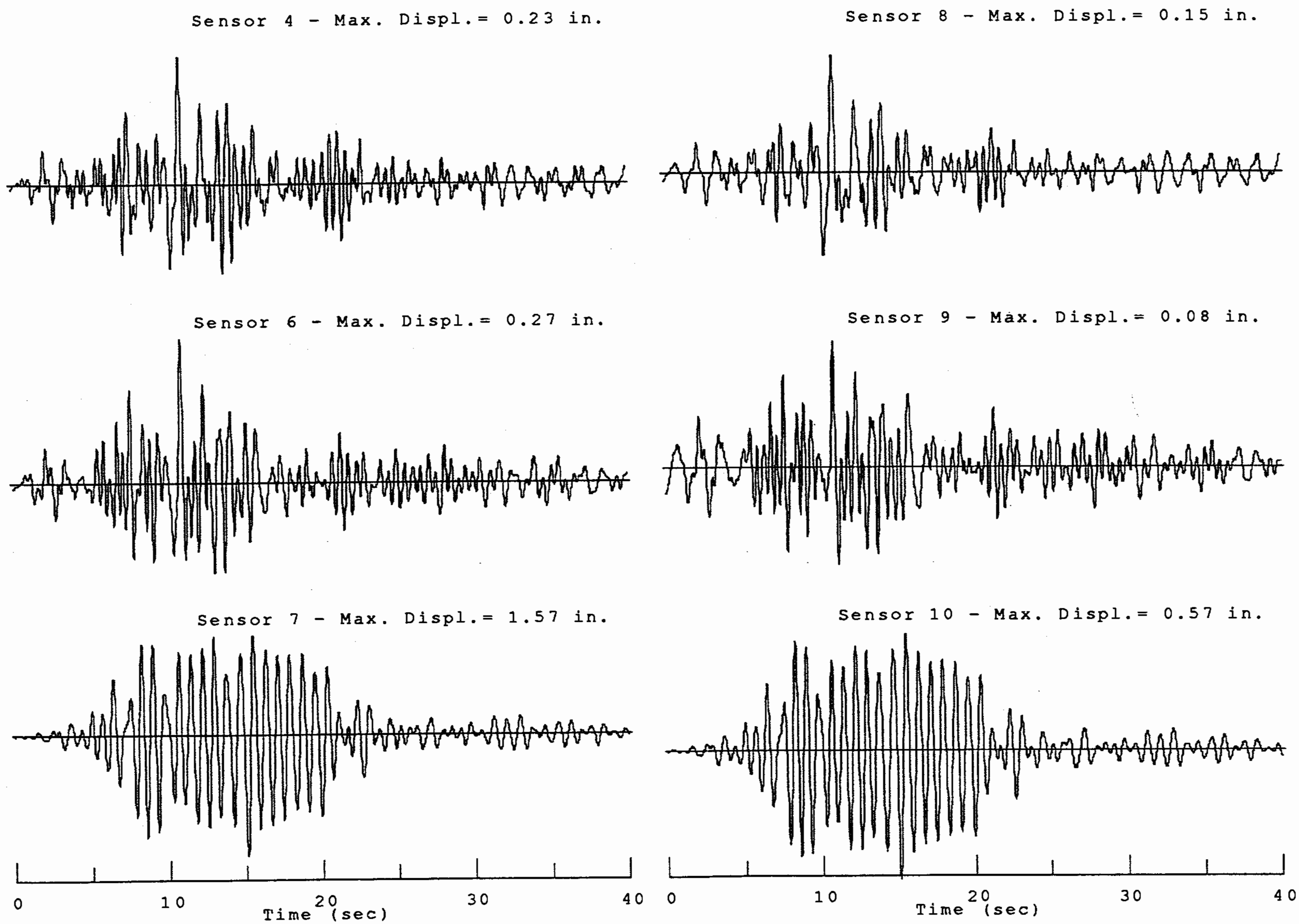

Fig. 5.14 Displacement Time Histories to be Imposed on a 3-D Mathematical Model of CSMIP356

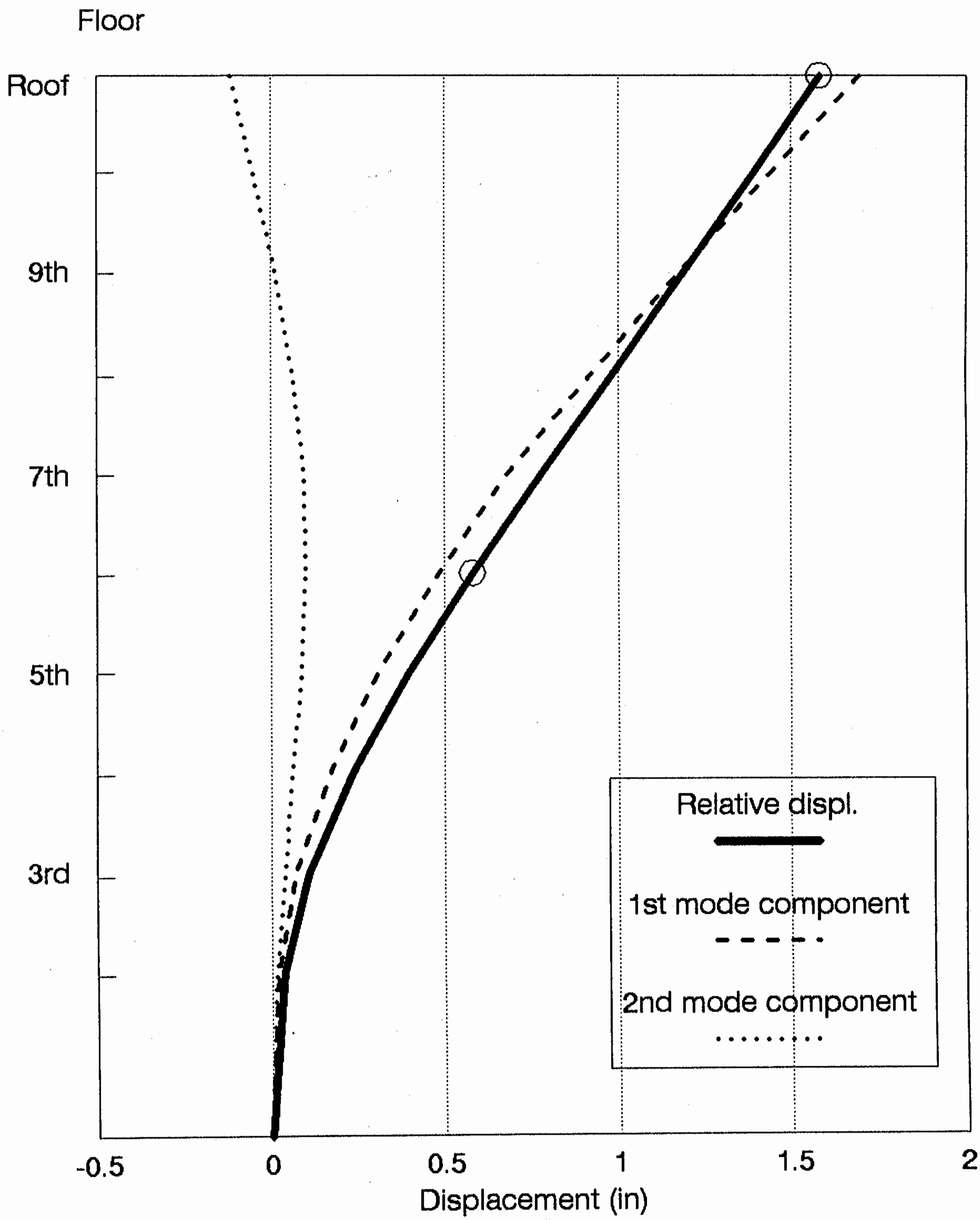

Fig. 5.15 Lateral Displacement Profile at Peak Response

(CSMIP356, N-S)

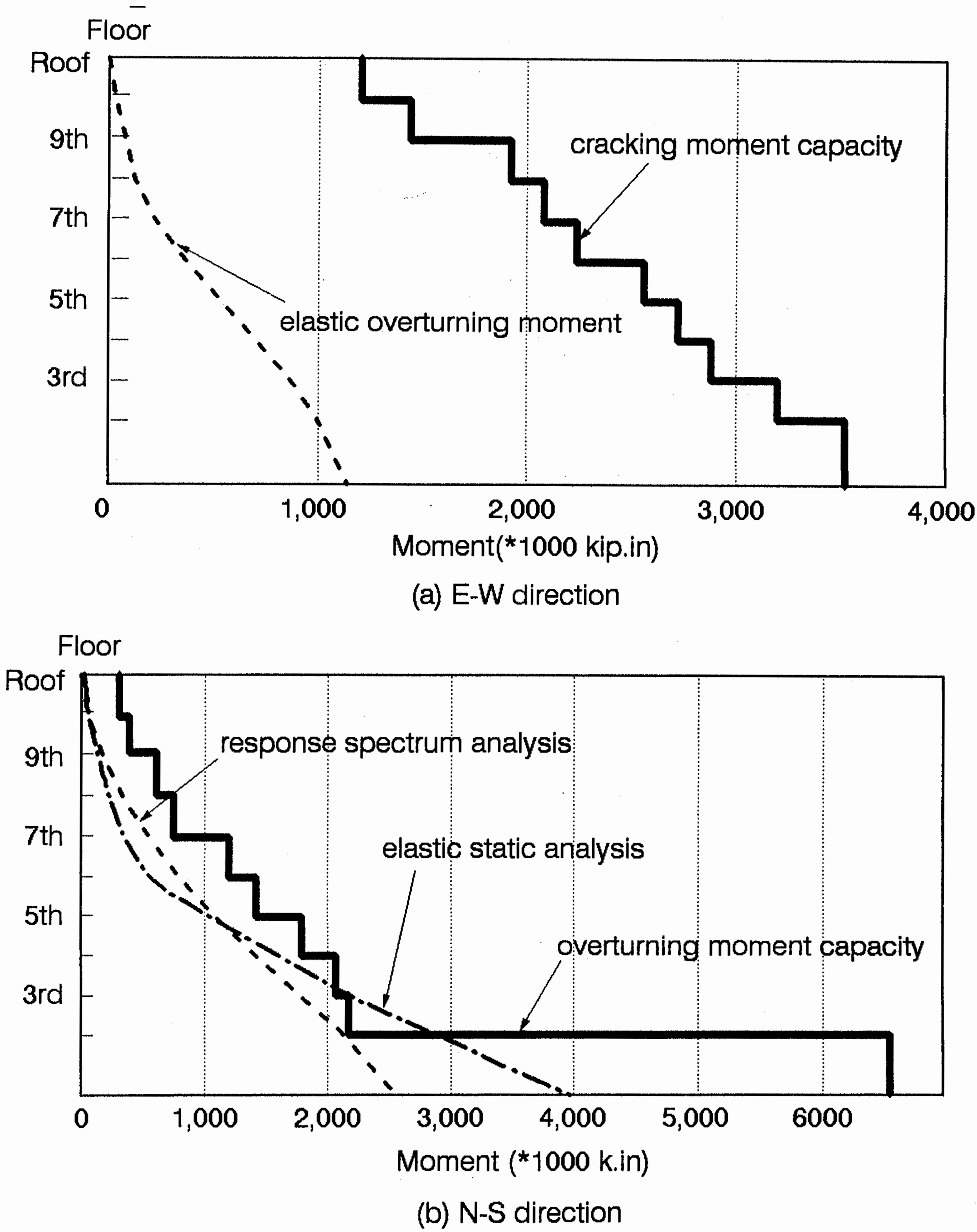

Fig. 5.16 Comparison of Overturning and Cracking Moments

(CSMIP356, Elastic Model)

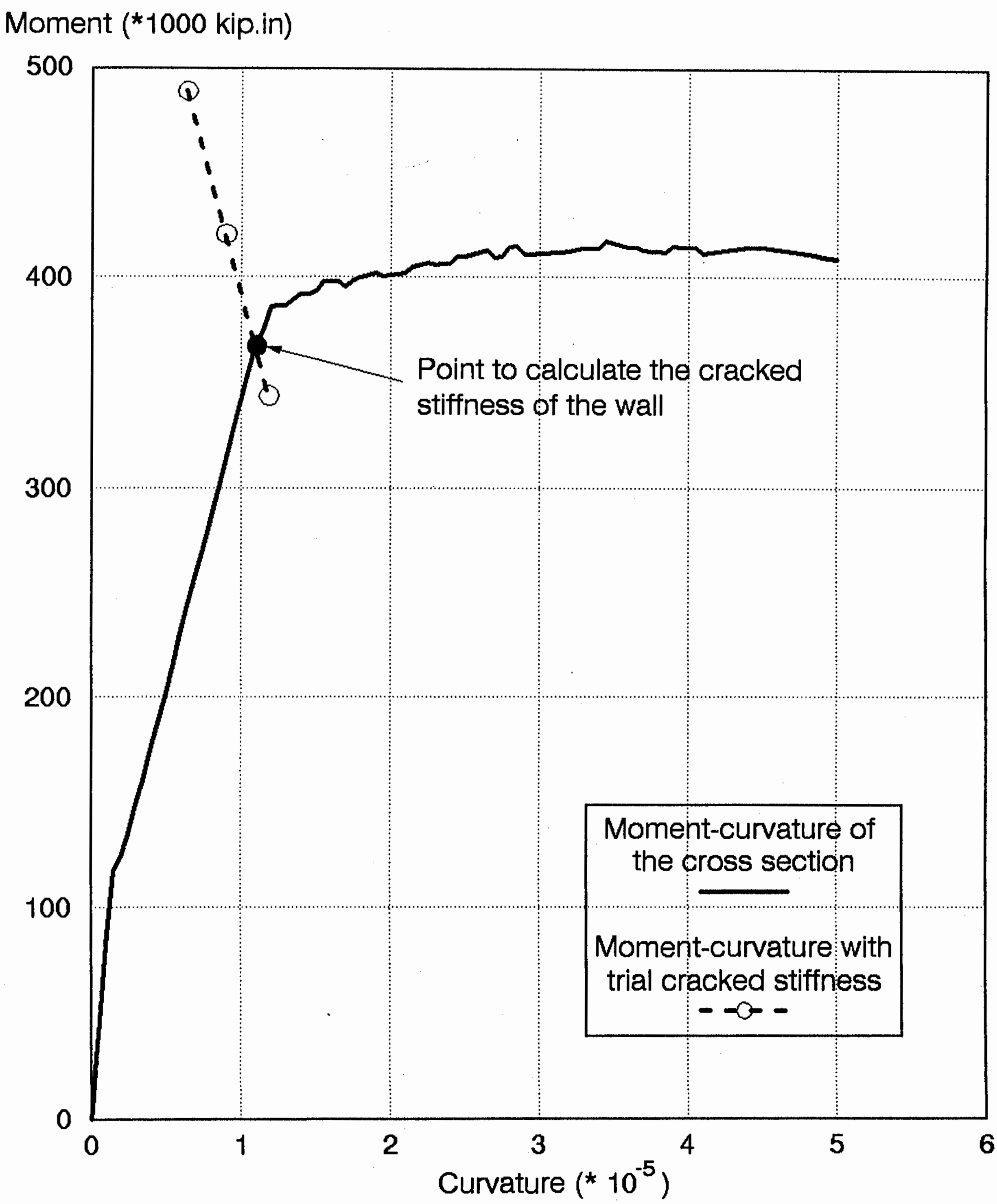

Fig. 5.17 Iterative Procedure to Establish Cracked Stiffness of Wall Section 19

(CSMIP356)

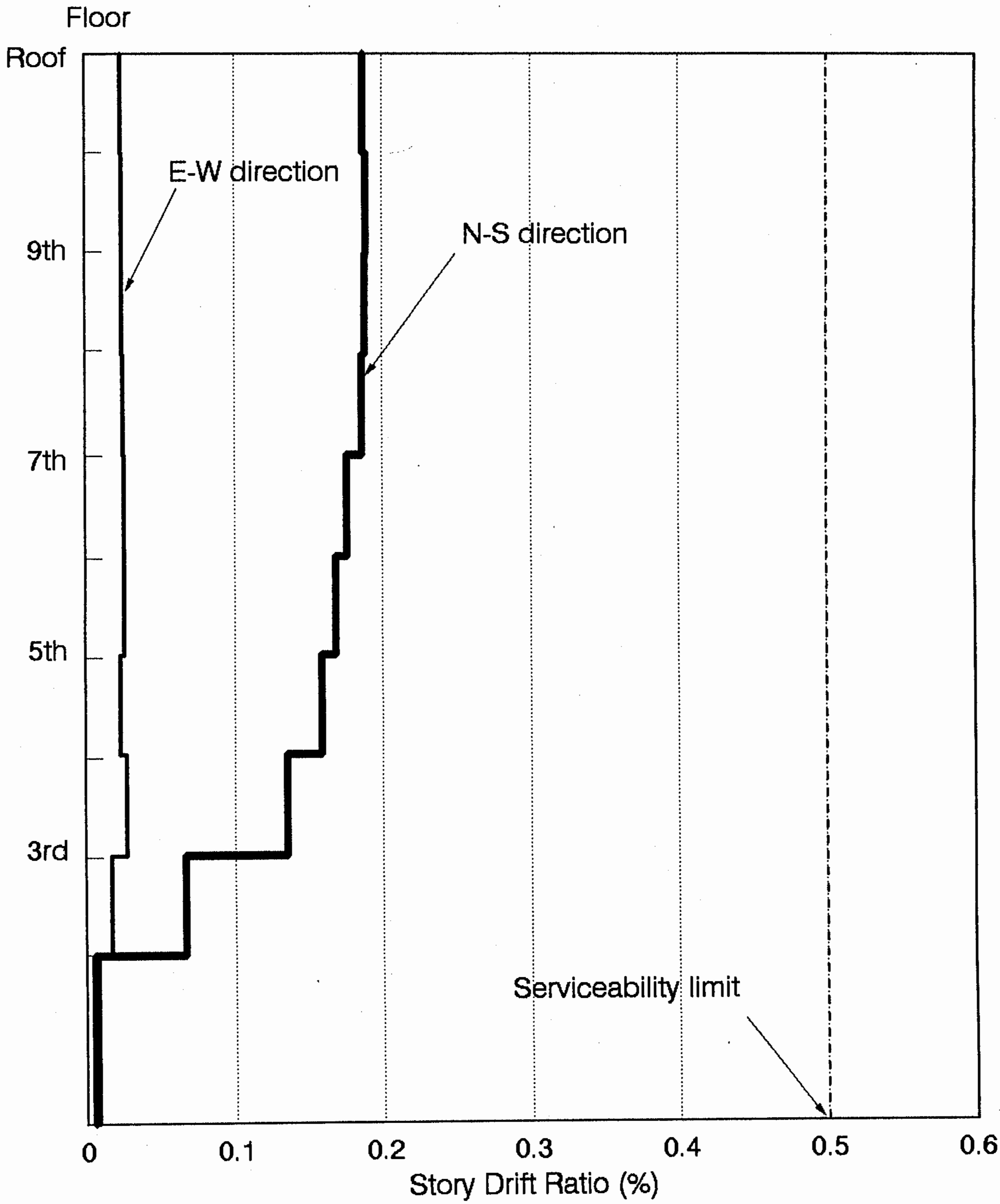

Fig. 5.18 Story Drift Ratios Produced by Loma Prieta Earthquake

(CSMIP356)

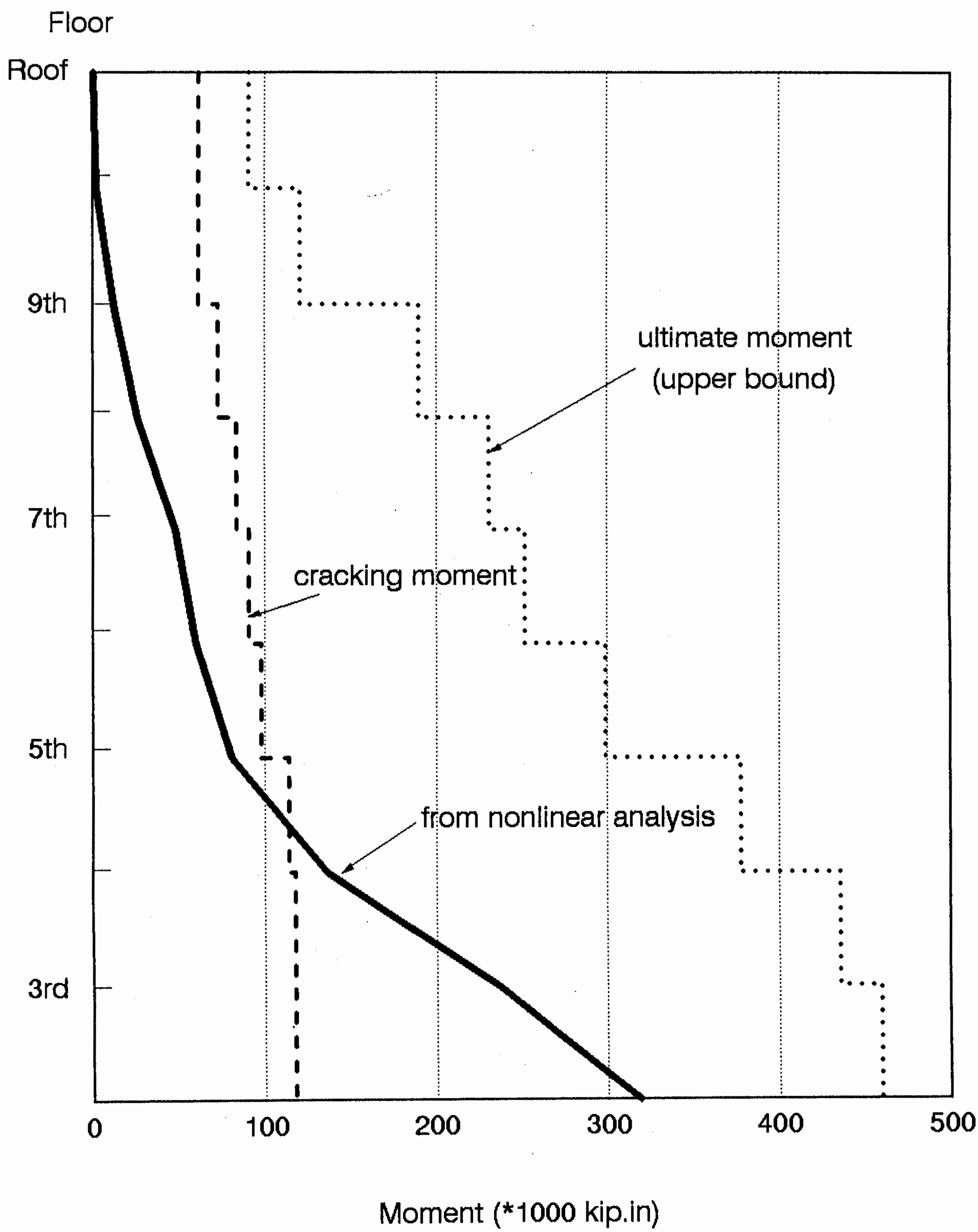

Fig. 5.19 Bending Moments along Axis 1A from Nonlinear Analysis

(CSMIP356, N-S)

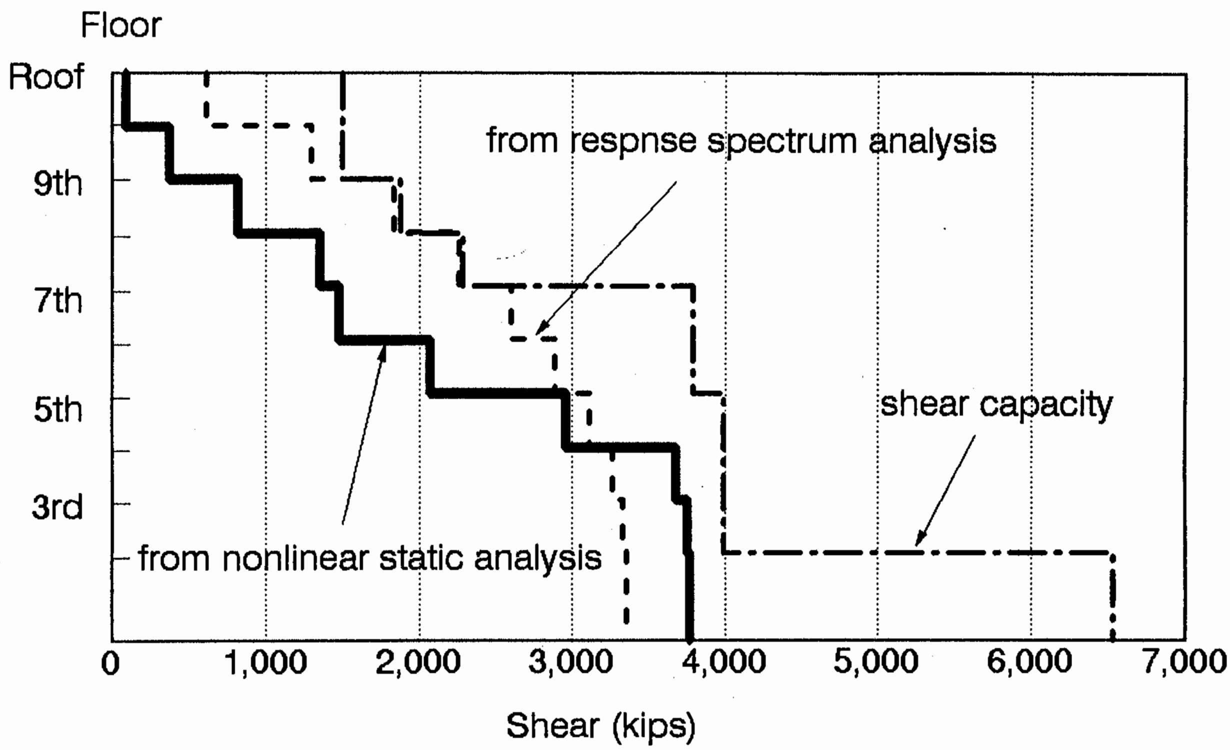

(a) Story Shears

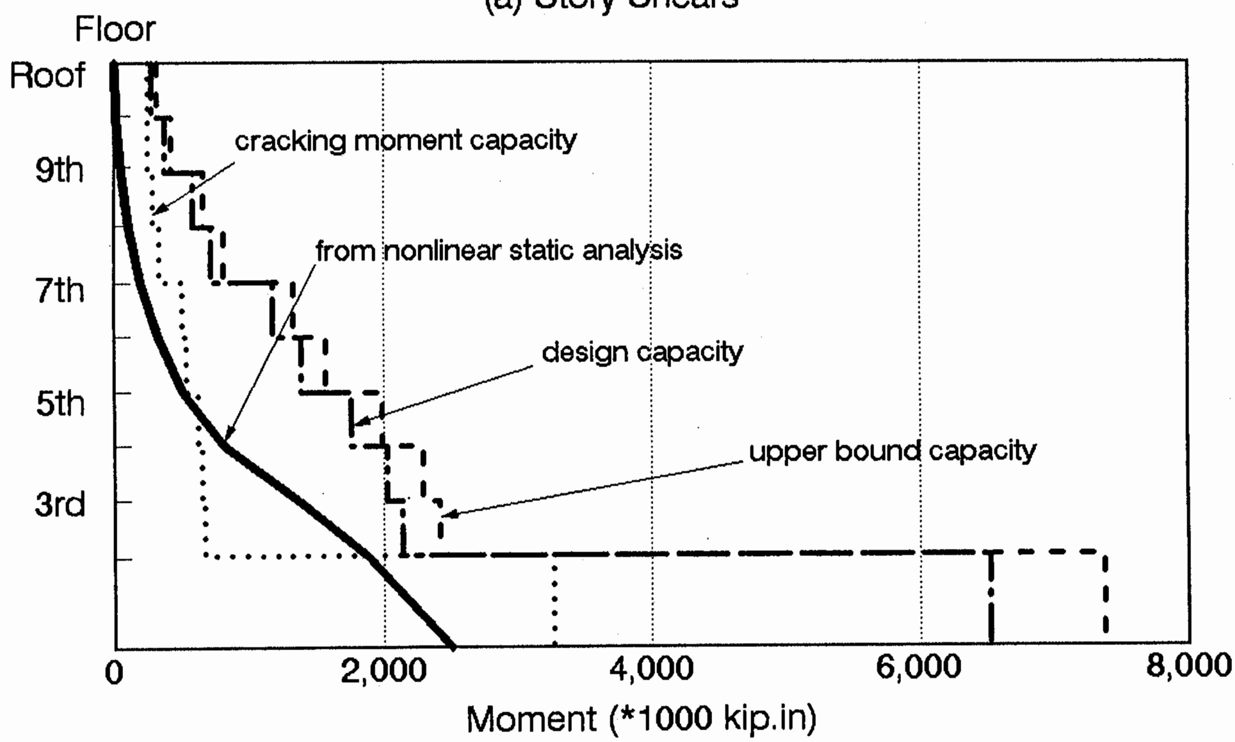

(b) Overturning Moment

Fig. 5.20 Story Shears and Overturning Moments Produced by Loma Prieta Earthquake (CSMIP356, Inelastic Model)

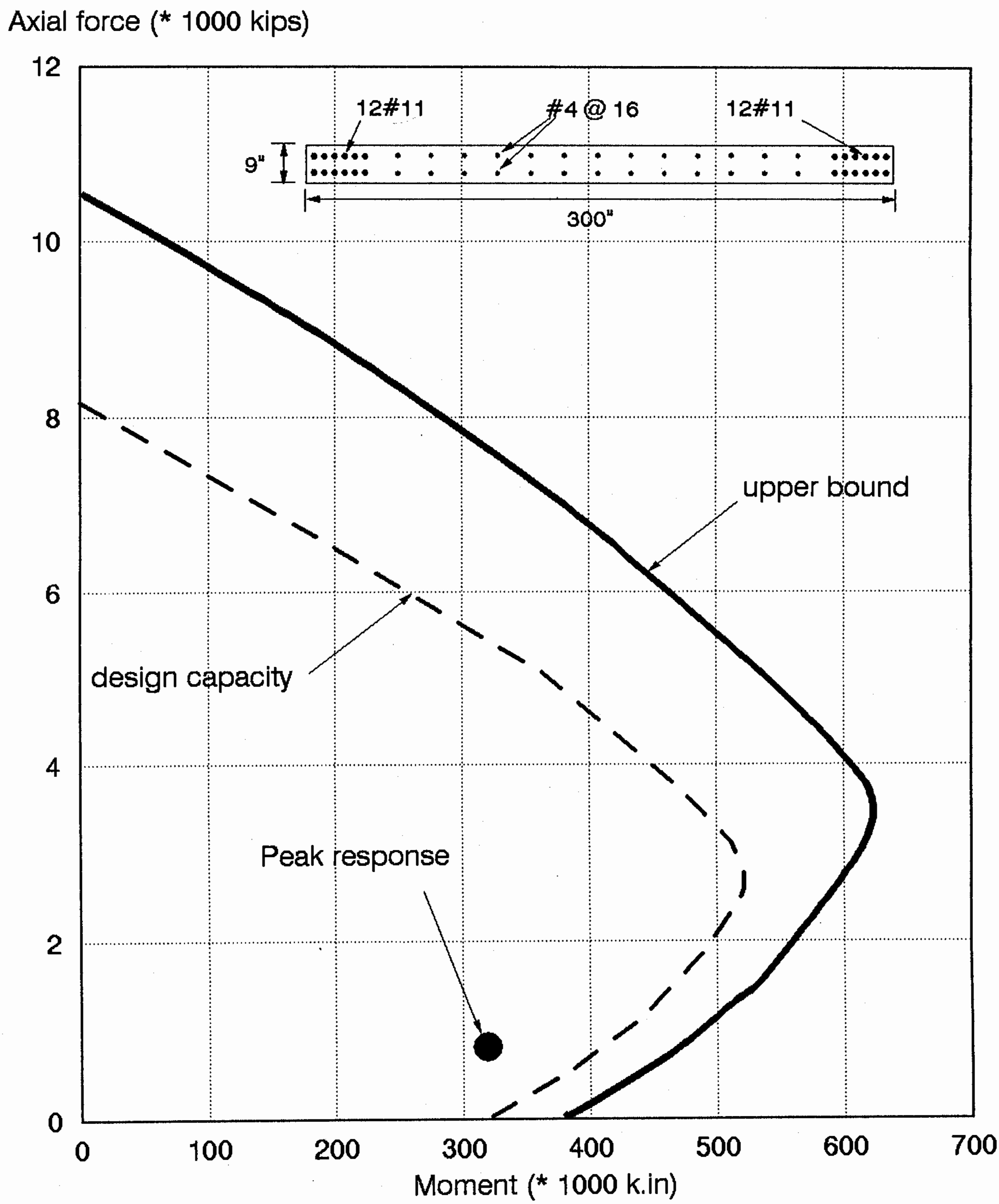

Fig. 5.21 Axial Forces vs. Moment Interaction Diagram

(CSMIP356, Section 19)

San Jose - 10-story Commercial Bldg.

No. of Stories above/below ground: 10/1
Plan Shape: Rectangular
Base Dimensions: 190′ x 96′
Typical Floor Dimensions: 190′ x 82′
Design Date: 1964
Construction Date: 1967

Vertical Load Carrying System:
Concrete floor slabs supported by concrete pan joists and concrete frames.
Lateral Force Resisting System:
End concrete shear walls in transverse direction; moment-resistant concrete frame in longitudinal direction.
Foundation Type:
Mat foundation.

Fig. 6.1 San Jose 10-story Commercial Building (CSMIP355, Shakal, et al., 1989)

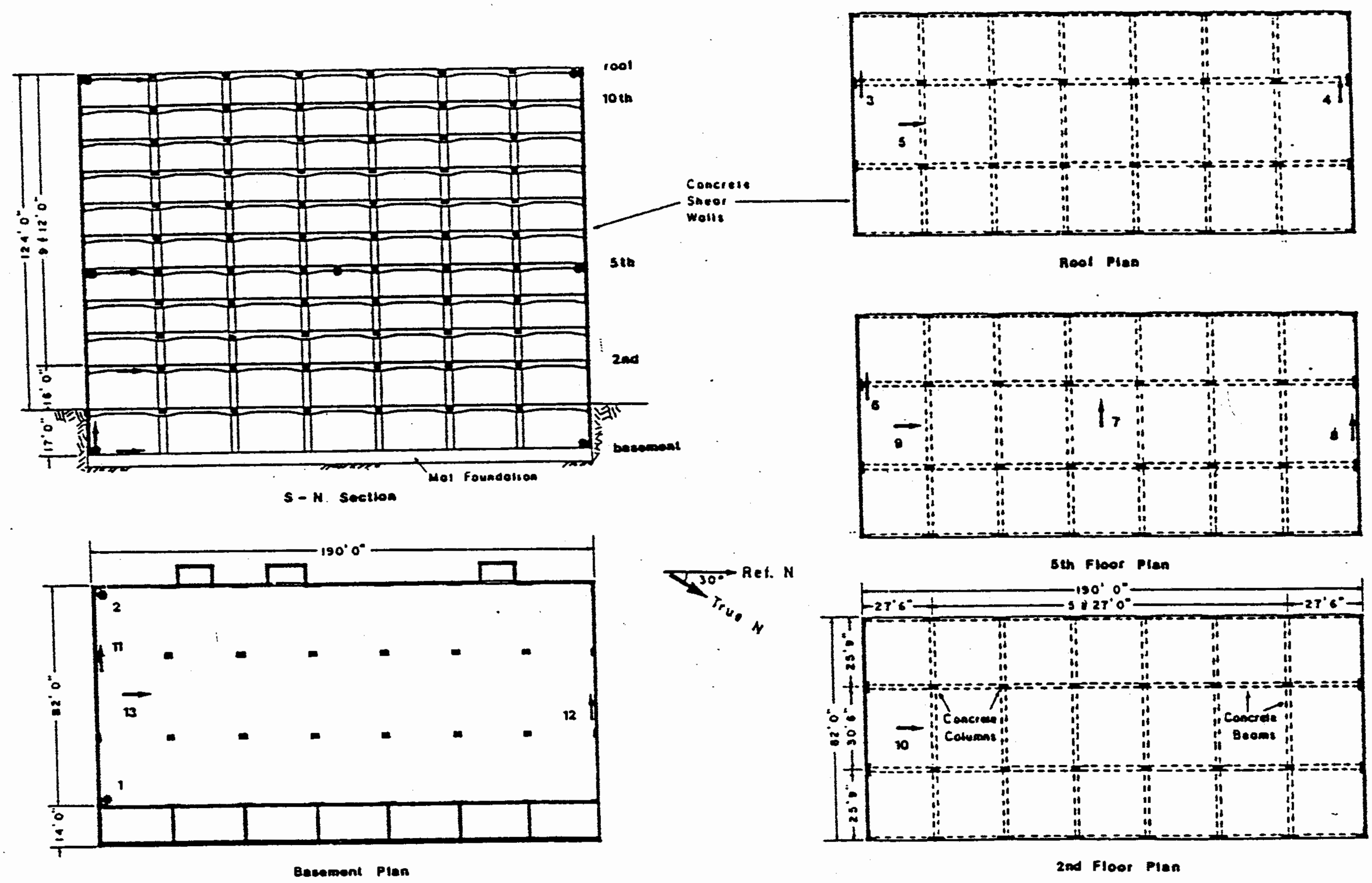

Fig. 6.2 General Layout of Building CSMIP355 (Shakal, et al., 1989)

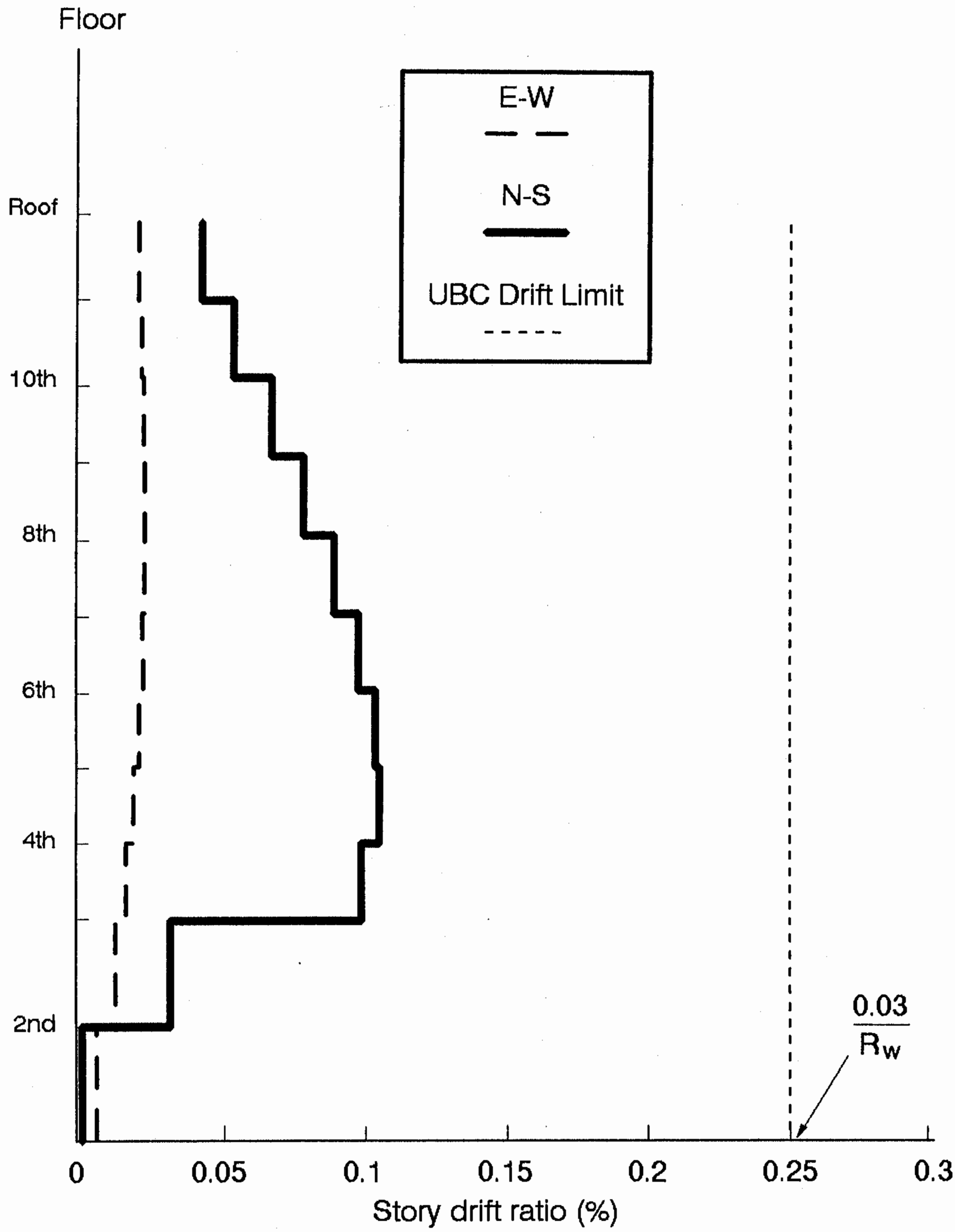

Fig. 6.3 Story Drift Ratios for the 1991 UBC Design

(CSMIP355)

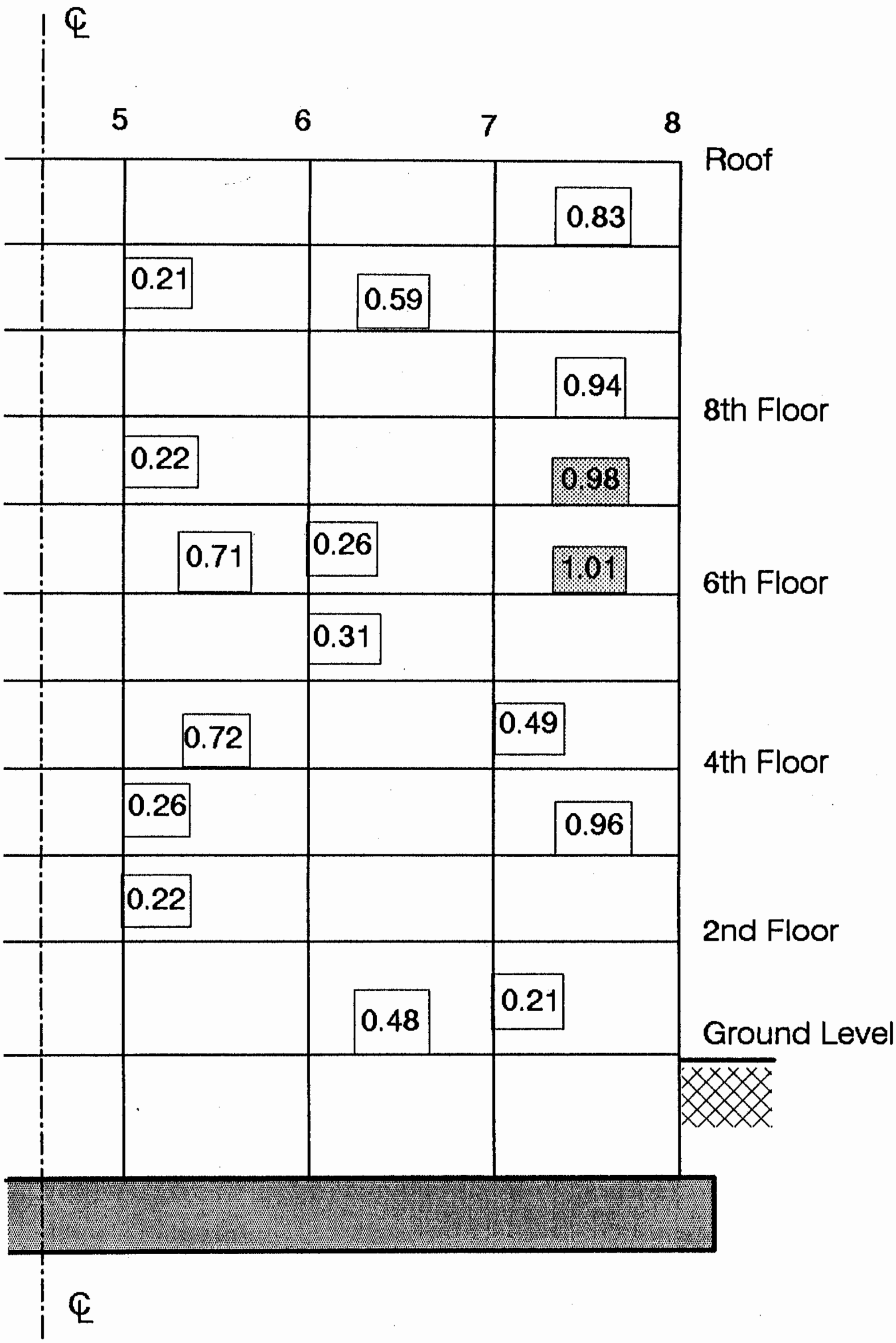

Fig. 6.4 Member Moment Ratios for the 1991 UBC Design

(CSMIP355, N-S Interior Frame)

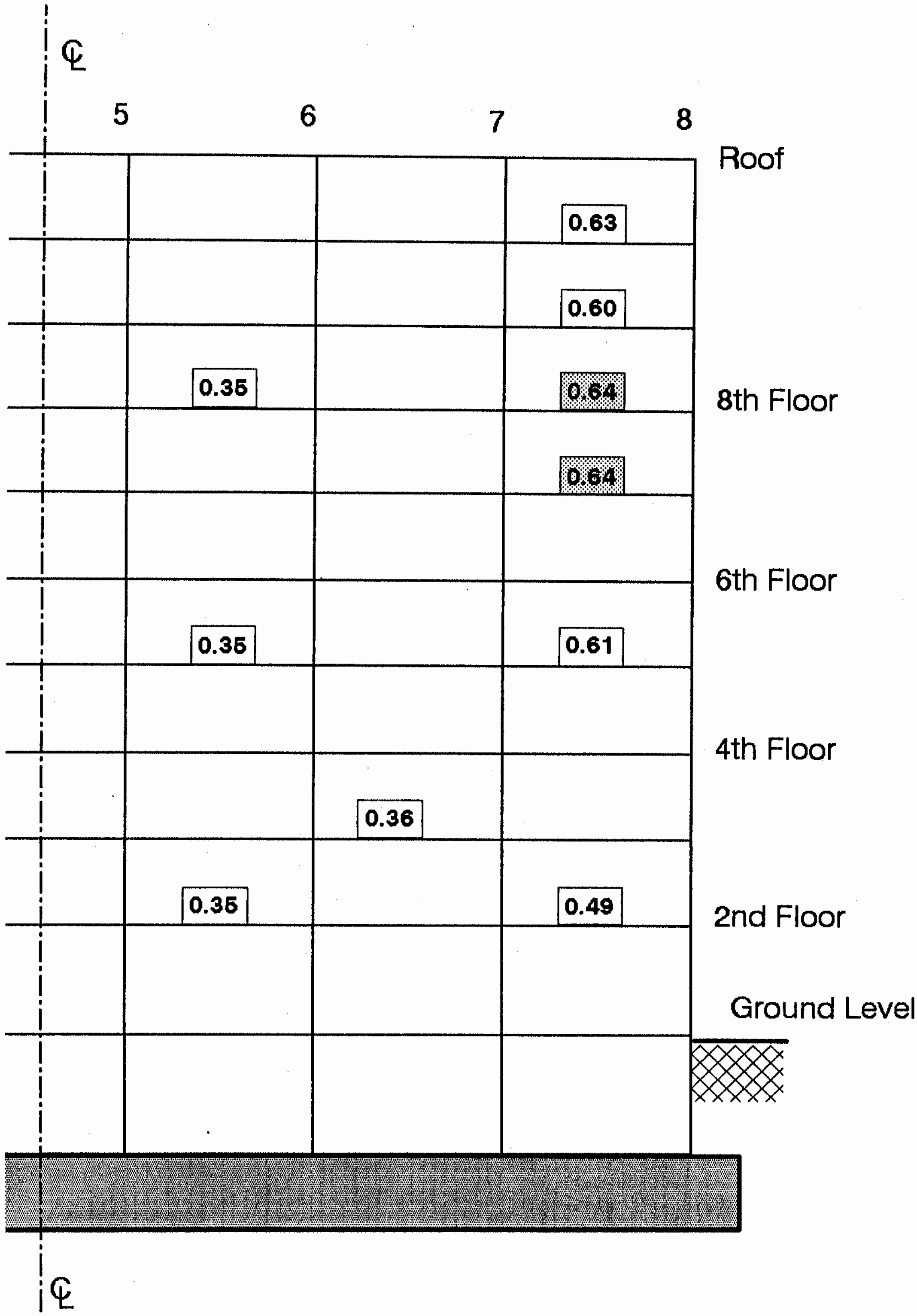

Fig. 6.5 Moment Ratios Due to Gravity Loads

(CSMIP355, N-S Interior Frame)

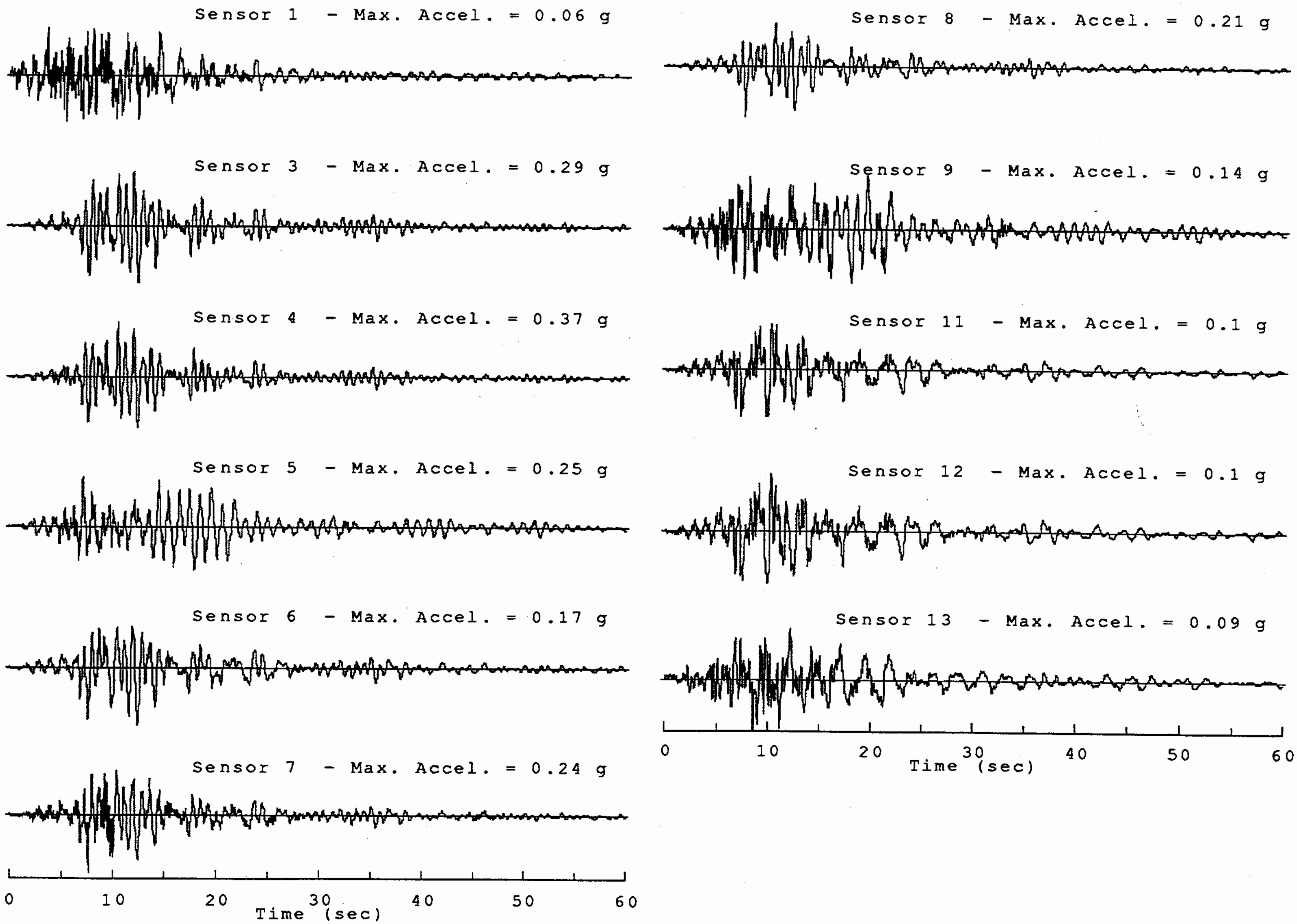

Fig. 6.6 Building CSMIP355 Acceleration Records

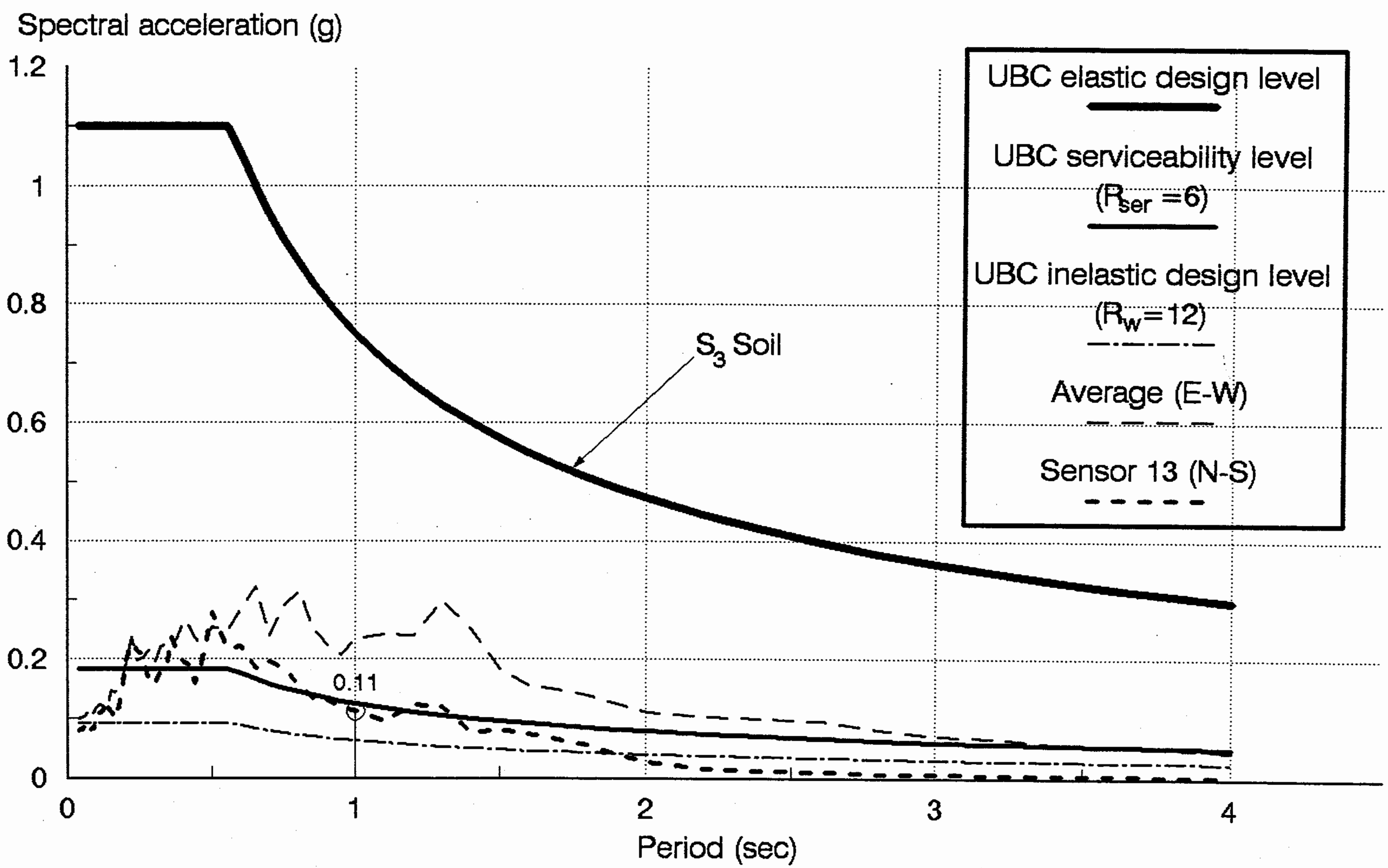

Fig. 6.7 UBC Design Spectra and the Elastic Response Spectra of the Base

Acceleration Records (CSMIP355, 5% damping)

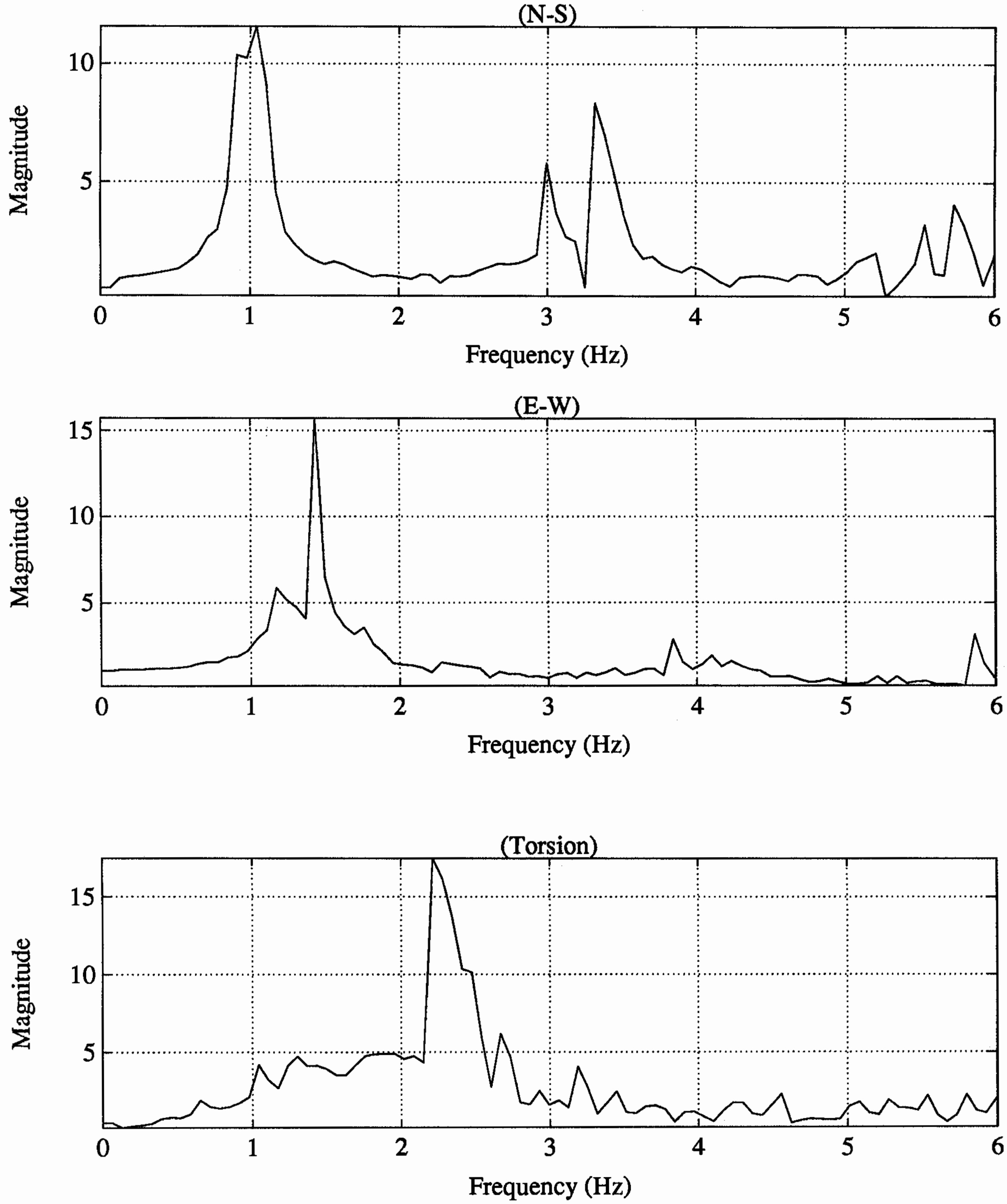

Fig. 6.8 Magnitude of Acceleration Transfer Functions between the Base and the Roof (CSMIP 355)

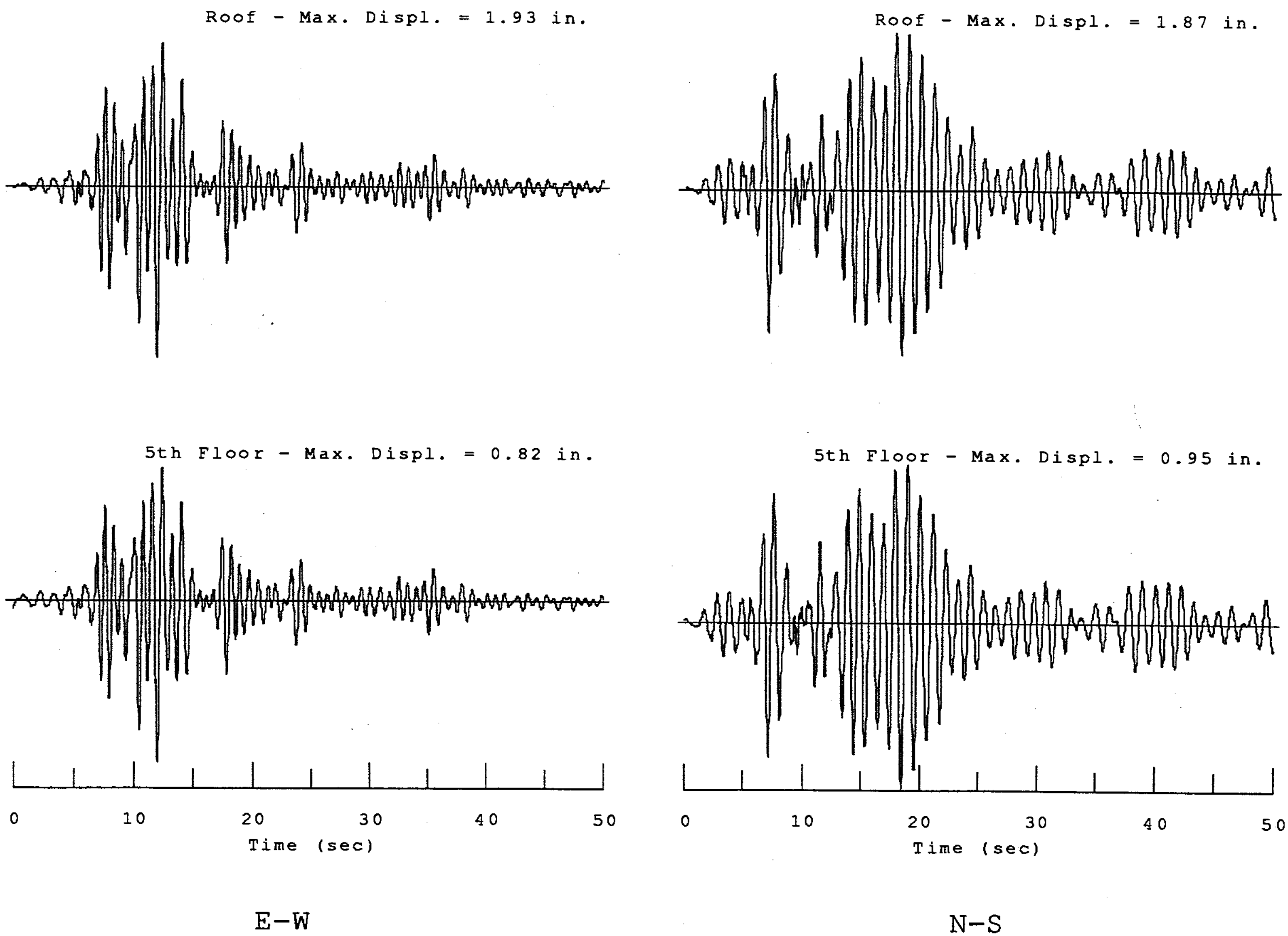

Fig. 6.9 Relative Displacement Time Histories at Center of Mass (CSMIP355)

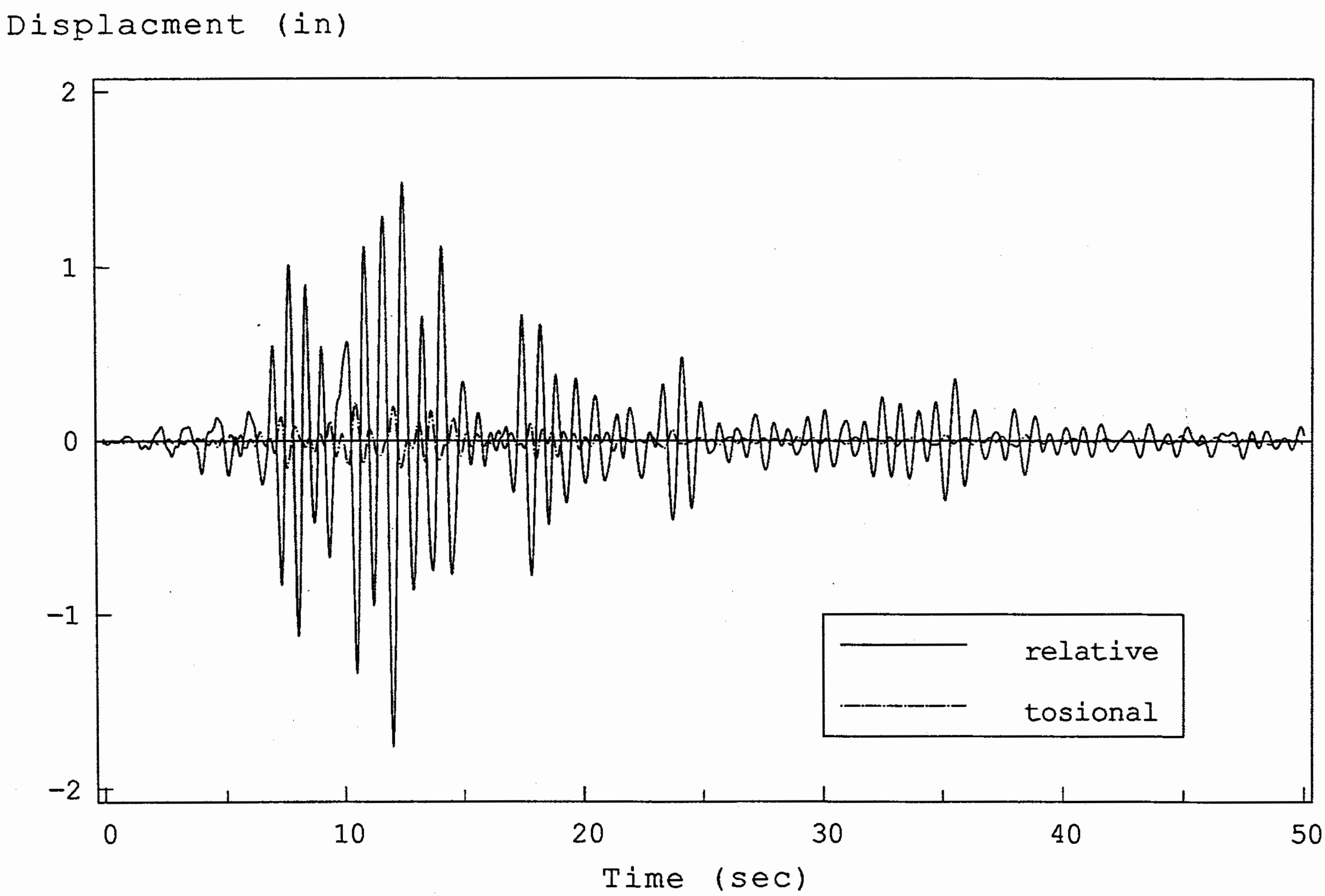

Fig. 6.10 Relative and Torsional Displacements at Roof Level

(CSMIP355, Sensor 3)

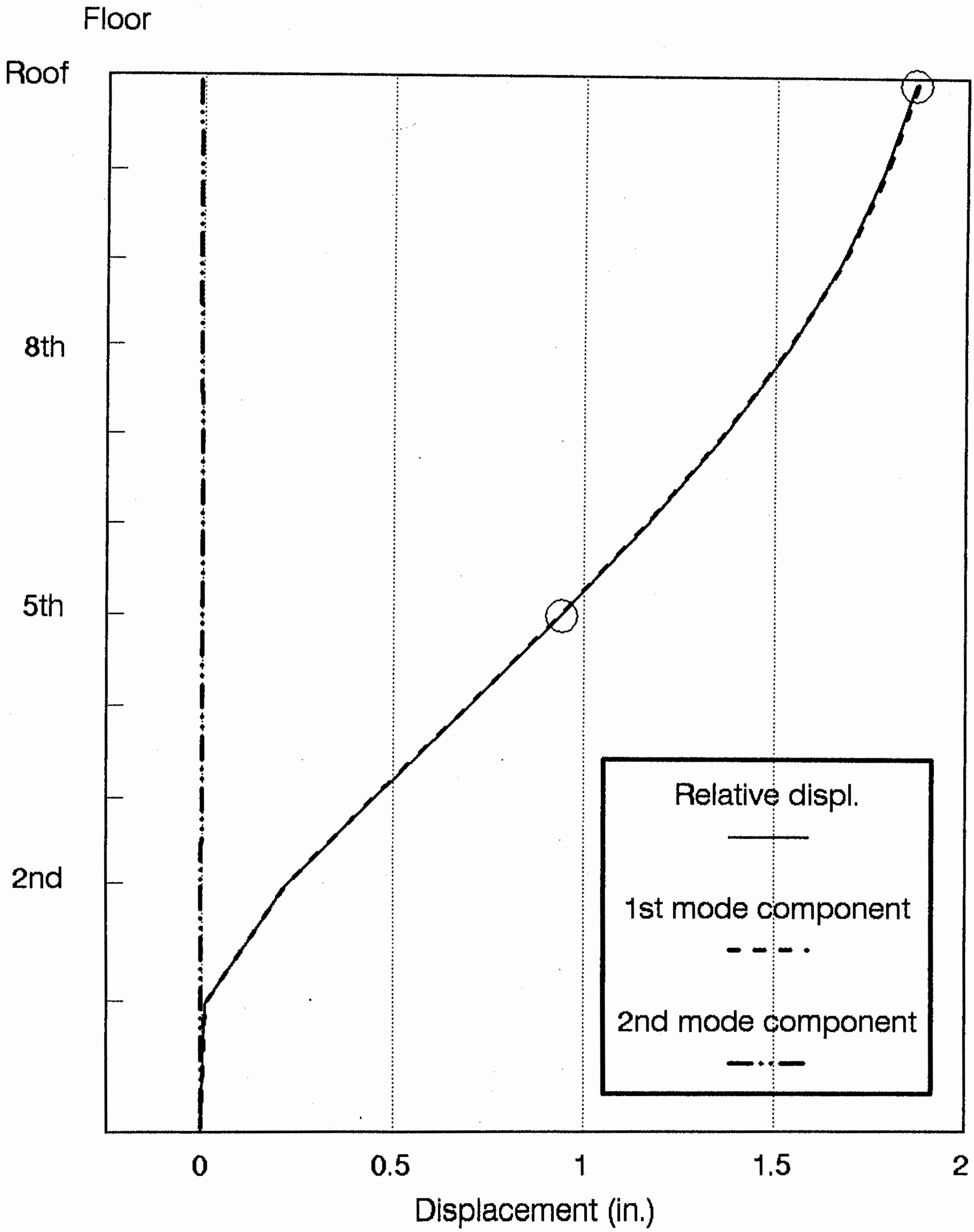

Fig. 6.11 Lateral Displacement Profile at Peak Response

(CSMIP355, N-S)

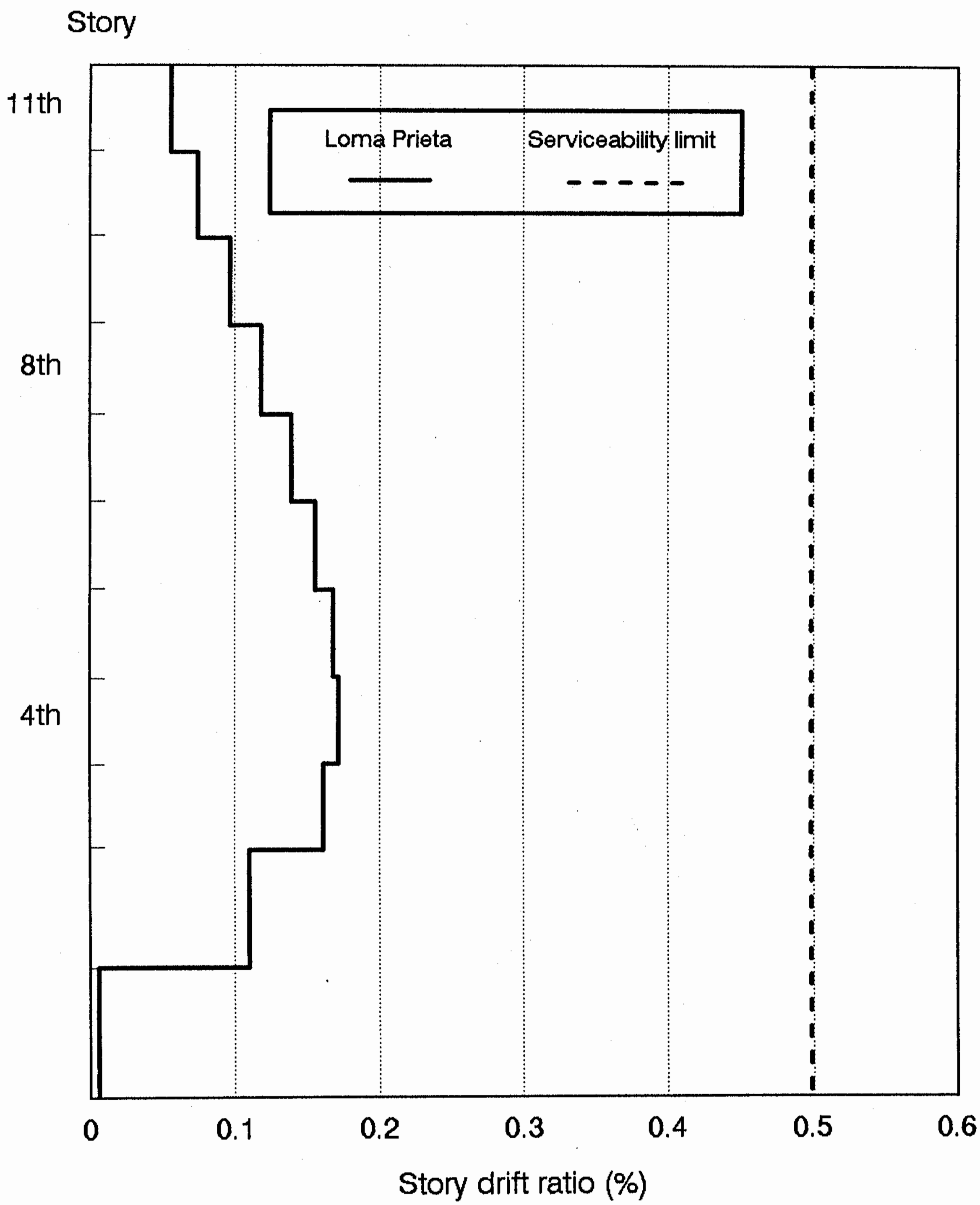

Fig. 6. 12 Story Drift Ratios from Loma Prieta Earthquake

(CSMIP355, N-S)

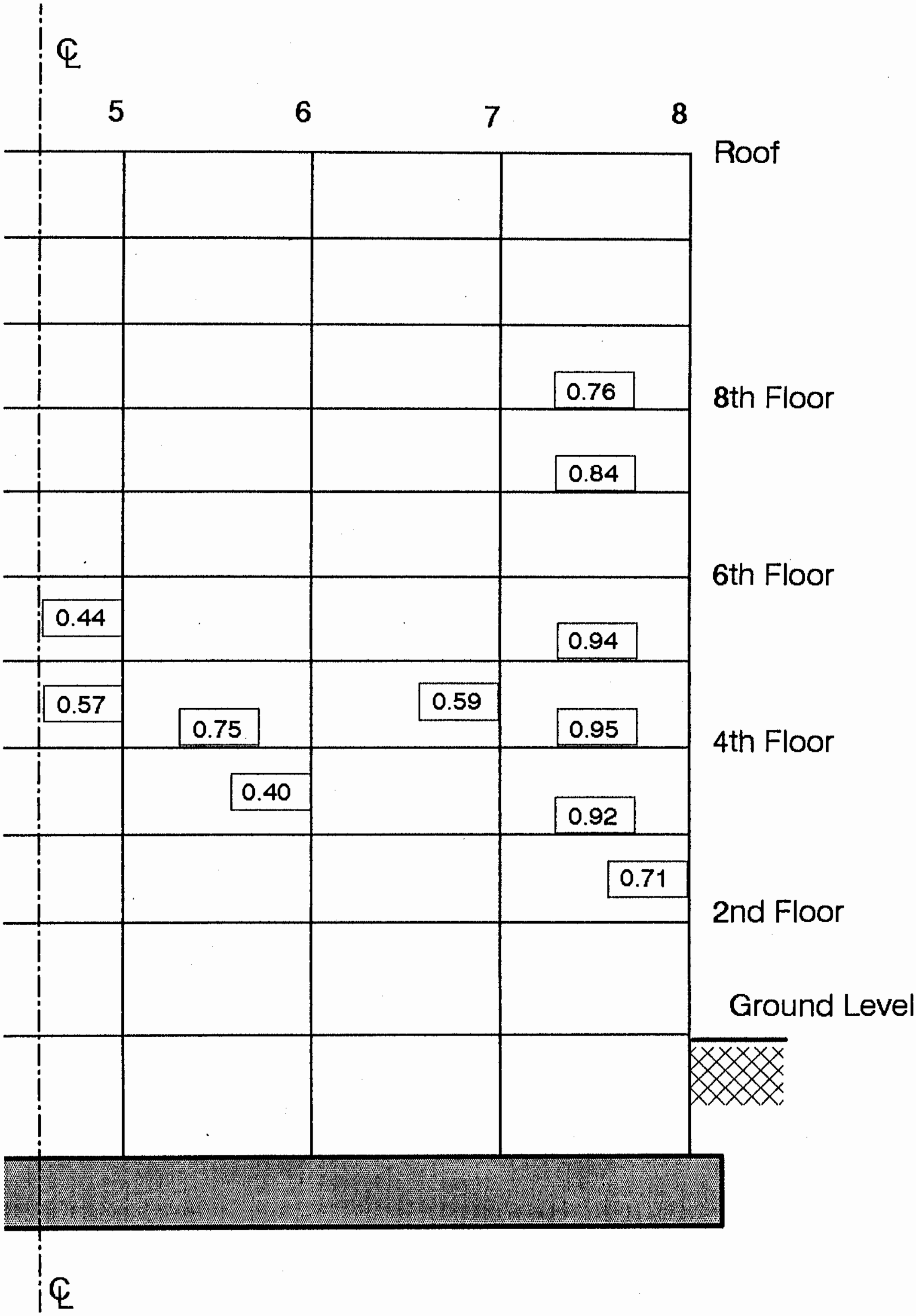

Fig. 6.13 Moment Ratios from Loma Prieta Earthquake

(CSMIP355, N-S Interior Frame)

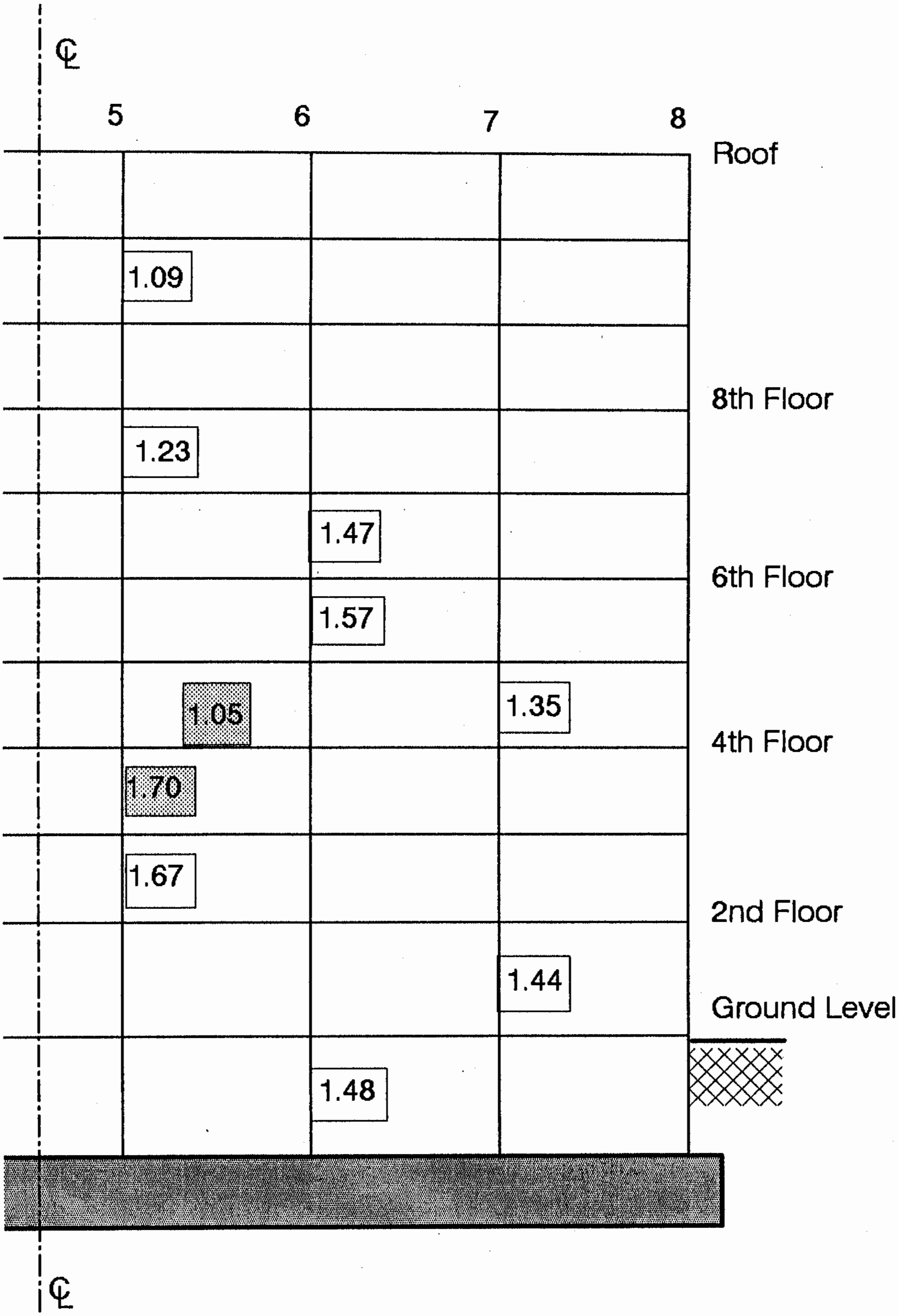

Fig. 6.14 Ratios between Member Forces Produced by Loma Prieta Earthquake and the UBC Design Forces (CSMIP355, N-S Interior Frame)

LIST OF CSMIP DATA UTILIZATION REPORTS

California Department of Conservation
Division of Mines and Geology
Office of Strong Motion Studies
California Strong Motion Instrumentation Program (CSMIP)

The California Strong Motion Instrumentation Program (CSMIP) publishes data utilization reports as part of the Data Interpretation Project. These reports were prepared by investigators funded by CSMIP. Results obtained by the investigators were summarized in the papers included in the proceedings of the annual seminar. These reports and seminar proceedings are available from CSMIP at nominal cost. Requests for the reports, seminar proceedings and/or for additional information should be addressed to: Data Interpretation Project Manager, Office of Strong Motion Studies, Division of Mines and Geology, California Department of Conservation, 801 K Street, MS 13-35, Sacramento, California 95814-3531. Phone: (916)322-3105

CSMIP/92-01 **"Evaluation of Soil-Structure Interaction in Buildings during Earthquakes,"** by G. Fenves and G. Serino, June 1992, 57 pp.

CSMIP/92-02 **"Seismic Performance Investigation of the Hayward BART Elevated Section,"** by W. Tseng, M. Yang and J. Penzien, September 1992, 61 pp.

CSMIP/93-01 **"Influence of Critical Moho Reflections on Strong Motion Attenuation in California,"** by P. Somerville, N. Smith and D. Dreger, December 1993, 84 pp.

CSMIP/93-02 **"Investigation of the Response of Puddingstone Dam in the Whittier Narrows Earthquake of October 1, 1987,"** by J. Bray, R. Seed and R. Boulanger, December 1993, 60 pp.

CSMIP/93-03 **"Investigation of the Response of Cogswell Dam in the Whittier Narrows Earthquake of October 1, 1987,"** by R. Boulanger, R. Seed and J. Bray, December 1993, 53 pp.

CSMIP/94-01 **"Torsional Response Characteristics of Regular Buildings under Different Seismic Excitation Levels,"** by H. Sedarat, S. Gupta, and S. Werner, January 1994, 43 pp.

CSMIP/94-02 **"Degradation of Plywood Roof Diaphragms under Multiple Earthquake Loading,"** by J. Bouwkamp, R. Hamburger and J. Gillengerten, February 1994, 32 pp.

CSMIP/94-03 **"Analysis of the Recorded Response of Lexington Dam during Various Levels of Ground Shaking,"** by F. Makdisi, C. Chang, Z. Wang and C. Mok, March 1994, 60 pp.

CSMIP/94-04 **"Correlation between Recorded Building Data and Non-Structural Damage during the Loma Prieta Earthquake of October 17, 1989,"** by S. Rihal, April 1994, 65 pp.

LIST OF CSMIP DATA UTILIZATION REPORTS (continued)

CSMIP/94-05	**"Simulation of the Recorded Response of Unreinforced Masonry (URM) Infill Buildings,"** by J. Kariotis, J. Guh, G. Hart and J. Hill, October 1994, 149 pp.
CSMIP/95-01	**"Seismic Response Study of the Hwy 101/Painter Street Overpass Near Eureka Using Strong-Motion Records,"** by R. Goel and A. Chopra, March 1995, 70 pp.
CSMIP/95-02	**"Evaluation of the Response of I-10/215 Interchange Bridge Near San Bernardino in the 1992 Landers and Big Bear Earthquakes,"** by G. Fenves and R. Desroches, March 1995, 132 pp.
CSMIP/95-03	**"Site Response Studies for Purpose of Revising NEHRP Seismic Provisions,"** by C.B. Crouse, March 1995, 68 pp.
CSMIP/96-01	**"An Investigation of UBC Serviceability Requirements from Building Responses Recorded During the 1989 Loma Prieta Earthquake,"** by C.-M. Uang and A. Maarouf, September 1996, 138 pp.
SMIP89	"SMIP89 Seminar on Seismological and Engineering Implications on Recent Strong-motion Data," Preprints, Sacramento, California, May 9, 1989
SMIP90	"SMIP90 Seminar on Seismological and Engineering Implications on Recent Strong-motion Data," Preprints, Sacramento, California, June 8, 1990
SMIP91	"SMIP91 Seminar on Seismological and Engineering Implications on Recent Strong-motion Data," Preprints, Sacramento, California, May 30, 1991
SMIP92	"SMIP92 Seminar on Seismological and Engineering Implications on Recent Strong-motion Data," Proceedings, Sacramento, California, May 21, 1992
SMIP93	"SMIP93 Seminar on Seismological and Engineering Implications on Recent Strong-motion Data," Proceedings, Sacramento, California, May 20, 1993, 114 pp.
SMIP94	"SMIP94 Seminar on Seismological and Engineering Implications on Recent Strong-motion Data," Proceedings, Los Angeles, California, May 26, 1994, 120 pp.
SMIP95	"SMIP95 Seminar on Seismological and Engineering Implications on Recent Strong-motion Data," Proceedings, San Francisco, California, May 16, 1995, 105 pp.
SMIP96	"SMIP96 Seminar on Seismological and Engineering Implications on Recent Strong-motion Data," Proceedings, Sacramento, California, May 14, 1996, 130 pp.